UNIVERSITY OF CALIFORNIA
RIVERSIDE

Formation and Genotoxicity of Novel Oxidatively Generated Tandem DNA Lesions and N^2-(1-carboxyethyl)-2′-deoxyguanosine

A Dissertation submitted in partial satisfaction
of the requirements for the degree of

Doctor of Philosophy

in

Environmental Toxicology

by

Yong Jiang

December 2009

Dissertation Committee:
Dr. Yinsheng Wang, Chairperson
Dr. David Eastmond
Dr. Connie Nugent

The Dissertation of Yong Jiang is approved:

_____

_____

_____

Committee Chairperson

University of California, Riverside

ACKNOWLEDGEMENTS

First of all, I would like to give my sincerest thanks to my advisor, Dr. Yinsheng Wang. He guided and supported me all along through my Ph.D. study. His enthusiasm and dedication to the research work greatly encouraged me over these years. At the moment when I finally completed my Ph.D. training and looked back all these years of research work, there were difficulties and hardships, but only the achievements and joys left and lasted ever after. It is of no question that, without Dr. Wang's help, I could not accomplish so much work in this thesis.

I would also like to thank my other committee members, Profs. David Eastmond and Connie Nugent. They were always very nice to me and gave me many helpful suggestions on my research. In addition, Profs. Robert Krieger and Janet Arey from ETOX program also helped me in many aspects.

I am grateful for the support from my labmates and staffs at UCR. I am proud that I was studying and working in such a wonderful research group. Everyone in the group was kind and accommodating to me, and gave me many generous help during the research work. Especially, I would like to thank Dr. Chunang Gu and Dr. Haizheng Hong, two former ETOX students and good labmates. They taught me a lot and led me to fit into the research work in a short time. I would also like to give my special thanks to one former labmate: Dr. Yuesong Wang, and two post-docs: Dr. Huachuan Cao and Dr.

Bifeng Yuan. We had many collaborating work and their efforts contributed greatly to the completion of my thesis.

I wish to extend my acknowledgement to Prof. John-Stephen A. Taylor for providing the construct for the overexpression of yeast pol η; Prof. Peter E.M. Gibbs, Prof. John M. Essigmann and Prof. Graham C. Walker for kindly providing the shuttle vector and *E. coli* strains; Prof. Myron F. Goodman for offering the recombinant *E. coli* DNA pol IV; Prof. Olga S. Fedorova for providing the expression vectors for hOGG1. I am also grateful that my research was supported by the funding from National Institutes of Health and the fellowships from the Environmental Toxicology Program of the University of California Riverside and the University of California Toxic Substances Research and Teaching Program.

I also want to thank the support and friendship from many good friends during my study in UCR: Dalin, Haiwei, Zhenshan, Yanhong, Haibo, Lei, Hongxia, Jianshuang, Congfang, Lijin, Chang and many more. They really made my life at UCR colorful and enjoyable.

At last, my deepest thanks belong to my beloved ones: my parents and my sister. They always understand me, unconditionally support me and bless me; and my lovely wife: Xilin; apparently, marrying her was another great achievement accomplished during my Ph.D. study. Their endless love brings me the power to overcome any difficulty. I love them very much.

COPYRIGHT ACKNOWLEDGEMENTS

The text and figures in Chapter 2, in part or in full, are a reprint of the material as it appears in *Biochemistry*, 2007, 46, p. 12757-12763. The co-author (Dr. Yinsheng Wang) listed in that publication directed and supervised the research which forms the basis of this Chapter. The co-author (Dr. Haizheng Hong) listed in that publication conducted experiments in LC-MS/MS identification. The co-author (Dr. Huachuan Cao) listed in that publication synthesized the isotope-labeled internal standard.

The text and figures in Chapter 3, in part or in full, are a reprint of the material as it appears in *Chem. Res. Toxicol.*, 2009, 22, p. 574-583. The co-author (Dr. Yinsheng Wang) listed in that publication directed and supervised the research which forms the basis of this Chapter. The co-author (Dr. Yuesong Wang) listed in that publication synthesized the lesion-bearing DNA substrates.

The text and figures in Chapter 4, in part or in full, are a reprint of the material as it appears in *Chem. Res. Toxicol.*, 2009, in submission. The co-author (Dr. Yinsheng Wang) listed in that publication directed and supervised the research which forms the basis of this Chapter. The co-author (Dr. Bifeng Yuan) listed in that publication conducted experiments in *in-vivo* replication study. The co-author (Dr. Yuesong Wang) listed in that publication synthesized the lesion-bearing DNA substrates.

The text and figures in Chapter 5, in part or in full, are a reprint of the material as it appears in *Proc. Natl. Acad. Sci.*, 2008, 105, p. 8679-8684. The co-author (Dr. Yinsheng

Wang) listed in that publication directed and supervised the research which forms the basis of this Chapter. The co-author (Dr. Bifeng Yuan) listed in that publication conducted experiments in *in-vivo* replication study. The co-author (Dr. Huachuan Cao) listed in that publication conducted experiments in LC-MS/MS identification. The co-author (Dr. Haizheng Hong) listed in that publication provided technical expertise in *in-vivo* replication study.

ABSTRACT OF THE DISSERTATION

Formation and Genotoxicity of Novel Oxidatively Generated Tandem DNA Lesions and N^2-(1-carboxyethyl)-2′-deoxyguanosine

by

Yong Jiang

Doctor of Philosophy, Graduate Program in Environmental Toxicology
University of California, Riverside, December 2009
Dr. Yinsheng Wang, Chairperson

Exogenous and endogenous agents can induce the formation of both single- and tandem-nucleobase lesions in DNA. In this dissertation, we assessed the formation and genotoxicity of three different types of DNA lesions; a novel guanine-thymine intrastrand cross-link lesion (G[8-5m]T), two tandem single-nucleobase lesions consisting of a thymidine glycol and an 8-oxo-7,8-dihydro-2′-deoxyguanosine [5′-(8-oxodG)-Tg-3′ and 5′-Tg-(8-oxodG)-3′], and a single nucleobase lesion, N^2-(1-carboxyethyl)-2′-deoxyguanosine (N^2-CEdG).

In Chapter 2, We demonstrated the dose-dependent induction of the G[8-5m]T cross-link in human HeLa-S3 cells upon exposure to γ-rays by LC-MS/MS. The *in-vitro* replication studies on the lesion-bearing substrate showed that the Klenow fragment of *Escherichia coli* (*E. coli*) DNA polymerase I stopped synthesis mostly after incorporating one nucleotide opposite the 3′-thymine moiety of the lesion. Yeast polymerase η, a translesion synthesis DNA polymerase, could replicate past the lesion with a markedly

reduced efficiency. However, it could also induce nucleotide misincorporation (i.e., dAMP and dGMP) opposite the 5′-guanine moiety of the G[8-5m]T. In Chapters 3 and 4, we developed an LC-MS/MS-based strategy for quantitative analysis and demonstrated the efficient formation of a tandem lesion, 5′-Tg-(8-oxodG)-3′, in calf thymus DNA upon exposure to Cu(II)/ascorbate along with H_2O_2 or γ- rays. Both *in-vitro* and *in-vivo* replication studies on two tandem lesions, 5′-(8-oxodG)-Tg-3′ and 5′-Tg-(8-oxodG)-3′, revealed that the tandem lesions blocked DNA replication mediated by the Klenow fragment and yeast pol η more readily than when the Tg or 8-oxodG was present alone and the mutagenicity of Tg or 8-oxodG differed while they were present alone or in tandem. Moreover, the activities of base excision repair enzymes were altered in substrates bearing the tandem lesions. The 5′-Tg-(8-oxodG)-3′ could also give rise to a substantial frequency of TG→GT tandem double mutation. These results support that complex lesions could exert a greater cytotoxic effect than when the composing lesions are present alone and the mutagenic properties of the tandem lesions could be markedly affected by the spatial arrangement of the component lesions.

In Chapter 5, we analyzed the formation and genotoxic properties of N^2-CEdG, demonstrated that this major stable DNA adduct could be induced by methylglyoxal (MG) in human cancer cells. We also found that N^2-CEdG is weakly mutagenic, and DinB (i.e., polymerase IV in *E. coli*) is the major DNA polymerase responsible for bypassing the lesion *in vivo*; the *E. coli* pol IV- and human polymerase κ-mediated nucleotide incorporation opposite this lesion is both accurate and efficient. Our results supported N^2-CEdG may constitute an important endogenous substrate for DinB DNA polymerase.

TABLE OF CONTENTS

LIST OF FIGURES

LIST OF TABLES

LIST OF SCHEMES

CHAPTER 1

General Introduction

This chapter will cover the general background of the research projects discussed in this dissertation.

Oxidative DNA Damage

The integrity of the human genome is constantly challenged by endogenous and exogenous agents, among which reactive oxygen species (ROS), i.e. superoxide anion ($O_2^{\bullet-}$), hydroxyl radical ($^{\bullet}OH$) and hydrogen peroxide (H_2O_2), can be generated from normal cellular aerobic metabolism or from interaction with exogenous sources such as ionizing radiation, ultraviolet light (UV) and anticancer agents (*1-5*). ROS can attack DNA molecules to induce a variety of lesions including single-nucleobase lesions, 2-deoxyribose modifications (*1, 5-7*), bulky adducts (*8, 9*), intra-/ interstrand cross-links (*10-16*), DNA-protein cross-links (*17-19*), and single- or double-strand breaks (SSB or DSB) (*1, 7*). It has been estimated that approximately 10^4 DNA bases can be oxidatively modified per cell per day (*20, 21*). The accumulation of DNA damage has been associated with the natural processes of ageing and numerous pathological conditions including cancer (*5, 22-24*), cardiovascular dysfunctions (*25*) and neurodegeneration (*26*).

Formation of Intrastrand Cross-link Lesions

It has been shown that intrastrand cross-link lesions, where two neighboring nucleobases in the same DNA strand are covalently bonded, can be induced in DNA upon ROS attack, which can be formed from exposure to γ rays (*15, 27, 28*) or Fenton reagents (*13, 29*). In this regard, studies have revealed several novel intrastrand cross-link lesions formed between neighboring C and G, G and T, T and A, C and A as well as G and mC (*10, 13, 15, 16, 28, 30-36*). The structures of several intrastrand cross-link lesions are shown in Figure 1-1.

Mechanisms have been proposed for the formation of intrastrand cross-link lesions. It was revealed that intrastrand cross-link lesions could be initiated from a single pyrimidine radical (*15, 30, 31, 34, 35, 37, 38*). In this respect, a hydroxyl radical ($^{\bullet}$OH) can be added to the C5 and C6 carbon atoms of cytosine, thymine or 5-methylcytosine; alternatively it can abstract a hydrogen atom from the 5-methyl group of thymine or 5-methylcytosine (*39*). The resulting pyrimidine base-centered secondary radicals may attack their neighboring purine bases to generate a covalent bond between two bases to form intrastrand cross-link lesions. It has been shown that the yields for the formation of these lesions are sequence- and distance-dependent, with the purine on the 5'-side favoring formation of the cross-link products than with the purine on the 3'-side, and the distance between the secondary radical of pyrimidine and the C8 of purine is also directly correlated with the yield of the cross-link lesion formation (*15, 40*).

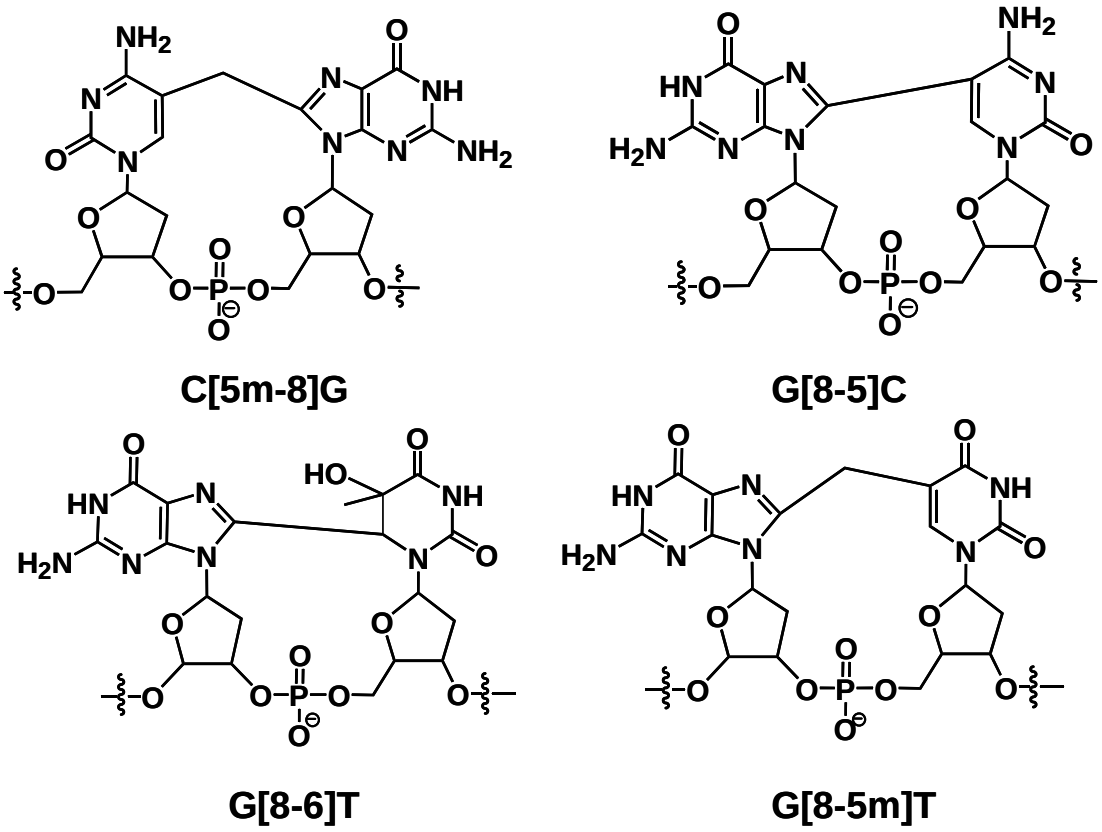

Figure 1-1 Structures of several oxidatively produced intrastrand cross-link lesions.

In this dissertation, we will discuss an intrastrand cross-link lesion, G[8-5m]T, where the C8 of guanine is covalently bonded with the methyl carbon of its neighboring 3'-thymine (structure shown in Figure 1-1). This lesion can be induced in an aqueous solution of duplex DNA upon exposure to γ- or X-rays (*15*). In addition, it was demonstrated that this lesion could be generated in calf thymus DNA upon treatment with the Fenton reagent, Cu(II)/H_2O_2/ascorbate, under aerobic conditions (*41*).

Formation of Single and Tandem Nucleobase DNA Lesions

Most oxidative modifications on a single nucleobase and 2-deoxyribose of DNA by ROS have been well studied and characterized. For instance, pyrimidine base lesions can be induced by the addition of the hydroxyl radical to the C5 and/or C6 positions of cytosine, thymine, or 5-methylcytosine, to form 5-hydroxy-6-yl and 6-hydroxy-5-yl radicals of the pyrimidine bases. The latter radicals can conjugate with OH^- or couple with water followed by deprotonation to render the corresponding pyrimidine glycols. Alternatively, hydrogen abstraction from the methyl group of thymine or 5-methylcytosine by the hydroxyl radical can initiate the formation of 5-hydroxymethyluracil (5-HmU), 5-formyluracil (5-FoU), 5-hydroxymethylcytosine (5-HmC) and 5-formylcytosine (*42*).

Purine base lesions can be induced by the hydroxyl radical addition to the C4, C5, or C8 of adenine and guanine. The generated secondary radicals are transformed to various products, such as 8-oxo-7,8-dihydro-2'-deoxyguanosine (8-oxodG), 8-oxo-7,8-dihydro-2'-deoxyadenosine (8-oxodA). These two oxidatively generated purine products

are known to undergo imidazole ring-opening to give 2,6-diamino-5-formamido-pyrimidine (Fapy-dG), and 4,6-diamino-5-formamido-pyrimidine (Fapy-dA), respectively (*43*).

Hydroxyl radicals can also attack the C-H bonds in 2-deoxyribose moiety of DNA to form carbon-centered radicals, resulting in 2-deoxyribose modification products, DNA strand breaks and base-free sites, such as lactone, abasic site and 2-deoxyribose ring-opening products (*39*).

In addition to the above single-base and 2-deoxyribose lesions, ROS can also induce the formation of cyclo lesions, which involve the formation of an additional bond between the nucleobase and the $C_{5'}$ carbon of the same nucleoside, e.g. 5',8-cyclo-2'-deoxyganosine, 5',8-cyclo-2'-deoxyadenosine, 5',6-cyclo-5,6-dihydrothymidine, and 5',6-cyclo-5,6-dihydro-2'-deoxyuridine (*44, 45*) .

Other than the above lesions, which are believed to occur frequently and predominately upon single ROS attack, complex or clustered DNA lesions, where two or more damaged nucleosides are located within 1-2 helical turns of DNA, can form upon interaction with ROS. Example lesions include those formed upon exposure to ionizing radiation (*46-49*). As a subset of clustered lesions, tandem lesions, consisting of two neighboring damaged nucleotides on the same DNA strand, could be initiated from a single hydroxyl radical attack (*50*), which can be induced from ionizing radiation (*46*) or Fenton reagents (*51*). For example, a tandem lesion, with an 8-oxodG and a formamido (dβF) moiety being neighboring to each other, was first reported to form in short

oligodeoxyribonucleotides (ODNs) upon exposure to γ-rays or Fenton-type reagents under aerobic conditions (Figure 1-2) (*46, 52*).

Multiple oxidation events in close proximity, for example, those occurred during ionizing radiation, may give rise to the formation of tandem lesions by inducing oxidation events on both neighboring nucleobases. In addition, a proposed mechanism for the tandem lesion formation under single oxidation event is that the single ROS attack may transform one nucleobase into an intermediate nucleobase radical, the latter radical can further attack its neighboring nucleobase rendering the formation of a tandem nucleobase lesion. This is similar as the well-studied formation of intrastrand cross-link lesions which can also be categorized as a type of tandem DNA lesions.

In this dissertation, we investigated the replication and repair of the tandem nucleobase lesions containing a neighboring thymidine glycol (or 5,6-dihydroxy-5,6-dihydrothymidine, Tg) and an 8-oxodG, which are major oxidatively induced lesions of thymidine and 2′-deoxyguanosine, respectively. The structures of the two positional isomers of this type of tandem lesions are shown in Figure 1-2.

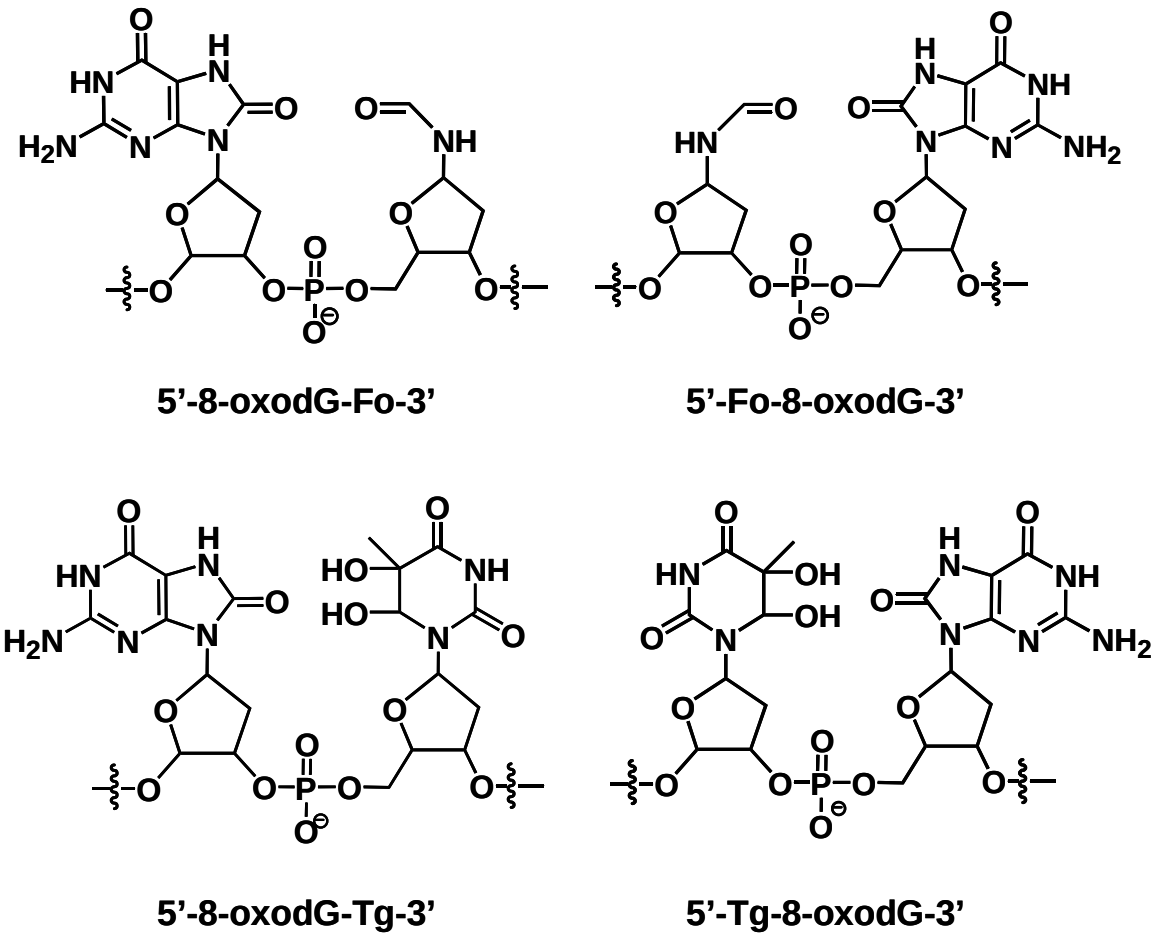

Figure 1-2 The structures of several oxidatively generated tandem nucleobase lesions.

Formation of N^2-(1-carboxyethyl)-2′-deoxyguanosine (N^2-CEdG)

Other than ROS, which constitutes a major endogenous source of DNA damage (*2*), DNA in living cells is also susceptible to damage from exposure to reactive carbonyl species, and methylglyoxal (MG) is one of them (*53*). MG is a byproduct of the nonenzymatic fragmentation of triose phosphates produced during glycolysis, a ubiquitous process conserved in all domains of life (*54*). The accumulation of MG in human cells can be enhanced by both endogenous factors, including aging, hyperglycemia, inflammation, oxidative stress, diabetes, and uremia (*55-57*), and exogenous sources, including cigarette smoke (*58*), food, and beverages (*58, 59*). In this regard, treatment of human red blood cells with increasing concentrations of glucose *in vitro* can result in increases of intracellular MG concentration (*60*). The MG concentration was also found to be elevated in the kidney (cortex and medulla), lens, and blood of streptozotocin-induced diabetic rats (*61*) and in blood samples of diabetic patients (*57*).

N^2-CEdG was the major stable adduct formed in calf thymus DNA upon exposure to MG at physiological concentration and temperature (*62*). The formation and structures of the two diastereomers of N^2-CEdG are shown in Figure 1-3. This lesion can also be detected in urine samples from healthy humans at levels ranging from 1.2- to 117-ng N^2-CEdG equivalent per milligram of creatinine (*63*). In another study, the level of the lesion was enhanced in the kidney and aorta of patients with diabetic nephropathy and uremic atherosclerosis, respectively (*64*).

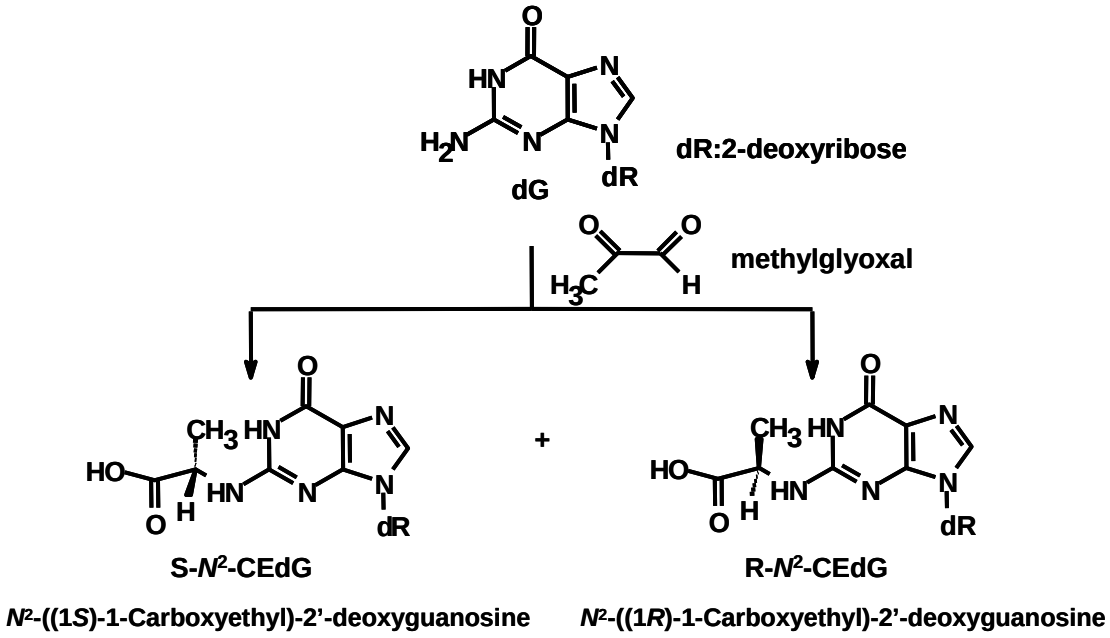

Figure 1-3 The formation of N^2-CEdG from methylglyoxal.

In this dissertation, we employed LC-MS/MS and measured the formation of N^2-CEdG in human cells, with or without treatment of methylglyoxal or glucose. We also assessed how the lesion perturbs the fidelity and efficiency of DNA replication both *in vitro* and *in vivo.*

Replication of Cross-link Lesions, Tandem Lesions and N^2-CEdG by Purified DNA Polymerases

To ensure the integrity and stability of genome against deleterious effects of DNA damage, cells have developed various strategies to protect themselves, including multiple levels of intracellular signaling to indicate the presence of damage, intricate DNA repair systems for removing DNA lesions, and certain tolerance mechanisms during DNA replication process. Despite replicative DNA synthesis is a faithful event which requires undamaged DNA and high-fidelity DNA polymerases, if lesions escape the complicated network of DNA repair, cells have developed processes, as a backup pathway, for tolerating unrepaired, or repair-resistant DNA lesions when the genome is replicated. A major mechanism proposed is translesion synthesis (TLS) (*65, 66*). A model of TLS, namely "DNA polymerase switch model", proposed that the replicative polymerase blocked by DNA damage is transiently replaced by one (or several) TLS polymerases, which insert only a few nucleotides opposite the lesion and beyond the lesion site before dissociating from replication fork and resuming regular DNA synthesis (*67*). During TLS, either the correct (error-free) or the incorrect (error-prone) nucleotide can be inserted, depending on the nature of the DNA lesion and the nucleotide preference of the engaged

specialized polymerase. Thus, TLS allows replication to continue and contributes to cell survival but can result in induced mutagenesis and increased cancer risk.

Relative to single nucleobase lesions, the presence of complex or bulky DNA lesions, i.e. tandem nucleobase lesions and cross-link lesions could lead to more DNA strand distortion. It has been demonstrated that G[8-5]C, G[8-5m]T and G[8-5m]C destabilized the DNA duplex, which increased the free energy for duplex formation at 37°C by 4.0, 5.4 and 3.6 kcal/mol, respectively (*68, 69*). Likewise, 5'-(8-oxodG)-Tg-3' or 5'-Tg-(8-oxodG)-3' tandem lesions destabilized the duplex by increasing the free energy for duplex formation at 25°C with 5.1 kcal/mol (*70*).

Most TLS polymerases, including pol η, pol ι, pol κ and Rev1 in mammalian cells (*65*), and pol IV and V in *E. coli* (*71*), belong to the Y-family of DNA polymerases. They have been well characterized for their lesion-bypassing properties *in vitro* (*67*). Unlike replicative polymerases, mostly TLS polymerases do not have highly constrained active sites and lack the 3'-5' proofreading exonuclease activity, resulting in low fidelity in replicating undamaged DNA.

The biological significance of TLS polymerases is highlighted by DNA polymerase η (pol η), which is encoded by the RAD30 gene in budding yeast *Saccharomyces cerevisiae* (*72*) and the variant form of xeroderma pigmentosum (XP-V) gene in humans (*73*). Pol η can bypass efficiently the TT cyclobutane pyrimidine dimer (CPD) in an error-free manner (*72, 74*). In addition to pol η, pol ι encoded by RAD30B in humans can bypass abasic sites and another major photoproduct, i.e. the pyrimidine(6-

4)pyrimidone product (*67*). Other than thymine dimers, pol η was reported to bypass many other DNA lesions, such as some bulky lesions, i.e. N^2-benzo[*a*]pyrene-7,8-diol-9,10-epoxide-dG (N^2-BPDE-dG), cisplatin-DNA adducts, and even Tg and 8-oxodG (*75-78*).

Two major oxidatively induced single-nucleobase lesions, 8-oxodG and Tg, have been extensively studied. 8-oxodG is a major mutagenic lesion and can result in G → T transversion mutations (*79, 80*). In contrast, thymidine glycol lacks mutagenicity under most conditions (*81-84*), but effectively blocks DNA replication (*85, 86*). It can be bypassed by TLS DNA polymerases including yeast pol η and ζ as well as human pol κ and all three polymerases preferentially insert a dA opposite the lesion (*82, 87, 88*). On the other hand, 8-oxodG can also be bypassed by various DNA polymerases, and both dC and dA can be inserted opposite the lesion (*89, 90*).

Most intrastrand cross-link lesions mentioned above and dimeric TT photo-products share close structural similarity. Our previous *in-vitro* replication study on an intrastrand cross-link lesion, G[8-5]C, also showed that it can either stall DNA replication performed by high-fidelity replicative polymerases or give rise to mutations by yeast pol η (*27*). In addition, since a similar conformational change can be induced by tandem lesions, it could be proposed that certain translesion synthesis enzyme(s), i.e. pol η, may play an important role in intrastrand cross-link- or tandem lesion-induced mutagenesis, if the replication of the lesion is blocked by replicative polymerases.

Among the Y-family DNA polymerases, DinB (also known as pol IV in *Escherichia coli* and pol κ in mammalian cells) is conserved in all domains of life. Previous studies demonstrated that *E. coli* pol IV and human pol κ can insert preferentially the correct nucleotide, dCMP, opposite a number of N^2-dG lesions (*91, 92*). It was also found that the DinB polymerase is capable of bypassing the N^2-dG adduct induced by BPDE (*75, 93-95*), a cigarette smoke carcinogen, and pol κ was observed to be overexpressed in lung tumor specimens (*96*). In this dissertation, one goal is to examine if N^2-CEdG is a substrate for DinB polymerase.

The study of *In-vitro* mutagenesis on a lesion can be achieved from steady-state enzyme kinetic analyses (*97-99*). The efficiency and fidelity of nucleotide incorporation can be determined by measuring the velocities for the incorporation of one nucleotide at a time and fitting the velocity data with the Michaelis-Menten equation ($V_{obs} = \frac{V_{\max} \times [dNTP]}{K_m + [dNTP]}$).

Repair of Complex DNA Lesions

Several repair systems are involved in repairing different types of DNA damage, such as base excision repair (BER) for single-nucleobase lesions, nucleotide excision repair (NER) for major DNA photo-products and bulky DNA adducts, homologous recombination (HR) and non-homologous end-joining (NHEJ) for double-strand breaks, as well as mismatch repair (MMR) for nucleobase mispairs (*3, 5, 100-102*). However, for complex or clustered DNA lesions, owing to the intrinsic chemical and structural

diversities of the different lesions involved and their close proximity, they are often more difficult to repair than when individual lesions are present alone (*100, 103-109*).

With respect to the repair of two major single nucleobase lesions, in eukaryotes, the majority of 8-oxodG is removed via BER pathway by 8-oxodG glycosylases (OGGs); As a second line of defense to prevent G → T transversions during replication, bacteria and most eukaryotes have a mismatch DNA glycosylase called MutY, which removes the dA that is mispaired with the 8-oxodG. Thymidine glycol is a substrate for the glycosylase activity of the endonuclease III in bacteria, this important enzyme is highly conserved in evolution from bacteria to human cells (*110-112*). In addition to BER, both Tg and 8-oxodG can also be excised from DNA by NER enzymes *in vitro* (*113*).

Several studies assessed the replication and repair of tandem single-nucleobase lesions. For example, the base-excision activities for a tandem lesion with Tg neighboring a 2-deoxyribonolactone are inhibited (*114*); the repair process on a tandem lesion may generate persistent single-strand breaks (*106*). In addition, the mutation frequency of an 8-oxodG is enhanced by a certain second lesion nearby due to inhibition of the repair machinery for 8-oxodG by the presence of another lesion (*106, 115*). More studies showed that the excision, by purified BER enzymes or by cell extracts, of clustered DNA lesions is indeed compromised, and that the effects vary depending on the types of lesions involved and their spatial distribution (*100, 104, 107, 116-118*).

NER pathway can repair those lesions that can distort the DNA helical structure. ROS-induced intrastrand cross-link lesions or tandem lesions, due to the increased

structural destabilization, may also allow the lesions to be more efficiently excised by the NER than the BER pathway. Indeed, several ROS-induced intrastrand cross-link lesions were found to be substrates for NER enzymes as manifested by the binding and incision of the lesion-bearing duplex DNA substrates by the *E. coli* UvrABC excision nuclease (*119*). Another study also indicated tandem nucleobase lesions may be recognized and incised by the bacterial NER repair system (*100*). NER is a particularly important mechanism by which the cell removes the vast majority of UV-induced DNA damage, mostly in the form of CPD and 6-4 PP photoproducts, and various bulky DNA adducts, i.e., BPDE-DNA adduct (*101*). Unlike BER machinery which recognizes and removes damaged bases by specific DNA glycosylases, the NER machinery recognizes distortions to the DNA double helix and leads to the removal of a short single-stranded DNA segment conaining the lesion, which creates a single-strand gap in the DNA. The latter is subsequently filled in by DNA polymerase with the undamaged strand as a template, and finally the nick is sealed by DNA ligase(s) (*120*).

Application of Mass Spectrometry (MS) in Identification and Quantification of DNA Modifications

Nowadays, mass spectrometry is becoming a powerful tool for nucleic acid research. It has major advantages for the characterization and quantification of DNA modifications. Historically the major role of MS in the determination of DNA lesions had been limited to providing structural information about new DNA adducts (*121*). Gas chromatography-mass spectrometry (GC-MS) was previously used to quantify DNA

adducts. However, only non-polar/volatile compounds can be analyzed by GC-MS. Derivatization at high temperature is needed prior to subjecting a sample to GC-MS analysis because most DNA adducts are non-volatile/polar. Thus, the measurements are not accurate because the derivatization may lead to artificial formation of certain adducts (*122, 123*).

The advent of liquid chromatography-mass spectrometry (LC-MS), together with the introduction of electrospray ionization (ESI) and atmospheric pressure chemical ionization (APCI), has led to widespread application of MS in the analysis of non-volatile and thermally labile compounds. Assessing DNA adducts by LC-MS has been proven to be a sensitive and reliable method for quantifying DNA adducts when compared to other analytical approaches, such as ^{32}P post-labeling and immunoassays. Accurate and reproducible data can be obtained by employing isotope dilution techniques together with LC-tandem MS (LC-MS/MS) analysis. The detection limits can reach as low as 0.2-2.0 adducts per 10^8 unmodified nucleosides. In addition, MS can offer structural information and is capable of analyzing DNA adducts with unknown structures (*123*).

The identification and quantification of certain DNA modifications formed in isolated or cellular DNA can be achieved by enzymatic digestion coupled with LC-MS/MS analysis. After enzymatic digestion, unmodified nucleobases and single-nucleobase lesions in DNA are liberated as mononucleosides or nucleotides depending on the enzymes employed; certain lesions, i.e. intrastrand cross-link lesions can be released as a dinucleoside monophosphate. These lesion-carrying small molecules can be analyzed

by LC-MS/MS for compound identification and quantification (*10, 13, 27*). Other methods may also improve the sensitivity for lesion detection, for example, chemical derivatization of 5-formyl-2'-deoxyuridine with Girard reagent T can enhance substantially the detection limit of the lesion by LC-MS/MS analysis (*124*).

LC-MS/MS-based Strategy for *In-vitro* and *In-vivo* Replication Studies

Two major types of fragment ions, w_n and [a_n-base] are generated during the fragmentation of ODNs in a mass spectrometer. The mass difference between two adjacent w_n or [a_n-base] corresponds to the mass of a nucleotide. Viewing that nucleotides bearing an A, C, G, or T have unique masses, the sequences of ODNs can be determined by MS/MS (*125*), which leads to another important application of MS in nucleic acid research: sequencing. The capability to sequence and quantify short ODNs renders MS a powerful tool for mutagenesis studies of modified DNA.

LC-MS/MS method had been introduced for investigating the multiple bypass mechanisms of polymerases toward DNA lesions *in vitro* by Guengerich et al. (*92, 126*) and our group (*127*). It turned out that this method provides an efficient route for determining the identities and distributions of various replication products resulting from the polymerase reaction in the presence of all four dNTPs, which, relative to the conditions used for steady-state kinetic measurements, mimics better the replication conditions *in vivo*.

Strategies have also been developed to assess the mutagenicity and cytotoxicity of a specific lesion in cells. In most previous *in-vivo* mutagenesis studies, researchers

applied genotoxic agents to introduce specific DNA lesions into the genome, which usually are site-undirected and may be contaminated with other non-specific lesions. To overcome those drawbacks, strategies have been developed for the site-directed mutagenesis study by inserting a structurally defined lesion into the genome of a vector that can be introduced into cells and replicated there. The replication and repair of the vector would be performed by the endogenous enzymes of the host and in a cellular environment providing the natural level of precursors for DNA synthesis (*128*). Moreover, the relative toxic effects of different lesions can be measured, and polymerase-specific analysis can be achieved by using certain polymerase-deficient or knockout cell lines as hosts.

Restriction endonuclease and post-labeling (REAP) and competitive replication and adduct bypass (CRAB) assays were introduced by Essigmann and coworkers to measure quantitatively the mutation frequency and lesion bypass efficiency of a site-specifically incorporated and structurally defined DNA lesion in cells (*129-131*). In these assays, the replication products of the lesion in the vector was extracted after replication, the sequence of interest was amplified by PCR, and short ODNs containing replication products were obtained by digestion with restriction endonucleases prior to sequencing and quantification analysis. Instead of ^{32}P post-labeling and thin-layer chromatography analysis which were used by Essigmann and coworkers, LC-MS/MS was recently introduced for unambiguous identification and accurate quantification of replication products; especially since the method can allow for the identification of unexpected replication products (*132*).

Scope of This Dissertation

To understand the biological significance of several oxidative DNA lesions, for example, intrastrand cross-links and tandem lesions, it's important to characterize and quantify their formation in isolated DNA upon exposure to certain biologically relevant ROS-inducing systems, i.e. γ rays or Fenton-type reagents; or more importantly, to investigate if the lesions can be formed in cells, i.e. N^2-CEdG. It is also of great importance to assess the cytotoxic and mutagenic properties of these lesions both *in vitro* and *in vivo*, so as to gain further insights into their influences on genome integrity and cell viability if they are produced in living organisms. The knowledge gained from these studies may also contribute to an understanding of oxidative DNA damage-related pathological conditions, i.e. cancer development, neurodegeneration and diabetes.

In this dissertation we attempt to attain the following objectives: 1). To identify and quantify the formation of a DNA intrastrand cross-link lesion, G[8-5m]T, induced in cells upon exposure to γ rays and to investigate its *in-vitro* replication properties with several purified DNA polymerases. 2). To identify and quantify the formation of a tandem lesion, 5'-Tg-(8-oxodG)-3', in isolated DNA upon exposure to Fenton-type reagents by LC-MS/MS. 3). To assess both the *in-vitro* and *in-vivo* replication properties of tandem lesions; 5'-Tg-(8-oxodG)-3' and 5'-(8-oxodG)-Tg-3'. 4). To identify and quantify the formation of N^2-CEdG adducts in cells with LC-MS/MS analysis and to reveal the translesion synthesis polymerase(s) involved in bypassing this lesion.

References:

(1) Dizdaroglu, M., Jaruga, P., Birincioglu, M., and Rodriguez, H. (2002) Free radical-induced damage to DNA: mechanisms and measurement. *Free Radic. Biol. Med. 32*, 1102-15.

(2) Finkel, T., and Holbrook, N. J. (2000) Oxidants, oxidative stress and the biology of ageing. *Nature 408*, 239-47.

(3) Lindahl, T. (1999) DNA lesions generated in vivo by reactive oxygen species, their accumulation and repair. *NATO ASI Ser., Ser. A 302*, 251-257.

(4) Nakabeppu, Y., Tsuchimoto, D., Ichinoe, A., Ohno, M., Ide, Y., Hirano, S., Yoshimura, D., Tominaga, Y., Furuichi, M., and Sakumi, K. (2004) Biological significance of the defense mechanisms against oxidative damage in nucleic acids caused by reactive oxygen species: from mitochondria to nuclei. *Ann. N. Y. Acad. Sci. 1011*, 101-11.

(5) Cooke, M. S., Evans, M. D., Dizdaroglu, M., and Lunec, J. (2003) Oxidative DNA damage: mechanisms, mutation, and disease. *FASEB J. 17*, 1195-214.

(6) Cadet, J., Delatour, T., Douki, T., Gasparutto, D., Pouget, J. P., Ravanat, J. L., and Sauvaigo, S. (1999) Hydroxyl radicals and DNA base damage. *Mutat. Res. 424*, 9-21.

(7) Cadet, J., Berger, M., Douki, T., and Ravanat, J. L. (1997) Oxidative damage to DNA: formation, measurement, and biological significance. *Rev. Physiol. Biochem. Pharmacol. 131*, 1-87.

(8) Randerath, K., Reddy, M. V., and Disher, R. M. (1986) Age- and tissue-related DNA modifications in untreated rats: detection by 32P-postlabeling assay and possible significance for spontaneous tumor induction and aging. *Carcinogenesis 7*, 1615-7.

(9) Randerath, K., Randerath, E., Zhou, G. D., and Li, D. H. (1999) Bulky endogenous DNA modifications (I-compounds) - possible structural origins and functional implications. *Mutation Research-Fundamental and Molecular Mechanisms of Mutagenesis 424*, 183-194.

(10) Hong, H., and Wang, Y. (2005) Formation of intrastrand cross-link products between cytosine and adenine from UV irradiation of d((Br)CA) and duplex DNA containing a 5-bromocytosine. *J. Am. Chem. Soc. 127*, 13969-77.

(11) Hong, I. S., and Greenberg, M. M. (2005) DNA interstrand cross-link formation initiated by reaction between singlet oxygen and a modified nucleotide. *Journal of the American Chemical Society 127*, 10510-10511.

(12) Hong, I. S., and Greenberg, M. M. (2005) Efficient DNA interstrand cross-link formation from a nucleotide radical. *Journal of the American Chemical Society 127*, 3692-3693.

(13) Hong, H., Cao, H., Wang, Y., and Wang, Y. (2006) Identification and quantification of a guanine-thymine intrastrand cross-link lesion induced by Cu(II)/H2O2/ascorbate. *Chem. Res. Toxicol. 19*, 614-21.

(14) Hong, I. S., Ding, H., and Greenberg, M. M. (2006) Oxygen independent DNA interstrand cross-link formation by a nucleotide radical. *Journal of the American Chemical Society 128*, 485-491.

(15) Bellon, S., Ravanat, J. L., Gasparutto, D., and Cadet, J. (2002) Cross-linked thymine-purine base tandem lesions: synthesis, characterization, and measurement in gamma-irradiated isolated DNA. *Chem. Res. Toxicol. 15*, 598-606.

(16) Zhang, Q., and Wang, Y. (2005) Generation of 5-(2'-deoxycytidyl)methyl radical and the formation of intrastrand cross-link lesions in oligodeoxyribonucleotides. *Nucleic Acids Res. 33*, 1593-603.

(17) Wang, T. S., Hsu, T. Y., Chung, C. H., Wang, A. S. S., Bau, D. T., and Jan, K. Y. (2001) Arsenite induces oxidative DNA adducts and DNA-protein cross-links in mammalian cells. *Free Radical Biology and Medicine 31*, 321-330.

(18) Shakhova, I. K., and Lomova, T. Y. (1985) The Induction and Repair of the DNA-Protein Cross-Links at Different Replication Activity Levels in the Chinese Hamsters Cultured-Cells. *Mutation Research 147*, 320-320.

(19) Brambilla, G., Sciaba, L., Faggin, P., Finollo, R., Bassi, A. M., Ferro, M., and Marinari, U. M. (1985) Methylglyoxal-Induced DNA-Protein Cross-Links and Cyto-Toxicity in Chinese-Hamster Ovary Cells. *Carcinogenesis 6*, 683-686.

(20) Shigenaga, M. K., Gimeno, C. J., and Ames, B. N. (1989) Urinary 8-hydroxy-2'-deoxyguanosine as a biological marker of in vivo oxidative DNA damage. *Proc. Natl. Acad. Sci. U. S. A. 86*, 9697-701.

(21) Loft, S., Vistisen, K., Ewertz, M., Tjonneland, A., Overvad, K., and Poulsen, H. E. (1992) Oxidative DNA damage estimated by 8-hydroxydeoxyguanosine excretion in humans: influence of smoking, gender and body mass index. *Carcinogenesis 13*, 2241-7.

(22) Jackson, A. L., and Loeb, L. A. (2001) The contribution of endogenous sources of DNA damage to the multiple mutations in cancer. *Mutat. Res. 477*, 7-21.

(23) Ames, B. N. (1989) Endogenous oxidative DNA damage, aging, and cancer. *Free Radic. Res. Commun. 7*, 121-8.

(24) Olinski, R., Gackowski, D., Rozalski, R., Foksinski, M., and Bialkowski, K. (2003) Oxidative DNA damage in cancer patients: a cause or a consequence of the disease development? *Mutat. Res. 531*, 177-90.

(25) Bennett, M. R. (2001) Reactive oxygen species and death: oxidative DNA damage in atherosclerosis. *Circ. Res. 88*, 648-50.

(26) Rolig, R. L., and McKinnon, P. J. (2000) Linking DNA damage and neurodegeneration. *Trends Neurosci. 23*, 417-24.

(27) Gu, C. N., and Wang, Y. S. (2004) LC-MS/MS identification and yeast polymerase eta bypass of a novel gamma-irradiation-induced intrastrand cross-link lesion G[8-5]C. *Biochemistry 43*, 6745-6750.

(28) Zeng, Y., and Wang, Y. (2004) Facile formation of an intrastrand cross-link lesion between cytosine and guanine upon pyrex-filtered UV light irradiation of d((Br)CG) and duplex DNA containing 5-bromocytosine. *J. Am. Chem. Soc. 126*, 6552-3.

(29) Cao, H. C., and Wang, Y. S. (2007) Quantification of oxidative single-base and intrastrand cross-link lesions in unmethylated and CpG-methylated DNA induced by Fenton-type reagents. *Nucleic Acids Research 35*, 4833-4844.

(30) Box, H. C., Budzinski, E. E., Dawidzik, J. B., Gobey, J. S., and Freund, H. G. (1997) Free radical-induced tandem base damage in DNA oligomers. *Free Radic. Biol. Med. 23*, 1021-30.

(31) Box, H. C., Budzinski, E. E., Dawidzik, J. B., Wallace, J. C., and Iijima, H. (1998) Tandem lesions and other products in X-irradiated DNA oligomers. *Radiat. Res. 149*, 433-9.

(32) Box, H. C., Budzinski, E. E., Dawidzik, J. D., Wallace, J. C., Evans, M. S., and Gobey, J. S. (1996) Radiation-induced formation of a crosslink between base moieties of deoxyguanosine and thymidine in deoxygenated solutions of d(CpGpTpA). *Radiat. Res. 145*, 641-3.

(33) Romieu, A., Bellon, S., Gasparutto, D., and Cadet, J. (2000) Synthesis and UV photolysis of oligodeoxynucleotides that contain 5- (phenylthiomethyl)-2'-deoxyuridine: a specific photolabile precursor of 5-(2'-deoxyuridilyl)methyl radical. *Org. Lett. 2*, 1085-8.

(34) Zhang, Q., and Wang, Y. (2003) Independent generation of 5-(2'-deoxycytidinyl)methyl radical and the formation of a novel crosslink lesion between 5-methylcytosine and guanine. *J. Am. Chem. Soc. 125*, 12795-802.

(35) Zhang, Q., and Wang, Y. (2004) Independent generation of the 5-hydroxy-5,6-dihydrothymidin-6-yl radical and its reactivity in dinucleoside monophosphates. *J. Am. Chem. Soc. 126*, 13287-97.

(36) Liu, Z. J., Gao, Y., Zeng, Y., Fang, F., Chi, D., and Wang, Y. S. (2004) Isolation and characterization of a novel cross-link lesion in d(CpC) induced by one-electron photooxidation. *Photochemistry and Photobiology 80*, 209-215.

(37) Budzinski, E. E., Dawidzik, J. B., Rajecki, M. J., Wallace, J. C., Schroder, E. A., and Box, H. C. (1997) Isolation and characterization of the products of anoxic irradiation of d(CpGpTpA). *Int. J. Radiat. Biol. 71*, 327-36.

(38) Zhang, Q., and Wang, Y. (2005) Generation of 5-(2'-deoxycytidyl)methyl radical and the formation of intrastrand cross-link lesions in oligodeoxyribonucleotides. *Nucleic Acids Res. 33*, 1593-1603.

(39) von Sonntag, C. (1987) *The Chemical Basis of Radiation Biology*, Taylor & Francis, London.

(40) Zeng, Y., and Wang, Y. (2006) Sequence-dependent formation of intrastrand crosslink products from the UVB irradiation of duplex DNA containing a 5-bromo-2'-deoxyuridine or 5-bromo-2'-deoxycytidine. *Nucleic Acids Res. 34*, 6521-9.

(41) Hong, H., Cao, H., Wang, Y., and Wang, Y. (2006) Identification and quantification of a guanine-thymine intrastrand cross-link lesion induced by Cu(II)/H_2O_2/ascorbate. *Chem. Res. Toxicol. 19*, 614-621.

(42) Zuo, S., Boorstein, R. J., and Teebor, G. W. (1995) Oxidative damage to 5-methylcytosine in DNA. *Nucleic Acids Res. 23*, 3239-43.

(43) Steenken, S. (1989) Purine bases, nucleosides, and nucleotides: aqueous solution redox chemistry and transformation reactions of their radical cations and e- and OH adducts. *Chem. Rev. 89*, 503-20.

(44) Dizdaroglu, M. (1986) Free-radical-induced formation of an 8,5'-cyclo-2'-deoxyguanosine moiety in deoxyribonucleic acid. *Biochem. J. 238*, 247-54.

(45) Shaw, A. A., and Cadet, J. (1988) Formation of cyclopyrimidines via the direct effects of gamma radiation of pyrimidine nucleosides. *Int. J. Radiat. Biol. 54*, 987-97.

(46) Box, H. C., Dawidzik, J. B., and Budzinski, E. E. (2001) Free radical-induced double lesions in DNA. *Free Radic. Biol. Med. 31*, 856-68.

(47) Gulston, M., Fulford, J., Jenner, T., de Lara, C., and O'Neill, P. (2002) Clustered DNA damage induced by radiation in human fibroblasts (HF19), hamster (V79-4) cells and plasmid DNA is revealed as Fpg and Nth sensitive sites. *Nucleic Acids Research 30*, 3464-3472.

(48) Nikjoo, H., O'Neill, P., Wilson, W. E., and Goodhead, D. T. (2001) Computational approach for determining the spectrum of DNA damage induced by ionizing radiation. *Radiation Research 156*, 577-583.

(49) Sutherland, B. M., Bennett, P. V., Sutherland, J. C., and Laval, J. (2002) Clustered DNA damages induced by X rays in human cells. *Radiation Research 157*, 611-616.

(50) Box, H. C., Budzinski, E. E., Freund, H. G., Evans, M. S., Patrzyc, H. B., Wallace, J. C., and MacCubbin, A. E. (1993) Vicinal lesions in X-irradiated DNA? *Int. J. Radiat. Biol. 64*, 261-3.

(51) Bourdat, A.-G., Douki, T., Frelon, S., Gasparutto, D., and Cadet, J. (2000) Tandem Base Lesions Are Generated by Hydroxyl Radical within Isolated DNA in Aerated Aqueous Solution. *J. Am. Chem. Soc. 122*, 4549-4556.

(52) Budzinski, E. E., Dawidzik, J. D., Wallace, J. C., Freund, H. G., and Box, H. C. (1995) The radiation chemistry of d(CpGpTpA) in the presence of oxygen. *Radiat. Res. 142*, 107-9.

(53) De Bont, R., and van Larebeke, N. (2004) Endogenous DNA damage in humans: a review of quantitative data. *Mutagenesis 19*, 169-85.

(54) Fothergill-Gilmore, L. A., and Michels, P. A. (1993) Evolution of glycolysis. *Prog. Biophys. Mol. Biol. 59*, 105-235.

(55) Ramasamy, R., Yan, S. F., and Schmidt, A. M. (2006) Methylglyoxal comes of AGE. *Cell 124*, 258-60.

(56) Chaplen, F. W., Fahl, W. E., and Cameron, D. C. (1998) Evidence of high levels of methylglyoxal in cultured Chinese hamster ovary cells. *Proc. Natl. Acad. Sci. U S A 95*, 5533-8.

(57) Mclellan, A. C., Thornalley, P. J., Benn, J., and Sonksen, P. H. (1994) Glyoxalase System in Clinical Diabetes-Mellitus and Correlation with Diabetic Complications. *Clinical Science 87*, 21-29.

(58) Saint-Jalm, Y., and Moree-Testa, P. (1980) Study of nitrogen-containing compounds in cigarette smoke by gas chromatography-mass spectrometry. *J. Chromatogr 198*, 188-92.

(59) do Rosario, P. M., Cordeiro, C. A., Freire, A. P., and Nogueira, J. M. (2005) Analysis of methylglyoxal in water and biological matrices by capillary zone electrophoresis with diode array detection. *Electrophoresis 26*, 1760-7.

(60) Thornalley, P. J. (1988) Modification of the Glyoxalase System in Human Red Blood-Cells by Glucose Invitro. *Biochemical Journal 254*, 751-755.

(61) Phillips, S. A., Mirrlees, D., and Thornalley, P. J. (1993) Modification of the Glyoxalase System in Streptozotocin-Induced Diabetic Rats - Effect of the Aldose Reductase Inhibitor Statil. *Biochemical Pharmacology 46*, 805-811.

(62) Frischmann, M., Bidmon, C., Angerer, J., and Pischetsrieder, M. (2005) Identification of DNA adducts of methylglyoxal. *Chem. Res. Toxicol. 18*, 1586-92.

(63) Schneider, M., Georgescu, A., Bidmon, C., Tutsch, M., Fleischmann, E. H., Popov, D., and Pischetsrieder, M. (2006) Detection of DNA-bound advanced glycation end-products by immunoaffinity chromatography coupled to HPLC-diode array detection. *Mol. Nutr. Food Res. 50*, 424-9.

(64) Li, H., Nakamura, S., Miyazaki, S., Morita, T., Suzuki, M., Pischetsrieder, M., and Niwa, T. (2006) N-2-carboxyethyl-2 '-deoxyguanosine, a DNA glycation marker, in kidneys and aortas of diabetic and uremic patients. *Kidney International 69*, 388-392.

(65) Kannouche, P., and Stary, A. (2003) Xeroderma pigmentosum variant and error-prone DNA polymerases. *Biochimie 85*, 1123-32.

(66) Goodman, M. F. (2002) Error-prone repair DNA polymerases in prokaryotes and eukaryotes. *Annu. Rev. Biochem. 71*, 17-50.

(67) Friedberg, E. C., Wagner, R., and Radman, M. (2002) Specialized DNA polymerases, cellular survival, and the genesis of mutations. *Science 296*, 1627-30.

(68) Gu, C. N., and Wang, Y. S. (2005) Thermodynamic and in vitro replication studies of an intrastrand G[8-5]C cross-link lesion. *Biochemistry 44*, 8883-8889.

(69) Gu, C. N., Zhang, Q. B., Yang, Z. G., Wang, Y. S., Zou, Y., and Wang, Y. S. (2006) Recognition and incision of oxidative intrastrand cross-link lesions by UvrABC nuclease. *Biochemistry 45*, 10739-10746.

(70) Wang, Y. W., and Wang, Y. S. (2006) Synthesis and thermodynamic studies of oligodeoxyribonucleotides containing tandem lesions of thymidine glycol and 8-oxo-2 '-deoxyguanosine. *Chemical Research in Toxicology 19*, 837-843.

(71) Goodman, M. F., and Fygenson, K. D. (1998) DNA polymerase fidelity: from genetics toward a biochemical understanding. *Genetics 148*, 1475-82.

(72) Johnson, R. E., Prakash, S., and Prakash, L. (1999) Efficient bypass of a thymine-thymine dimer by yeast DNA polymerase, Poleta. *Science 283*, 1001-4.

(73) Masutani, C., Kusumoto, R., Yamada, A., Dohmae, N., Yokoi, M., Yuasa, M., Araki, M., Iwai, S., Takio, K., and Hanaoka, F. (1999) The XPV (xeroderma pigmentosum variant) gene encodes human DNA polymerase eta. *Nature 399*, 700-4.

(74) Masutani, C., Araki, M., Yamada, A., Kusumoto, R., Nogimori, T., Maekawa, T., Iwai, S., and Hanaoka, F. (1999) Xeroderma pigmentosum variant (XP-V) correcting protein from HeLa cells has a thymine dimer bypass DNA polymerase activity. *Embo J. 18*, 3491-501.

(75) Rechkoblit, O., Zhang, Y. B., Guo, D. Y., Wang, Z. G., Amin, S., Krzeminsky, J., Louneva, N., and Geacintov, N. E. (2002) trans-lesion synthesis past bulky benzo[a]pyrene diol epoxide N-2-dG and N-6-dA lesions catalyzed by DNA bypass polymerases. *Journal of Biological Chemistry 277*, 30488-30494.

(76) Kusumoto, R., Masutani, C., Iwai, S., and Hanaoka, F. (2002) Translesion synthesis by human DNA polymerase eta across thymine glycol lesions. *Biochemistry 41*, 6090-6099.

(77) Zhang, Y., Yuan, F., Wu, X., Rechkoblit, O., Taylor, J. S., Geacintov, N. E., and Wang, Z. (2000) Error-prone lesion bypass by human DNA polymerase η. *Nucleic Acids Res. 28*, 4717-24.

(78) Vaisman, A., Masutani, C., Hanaoka, F., and Chaney, S. G. (2000) Efficient translesion replication past oxaliplatin and cisplatin GpG adducts by human DNA polymerase eta. *Biochemistry 39*, 4575-4580.

(79) Wagner, J., Kamiya, H., and Fuchs, R. P. (1997) Leading versus lagging strand mutagenesis induced by 7,8-dihydro-8-oxo-2'-deoxyguanosine in Escherichia coli. *J Mol Biol 265*, 302-9.

(80) Tan, X., Grollman, A. P., and Shibutani, S. (1999) Comparison of the mutagenic properties of 8-oxo-7,8-dihydro-2'-deoxyadenosine and 8-oxo-7,8-dihydro-2'-deoxyguanosine DNA lesions in mammalian cells. *Carcinogenesis 20*, 2287-92.

(81) Hayes, R. C., Petrullo, L. A., Huang, H. M., Wallace, S. S., and LeClerc, J. E. (1988) Oxidative damage in DNA. Lack of mutagenicity by thymine glycol lesions. *J Mol Biol 201*, 239-46.

(82) Johnson, R. E., Yu, S. L., Prakash, S., and Prakash, L. (2003) Yeast DNA polymerase zeta (zeta) is essential for error-free replication past thymine glycol. *Genes Dev 17*, 77-87.

(83) Seki, M., Masutani, C., Yang, L. W., Schuffert, A., Iwai, S., Bahar, I., and Wood, R. D. (2004) High-efficiency bypass of DNA damage by human DNA polymerase Q. *Embo J 23*, 4484-94.

(84) Basu, A. K., Loechler, E. L., Leadon, S. A., and Essigmann, J. M. (1989) Genetic effects of thymine glycol: site-specific mutagenesis and molecular modeling studies. *Proc Natl Acad Sci U S A 86*, 7677-81.

(85) Clark, J. M., and Beardsley, G. P. (1986) Thymine glycol lesions terminate chain elongation by DNA polymerase I in vitro. *Nucleic Acids Res 14*, 737-49.

(86) Ide, H., Kow, Y. W., and Wallace, S. S. (1985) Thymine glycols and urea residues in M13 DNA constitute replicative blocks in vitro. *Nucleic Acids Res 13*, 8035-52.

(87) Kusumoto, R., Masutani, C., Iwai, S., and Hanaoka, F. (2002) Translesion synthesis by human DNA polymerase eta across thymine glycol lesions. *Biochemistry 41*, 6090-9.

(88) Fischhaber, P. L., Gerlach, V. L., Feaver, W. J., Hatahet, Z., Wallace, S. S., and Friedberg, E. C. (2002) Human DNA polymerase kappa bypasses and extends beyond thymine glycols during translesion synthesis in vitro, preferentially incorporating correct nucleotides. *J Biol Chem 277*, 37604-11.

(89) Zhang, Y., Yuan, F., Wu, X., Wang, M., Rechkoblit, O., Taylor, J. S., Geacintov, N. E., and Wang, Z. (2000) Error-free and error-prone lesion bypass by human DNA polymerase kappa in vitro. *Nucleic Acids Res 28*, 4138-46.

(90) Zhang, Y., Yuan, F., Wu, X., Taylor, J. S., and Wang, Z. (2001) Response of human DNA polymerase iota to DNA lesions. *Nucleic Acids Res 29*, 928-35.

(91) Jarosz, D. F., Godoy, V. G., Delaney, J. C., Essigmann, J. M., and Walker, G. C. (2006) A single amino acid governs enhanced activity of DinB DNA polymerases on damaged templates. *Nature 439*, 225-8.

(92) Choi, J. Y., Zang, H., Angel, K. C., Kozekov, I. D., Goodenough, A. K., Rizzo, C. J., and Guengerich, F. P. (2006) Translesion synthesis across 1,N^2-ethenoguanine by human DNA polymerases. *Chem. Res. Toxicol. 19*, 879-86.

(93) Zhang, Y., Yuan, F., Wu, X., Wang, M., Rechkoblit, O., Taylor, J. S., Geacintov, N. E., and Wang, Z. (2000) Error-free and error-prone lesion bypass by human DNA polymerase κ *in vitro*. *Nucleic Acids Res. 28*, 4138-46.

(94) Shen, X., Sayer, J. M., Kroth, H., Ponten, I., O'Donnell, M., Woodgate, R., Jerina, D. M., and Goodman, M. F. (2002) Efficiency and accuracy of SOS-induced DNA polymerases replicating benzo[*a*]pyrene-7,8-diol 9,10-epoxide A and G adducts. *J. Biol. Chem. 277*, 5265-74.

(95) Suzuki, N., Ohashi, E., Kolbanovskiy, A., Geacintov, N. E., Grollman, A. P., Ohmori, H., and Shibutani, S. (2002) Translesion synthesis by human DNA polymerase kappa on a DNA template containing a single stereoisomer of dG-(+)- or dG-(-)-anti-N-2-BPDE (7,8-dihydroxy-anti-9,10-epoxy-7,8,9,10-tetrahydrobenzo[a]pyrene). *Biochemistry 41*, 6100-6106.

(96) O-Wang, J., Kawamura, K., Tada, Y., Ohmori, H., Kimura, H., Sakiyama, S., and Tagawa, M. (2001) DNA polymerase κ, implicated in spontaneous and DNA damage-induced mutagenesis, is overexpressed in lung cancer. *Cancer Res. 61*, 5366-9.

(97) Goodman, M. F., Creighton, S., Bloom, L. B., and Petruska, J. (1993) Biochemical basis of DNA replication fidelity. *Crit. Rev. Biochem. Mol. Biol. 28*, 83-126.

(98) Kuchta, R. D., Mizrahi, V., Benkovic, P. A., Johnson, K. A., and Benkovic, S. J. (1987) Kinetic mechanism of DNA polymerase I (Klenow). *Biochemistry 26*, 8410-7.

(99) Creighton, S., Bloom, L. B., and Goodman, M. F. (1995) Gel fidelity assay measuring nucleotide misinsertion, exonucleolytic proofreading, and lesion bypass efficiencies. *Methods Enzymol. 262*, 232-56.

(100) Imoto, S., Bransfield, L. A., Croteau, D. L., Van Houten, B., and Greenberg, M. M. (2008) DNA tandem lesion repair by strand displacement synthesis and nucleotide excision repair. *Biochemistry 47*, 4306-4316.

(101) Balajee, A. S., May, A., and Bohr, V. A. (1999) DNA repair of pyrimidine dimers and 6-4 photoproducts in the ribosomal DNA. *Nucleic Acids Res 27*, 2511-20.

(102) Lindahl, T., and Wood, R. D. (1999) Quality control by DNA repair. *Science 286*, 1897-905.

(103) Bellon, S., Shikazono, N., Cunniffe, S., Lomax, M., and O'Neill, P. (2009) Processing of thymine glycol in a clustered DNA damage site: mutagenic or cytotoxic. *Nucleic Acids Research 37*, 4430-4440.

(104) Yang, N., Chaudhry, M. A., and Wallace, S. S. (2006) Base excision repair by hNTH1 and hOGG1: A two edged sword in the processing of DNA damage in gamma-irradiated human cells. *DNA Repair 5*, 43-51.

(105) Budworth, H., and Dianov, G. L. (2003) Mode of inhibition of short-patch base excision repair by thymine glycol within clustered DNA lesions. *Journal of Biological Chemistry 278*, 9378-9381.

(106) Budworth, H., Matthewman, G., O'Neill, P., and Dianov, G. L. (2005) Repair of tandem base lesions in DNA by human cell extracts generates persisting single-strand breaks. *Journal of Molecular Biology 351*, 1020-1029.

(107) David-Cordonnier, M. H., Cunniffe, S. M. T., Hickson, I. D., and O'Neill, P. (2002) Efficiency of incision of an AP site within clustered DNA damage by the major human AP endonuclease. *Biochemistry 41*, 634-642.

(108) Dobbs, T. A., Palmer, P., Maniou, Z., Lomax, M. E., and O'Neill, P. (2008) Interplay of two major repair pathways in the processing of complex double-strand DNA breaks. *DNA Repair 7*, 1372-1383.

(109) Lomax, M. E., Cunniffe, S., and O'Neill, P. (2004) 8-oxoG retards the activity of the ligase III/XRCC1 complex during the repair of a single-strand break, when present within a clustered DNA damage site. *DNA Repair 3*, 289-299.

(110) Aspinwall, R., Rothwell, D. G., Roldan-Arjona, T., Anselmino, C., Ward, C. J., Cheadle, J. P., Sampson, J. R., Lindahl, T., Harris, P. C., and Hickson, I. D. (1997) Cloning and characterization of a functional human homolog of Escherichia coli endonuclease III. *Proc Natl Acad Sci U S A 94*, 109-14.

(111) Hilbert, T. P., Chaung, W., Boorstein, R. J., Cunningham, R. P., and Teebor, G. W. (1997) Cloning and expression of the cDNA encoding the human homologue of the DNA repair enzyme, Escherichia coli endonuclease III. *J Biol Chem 272*, 6733-40.

(112) Ikeda, S., Biswas, T., Roy, R., Izumi, T., Boldogh, I., Kurosky, A., Sarker, A. H., Seki, S., and Mitra, S. (1998) Purification and characterization of human NTH1, a homolog of Escherichia coli endonuclease III. Direct identification of Lys-212 as the active nucleophilic residue. *J Biol Chem 273*, 21585-93.

(113) Reardon, J. T., Bessho, T., Kung, H. C., Bolton, P. H., and Sancar, A. (1997) In vitro repair of oxidative DNA damage by human nucleotide excision repair system: possible explanation for neurodegeneration in xeroderma pigmentosum patients. *Proc Natl Acad Sci U S A 94*, 9463-8.

(114) Bourdat, A. G., Gasparutto, D., and Cadet, J. (1999) Synthesis and enzymatic processing of oligodeoxynucleotides containing tandem base damage. *Nucleic Acids Res. 27*, 1015-24.

(115) Malyarchuk, S., Youngblood, R., Landry, A. M., Quillin, E., and Harrison, L. (2003) The mutation frequency of 8-oxo-7,8-dihydroguanine (8-oxodG) situated in a multiply damaged site: comparison of a single and two closely opposed 8-oxodG in Escherichia coli. *DNA Repair (Amst) 2*, 695-705.

(116) Pearson, C. G., Shikazono, N., Thacker, J., and O'Neill, P. (2004) Enhanced mutagenic potential of 8-oxo-7,8-dihydroguanine when present within a clustered DNA damage site. *Nucleic Acids Res. 32*, 263-270.

(117) David-Cordonnier, M. H., Laval, J., and O'Neill, P. (2000) Clustered DNA damage, influence on damage excision by XRS5 nuclear extracts and Escherichia coli Nth and Fpg proteins. *J. Biol. Chem. 275*, 11865-11873.

(118) Budworth, H., Dianova, I. I., Podust, V. N., and Dianov, G. L. (2002) Repair of clustered DNA lesions - Sequence-specific inhibition of long-patch base excision repair by 8-oxoguanine. *J. Biol. Chem. 277*, 21300-21305.

(119) Gu, C., Zhang,Q., Yang, Z., Zou, Y. and Wang, Y. (2006) Recognition and incision of oxidative intrastrand cross-link lesions by UvrABC nuclease. *Biochemistry*.

(120) Ura, K., and Hayes, J. J. (2002) Nucleotide excision repair and chromatin remodeling. *Eur J Biochem 269*, 2288-93.

(121) Koc, H., and Swenberg, J. A. (2002) Applications of mass spectrometry for quantitation of DNA adducts. *Journal of Chromatography B-Analytical Technologies in the Biomedical and Life Sciences 778*, 323-343.

(122) Collins, A. R., Cadet, J., Moller, L., Poulsen, H. E., and Vina, J. (2004) Are we sure we know how to measure 8-oxo-7,8-dihydroguanine in DNA from human cells? *Archives of Biochemistry and Biophysics 423*, 57-65.

(123) Singh, R., and Farmer, P. B. (2006) Liquid chromatography-electrospray ionization-mass spectrometry: the future of DNA adduct detection. *Carcinogenesis 27*, 178-196.

(124) Hong, H. H., and Wang, Y. S. (2007) Derivatization with girard reagent t combined with LC-MS/MS for the sensitive detection of 5-formyl-2 '-deoxyuridine in cellular DNA. *Analytical Chemistry 79*, 322-326.

(125) Mcluckey, S. A., Vanberkel, G. J., and Glish, G. L. (1992) Tandem Mass-Spectrometry of Small, Multiply Charged Oligonucleotides. *Journal of the American Society for Mass Spectrometry 3*, 60-70.

(126) Zang, H., Goodenough, A. K., Choi, J. Y., Irimia, A., Loukachevitch, L. V., Kozekov, I. D., Angel, K. C., Rizzo, C. J., Egli, M., and Guengerich, F. P. (2005) DNA adduct bypass polymerization by *Sulfolobus solfataricus* DNA polymerase Dpo4: analysis and crystal structures of multiple base pair substitution and frameshift products with the adduct 1,N^2-ethenoguanine. *J. Biol. Chem. 280*, 29750-64.

(127) Gu, C. N., and Wang, Y. S. (2007) In vitro replication and thermodynamic studies of methylation and oxidation modifications of 6-thioguanine. *Nucleic Acids Research 35*, 3693-3704.

(128) Singer, B., and Essigmann, J. M. (1991) Site-specific mutagenesis: retrospective and prospective. *Carcinogenesis 12*, 949-55.

(129) Delaney, J. C., and Essigmann, J. M. (1999) Context-dependent mutagenesis by DNA lesions. *Chem. Biol. 6*, 743-753.

(130) Delaney, J. C., and Essigmann, J. M. (2004) Mutagenesis, genotoxicity, and repair of 1-methyladenine, 3-alkylcytosines, 1-methylguanine, and 3-methylthymine in alkB Escherichia coli. *Proc. Natl. Acad. Sci. USA 101*, 14051-6.

(131) Delaney, J. C., and Essigmann, J. M. (2006) Assays for determining lesion bypass efficiency and mutagenicity of site-specific DNA lesions in vivo. *Methods Enzymol. 408*, 1-15.

(132) Hong, H., Cao, H., and Wang, Y. (2007) Formation and genotoxicity of a guanine-cytosine intrastrand cross-link lesion in vivo. *Nucleic Acids Res 35*, 7118-27.

CHAPTER 2

In-vivo Formation and *In-vitro* Replication of a Guanine-thymine Intrastrand Cross-link Lesion

Introduction

Excess generation of reactive oxygen species (ROS) *in vivo* can result in DNA damage (*1-3*), which include a multitude of single-nucleobase lesions (*4*) and a number of intrastrand cross-link lesions (*5-17*). In this respect, it was found that some intrastrand cross-link lesions, including G[8-5m]T where the C8 of guanine is covalently bonded to the methyl carbon of its neighboring 3'-thymine (structure shown in Figure 2-1), can be induced in an aqueous solution of duplex DNA upon exposure to γ- or X-rays (*10*). In addition, our study demonstrated that G[8-5m]T could be generated from calf thymus DNA upon treatment with Fenton reagent, Cu(II)/H_2O_2/ascorbate, under aerobic conditions (*18*).

Previous studies revealed that intrastrand cross-link lesions are initiated from a single pyrimidine radical (*6-8, 10, 12-14*). In this respect, hydroxyl radical ($^{\cdot}$OH) can abstract a hydrogen atom from the 5-methyl group of thymine (*19*), leading to the formation of the methyl radical of the nucleobase, which may attack its neighboring guanine base to yield the G[8-5m]T (*10*). In light of this underlying mechanism for the formation of the intrastrand cross-link lesions and the previous results from Fenton

system (*18*), we reasoned that the G[8-5m]T cross-link lesion might be induced in genomic DNA of eukaryotic cells upon exposure to ROS.

The presence of DNA lesions in replicating DNA may lead to the stalling of DNA replication, which may cause cell death. Moreover, lesions may give rise to mutations and result in numerous pathological conditions including carcinogenesis (*20*). Other than some frequently observed single mutations resulting from ROS-induced DNA lesions, e.g. C→T transitions and G→T transversions (*21*), CC→TT and mCG→TT tandem double mutations were shown to be induced by ROS generated from a variety of systems (*21-24*). It was suggested that ROS-induced intrastrand cross-link lesions formed between adjacent nucleotides might contribute to the tandem mutations (*22, 23*).

It is worth noting that one of our previous *in-vitro* replication studies on G[8-5]C showed that it can either stall DNA replication performed by some high fidelity replicative polymerase, such as T7 DNA polymerase and HIV reverse transcriptase, or lead to mutagenesis by a translesion synthesis polymerase, yeast polymerase η (pol η) (*17, 25*).

Herein, we demonstrated, for the first time, that the G[8-5m]T cross-link lesion could be induced, in a dose-dependent manner, in cultured human cells upon exposure to γ rays. In addition, we measured the steady-state kinetic parameters during DNA replication *in vitro* with a replicative DNA polymerase, Klenow fragment of *Escherichia coli* DNA polymerase I, and a member of "Y" superfamily polymerases, yeast DNA pol η. The latter is the gene product of Rad30 in budding yeast *Saccharomyces cerevisiae* (*26*) and the variant form of *Xeroderma pigmentosum* (XP-V) in humans (*27*).

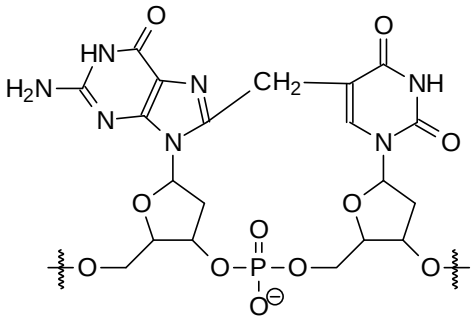

G[8-5m]T

Crosslink: 5’-ATGGCG[8-5m]TGCTATGATCCTAG-3’

Control: 5’-ATGGCGTGCTATGATCCTAG-3’

14 mer Primer: 5’-GCTAGGATCATAGC-3’

15 mer Primer: 5’-GCTAGGATCATAGCA-3’

Figure 2-1. (Top) Structure of the G[8-5m]T intrastrand cross-link. (Bottom) The substrates used for *in vitro* replication studies.

Experimental

Chemicals and enzymes

All oligodeoxyribonucleotides (ODNs) used in this study were purchased from Integrated DNA Technologies (Coraville, IA). [γ-^{32}P]ATP was obtained from Amersham Biosciences Co. (Piscataway, NJ). Other chemicals were purchased from Sigma-Aldrich (St. Louis, MO). Nuclease P1 and alkaline phosphatase were purchased from MP Biomedicals (Aurora, OH) and Sigma-Aldrich (St. Louis, MO), respectively. Snake venom phosphodiesterase and calf spleen phosphodiesterase were obtained from US Biological (Swampscott, MA). Klenow fragment (3'→5' exo$^-$) of the DNA polymerase I was purchased from New England Biolabs, Inc. (Ipswich, MA). Yeast polymerase η (pol η) was a kind gift from Prof. J.-S. A. Taylor at Washington University (St. Louis, MO). Hela-S3 cells were obtained from National Cell Culture Center (Minneapolis, MN).

Treatment of Hela-S3 cells with γ-rays and enzymatic digestion of DNA

Hela-S3 cells were centrifuged to remove the culture medium and resuspended in phosphate-buffered saline (PBS). The cell suspension (10^7 cells/mL) was exposed to γ-rays delivered by a Mark I ^{137}Cs Irradiator (JL Shepherd and Associates, San Fernando, CA), and the dose rate was 2.8 Gy/min. Immediately after the exposure, the cells were harvested by centrifugation and the nuclear DNA was isolated by phenol extraction.

The DNA was digested with four enzymes (nuclease P1, calf spleen phosphodiesterase, alkaline phosphatase, and snake venom phosphodiesterase) to release the intrastrand cross-link lesions as dinucleoside monophosphates following previously

published procedures (*28*). The digestion mixture was passed through a YM-10 Centricon membrane (Millipore, Billerica, MA) to remove the enzymes. The amount of nucleosides in the mixture was quantified by UV absorption spectroscopy and to the mixture was then added isotopically labeled d(G[8-5m]T), which carried two ^{15}N and a deuterium on the thymidine portion and was synthesized previously (*18*).

HPLC enrichment

The HPLC enrichment of d(G[8-5m]T) from the digestion mixture of cellular DNA was performed with a 4.6×50 mm Luna reverse-phase C18 column (5 μm in particle size, Phenomenex, Torrance, CA). A gradient of 5-min of 0-2% acetonitrile followed by a 55-min of 2-5% acetonitrile in 10 mM ammonium formate (pH 6.3) was employed and the flow rate was 0.60 mL/min. The fractions were collected in a wide retention time range to ensure that the cross-link product was completely collected. The collected fractions were dried in the Speed-vac, redissolved in 15 μL H_2O, and injected for LC-MS/MS analysis.

LC-MS/MS for the detection and quantification of G[8-5m]T

A 0.5×150 mm Zorbax SB-C18 column (particle size, 5 μm, Agilent) was used for the separation of the DNA hydrolysis samples, and the flow rate was 8.0 μL/min, which was delivered by an Agilent 1100 capillary HPLC pump (Agilent Technologies, Palo Alto, CA). A 60-min gradient of 0-30% acetonitrile in 20 mM ammonium acetate was employed for the analysis of HPLC-enriched d(G[8-5m]T). The effluent from the LC column was coupled to an LTQ linear ion-trap mass spectrometer (Thermo Fisher

Scientific, San Jose, CA), which was set up for monitoring the fragmentation of the $[M + H]^+$ ions of the labeled and unlabeled d(G[8-5m]T).

Preparation of substrates for in vitro replication studies

The G[8-5m]T-containing ODN for *in-vitro* replication studies was prepared following procedures described in a previous paper (*29*). Briefly, a dodecameric lesion-bearing substrate d(ATGGCG[8-5m]TGCTAT) was obtained from the 254-nm irradiation of a 5-phenylthiomethyl-2'-deoxyuridine-containing ODN. The lesion-bearing substrate was ligated with the 5'-phosphorylated d(GATCCTAG) in the presence of a template ODN, d(CCGCTCCCTAGGATCATAGCACGCCAT) (*17*). The desired lesion-containing 20-mer ODN was purified by 20% denaturing polyacrylamide gel electrophoresis (PAGE) and desalted by ethanol precipitation. The purity of the product was further confirmed by PAGE analysis (data not shown).

Primer extension assay

The 20-mer lesion-containing template or normal template (20 nM) with GT in lieu of the G[8-5m]T was annealed with a 5'-^{32}P-labeled 14-mer primer (10 nM) (Figure 2-1). To the duplex mixture were added a mixture of all four dNTPs as well as a DNA polymerase. The reaction was carried out at 37°C in a buffer containing 10 mM Tris-HCl (pH 7.5), 5 mM $MgCl_2$, and 7.5 mM DTT for 60 min. The concentrations of polymerases were indicated in the figures. The reaction was terminated by adding a 2 volume excess of formamide gel-loading buffer [80% formamide, 10 mM EDTA (pH 8.0), 1 mg/mL xylene cyanol, and 1 mg/mL bromophenol blue]. The products were resolved on 20%

(29:1) cross-linked polyacrylamide gels containing 8 M urea. Gel band intensities for the substrates and products were quantified by using a Typhoon 9410 Variable Mode Imager (Amersham Biosciences Co.) and ImageQuant version 5.2 (Amersham Biosciences Co.).

Steady-state kinetic measurements

The steady-state kinetic analyses were performed as described previously (*30, 31*). In this measurement, the primer-template duplex (10 nM) was incubated with either Klenow fragment (0.1 unit) or yeast polymerase η (5 ng) in the presence of an individual dNTP at various concentrations as indicated in the figures. The reaction was carried out at room temperature with the same reaction buffer as described for the primer extension assays. The dNTP concentration was optimized for different insertion reactions to allow for less than 20% primer extension (*31*). The observed rate of dNTP incorporation (V_{obs}) was plotted as a function of dNTP concentration, and the apparent K_m and V_{max} steady-state kinetic parameters for the incorporation of both the correct and incorrect nucleotides were determined by fitting the rate data with the Michaelis-Menten equation:

$$V_{obs} = \frac{V_{max} \times [dNTP]}{K_m + [dNTP]}.$$

The efficiency of nucleotide incorporation was determined by the ratio of V_{max} /K_m. The fidelity of nucleotide incorporation was then calculated by the frequency of misincorporation (f_{inc}) with the following equation:

$$f_{inc} = \frac{(V_{max} / K_m)_{incorrect}}{(V_{max} / K_m)_{correct}}.$$

Results

Identification and quantification of G[8-5m]T in Hela-S3 cells exposed to γ rays

Encouraged by the findings that G[8-5m]T could be induced in ODNs from exposure to γ-rays and in calf thymus DNA treated with Fenton reagents under aerobic conditions (*10, 18*), we set out to examine the formation of this type of lesion in human cells. To this end, we exposed cultured Hela-S3 cells to a series of doses of γ-rays, isolated nuclear DNA immediately after the exposure, and digested the DNA by using four enzymes (See Experimental). This digestion method was proven to be efficient in liberating both single-base and intrastrand-cross-link lesions (*18*). We then added the isotope-labeled d(G[8-5m]T) to the digestion mixture, removed most unmodified nucleosides by HPLC, and subjected the d(G[8-5m]T)-containing HPLC fractions to LC-MS/MS and LC-MS/MS/MS (MS^3) analyses.

Our LC-MS results revealed that G[8-5m]T could be induced in cultured human cells upon exposure to γ-ray exposure. In this context, we observed a peak in the SIC for the *m/z* 570→472 transition for the DNA sample obtained from the cell (Figure 2-2). Moreover, the product-ion spectrum of the $[M + H]^+$ ion of this fraction showed the presence of the fragment ion of *m/z* 472, which is attributed to the elimination of a 2-deoxyribose (*18*). Corresponding analysis of DNA samples obtained from control cells without γ-ray exposure revealed that the G[8-5m]T was not detectable.

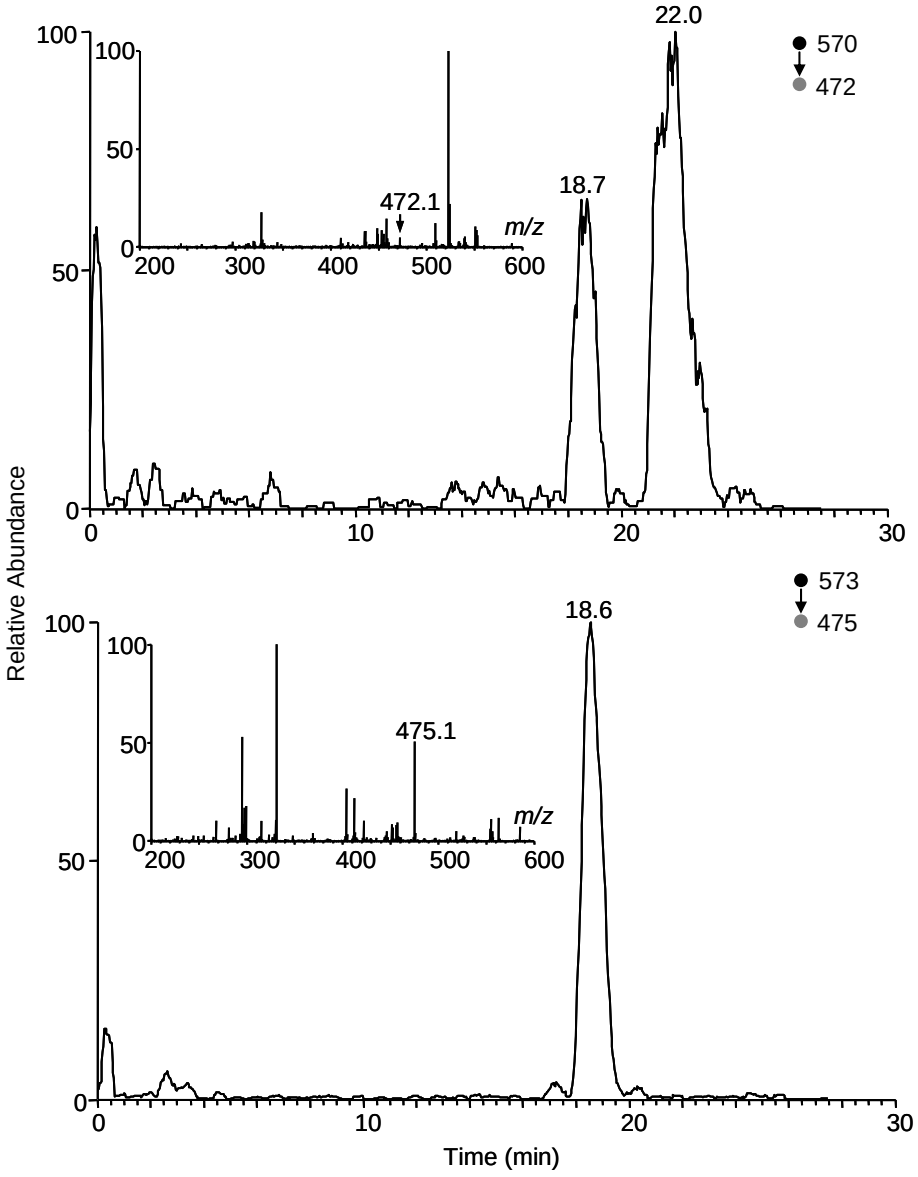

Figure 2-2. Selected ion chromatograms (SICs) for the monitoring of the *m/z* 570→472 (a, for G[8-5m]T and 573 →475 (b, for labeled G[8-5m]T transitions in the γ-ray irradiated cellular DNA samples after enzymatic digestion . Shown in the insets are the product-ion spectra of the $[M + H]^+$ ions of the unlabeled and labeled G[8-5m]T.

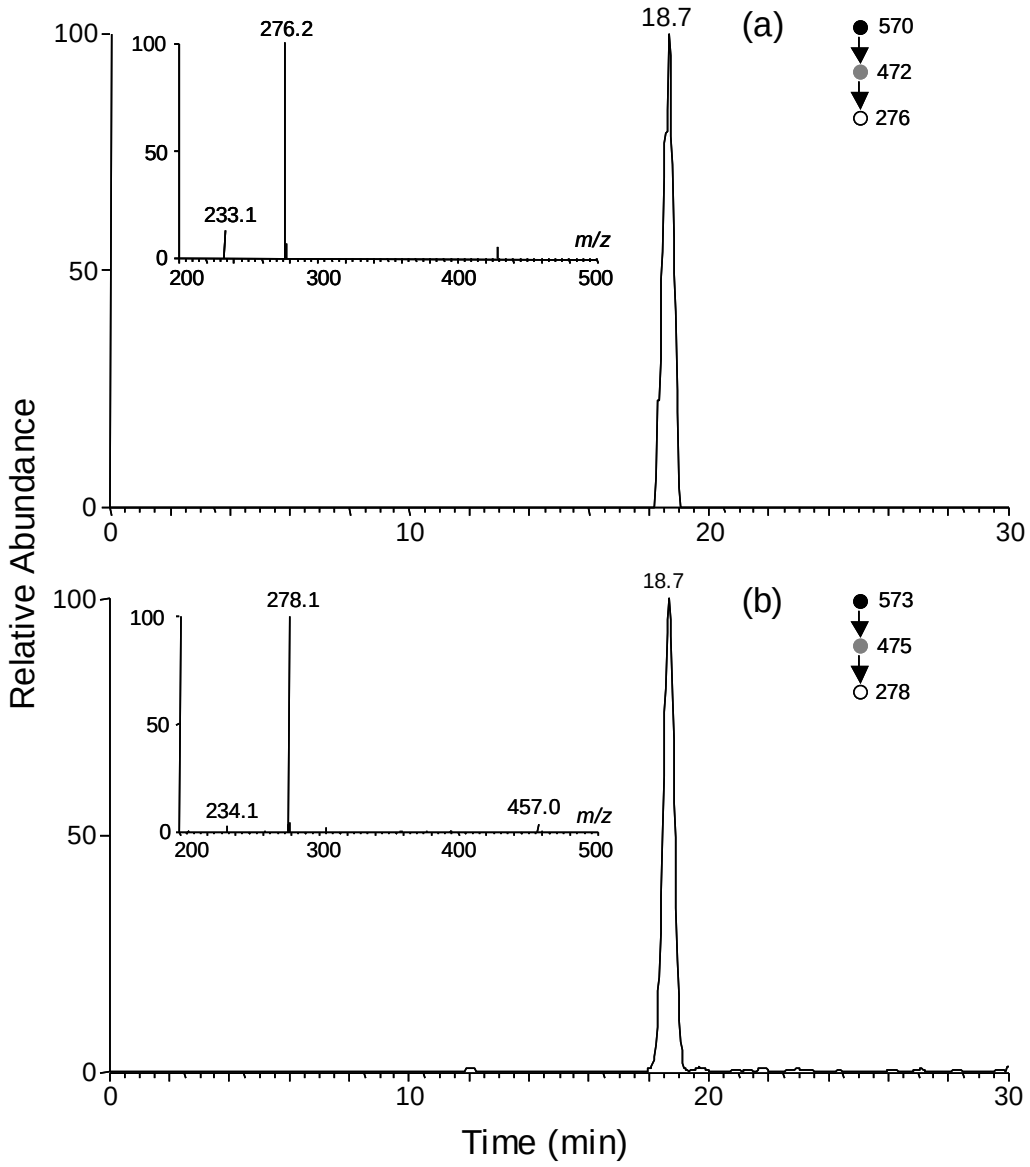

Figure 2-3. SICs for monitoring the *m/z* 570→472→276 (a, for unlabeled G[8-5m]) and *m/z* 573→475→278 (b, for labeled G[8-5m]T) transitions in the γ-ray treated DNA after enzymatic digestion. Shown in the insets are the MS^3 results for the unlabeled and labeled G[8-5m]T.

Other than the characteristic fragment ions found in the MS/MS for the internal standard and the analyte, ions from impurities were also present (Figure 2-2). To afford unambiguous detection of the lesion, we set up the instrument to monitor the further cleavage of the ion of *m/z* 472 to obtain a product-ion spectrum, i.e. MS^3, of high quality (Figure 2-3). In this respect, collisional activation of the ion of *m/z* 472 results in the formation of a dominant fragment ion of *m/z* 276, which is attributed to the protonated ion of the cross-linked nucleobase component. Moreover, the LC-MS^3 results revealed the dose-dependent formation of this lesion in Hela-S3 cells (Figure 2-4, and calibration curve is shown in Figure 2-5). It is worth noting that the rate for the formation of the G[8-5m]T lesion is approximately 0.050 lesions per 10^9 nucleosides per Gy, which is approximately 200 times lower than what we found for the rate of the formation of 5-formyl-2'-deoxyuridine (0.011 lesions per 10^6 nucleotides per Gy) under identical exposure conditions (*32*).

In vitro replication studies of the G[8-5m]T cross-link lesion

The G[8-5m]T-bearing 12mer ODN substrate was obtained from the 254 nm-irradiation of a 5-phenythiomethyl-2'-deoxyuridine-containing ODN following previously reported procedures (*29*). This lesion-carrying ODN was further ligated with a 5'-phosphorylated 8-mer ODN to construct a 20-mer lesion-containing substrate as a template for *in vitro* replication studies (Figure 2-1).

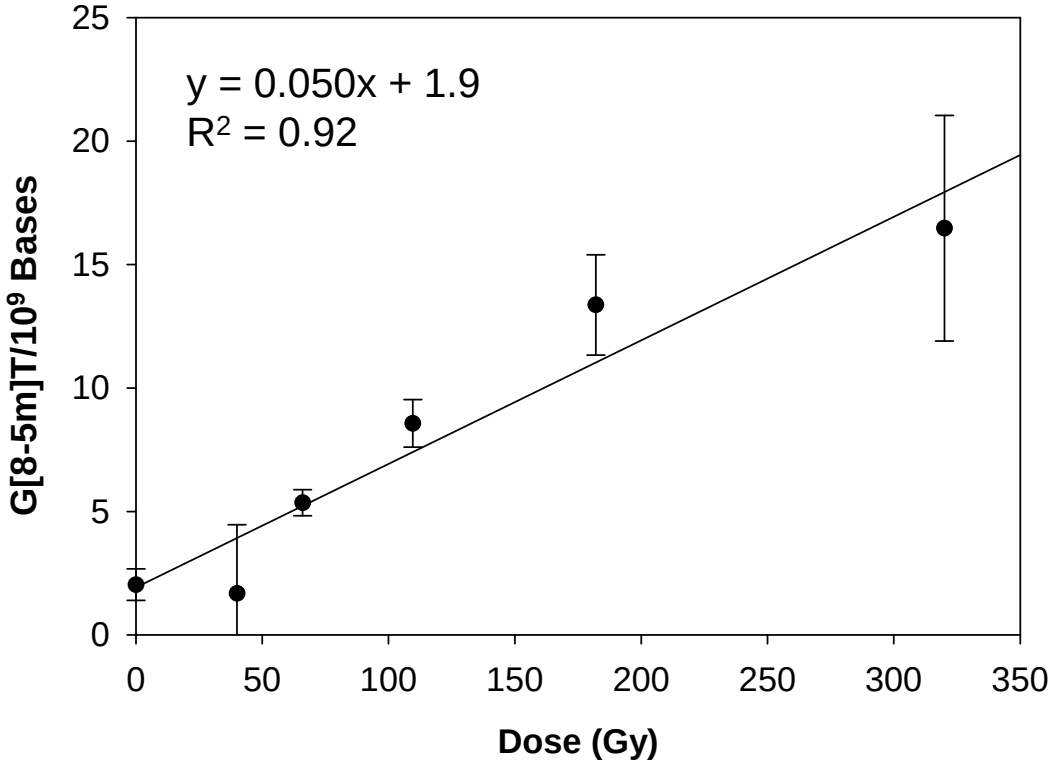

Figure 2-4. Dose-dependent formation of G[8-5m]T in Hela-S3 cells upon exposure to γ-rays. The values represent the means ± SD from three independent exposure and quantification experiments.

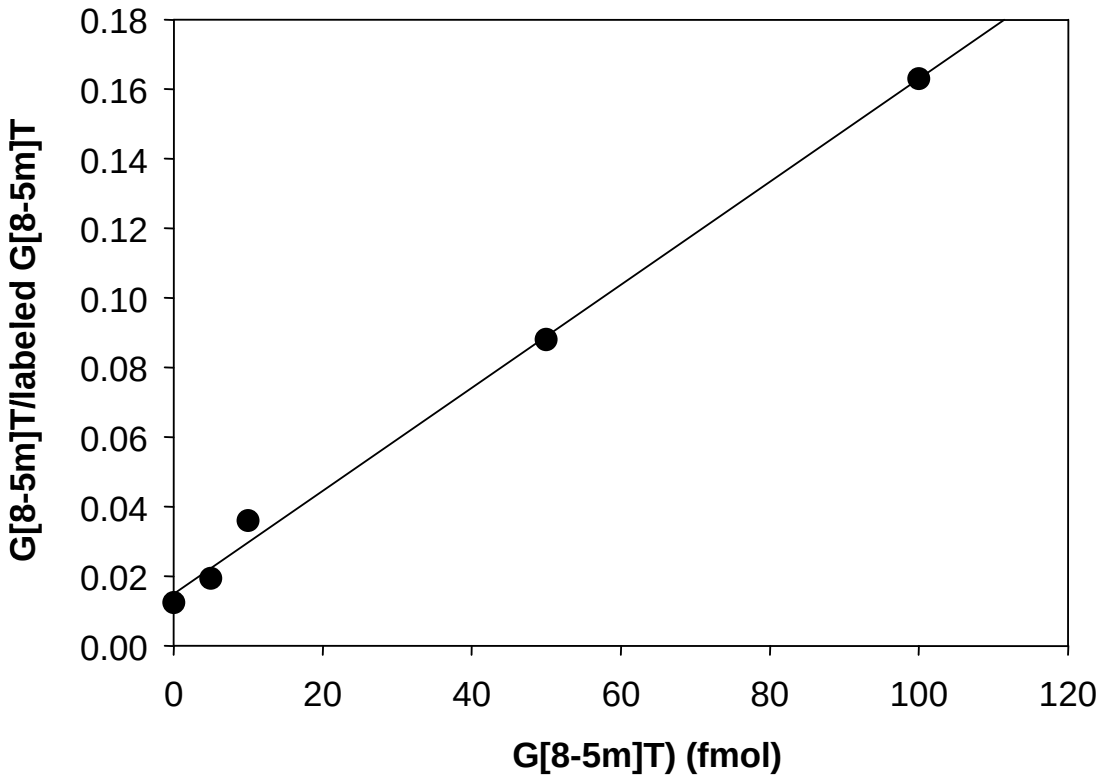

Figure 2-5. Calibration curves for the quantifications of G[8-5m]T. The amounts of labeled G[8-5m]T is 500 fmol

Firstly, we examined the general replication properties of G[8-5m]T by performing primer extension assays with Klenow fragment and yeast pol η. The primer extension assay results with Klenow fragment showed that, in the presence of all four dNTPs, the synthesis stopped mostly after the incorporation of the first nucleotide opposite the 3'-T of the lesion. A small portion of the reaction product carried an additional nucleotide opposite the 5'-G of the lesion, and only trace amount of full-length products could be detected (Figure 2-6a). This result is consistent with what was observed by Bellon and coworkers (*33*). On the other hand, the primer extension assay with yeast pol η showed that this polymerase can bypass partially the G[8-5m]T intrastrand cross-link when all four dNTPs are present. However, a considerable amount of short replication products with the addition of one or two nucleotides opposite the lesion site was also found (Figure 2-6b).

Next, we determined the steady-state kinetic parameters for nucleotide incorporation opposite the damaged nucleobases in the G[8-5m]T lesion-containing substrate and G and T in the undamaged substrate as a control by both Klenow fragment and yeast pol η (Figure 2-7 and Figure 2-8). The steady-state kinetic parameters for nucleotide incorporation mediated by the two polymerases are summarized in Tables 2-1&2-2).

Relative to the unmodified substrate, the efficiency for Klenow fragment to incorporate the correct nucleotide, dAMP, opposite the modified 3'-thymine moiety of G[8-5m]T was reduced by only two-fold. Decreased incorporation efficiencies, i.e. by 2-10 times, were also found for the other three nucleotides. Thus, the incorporation of

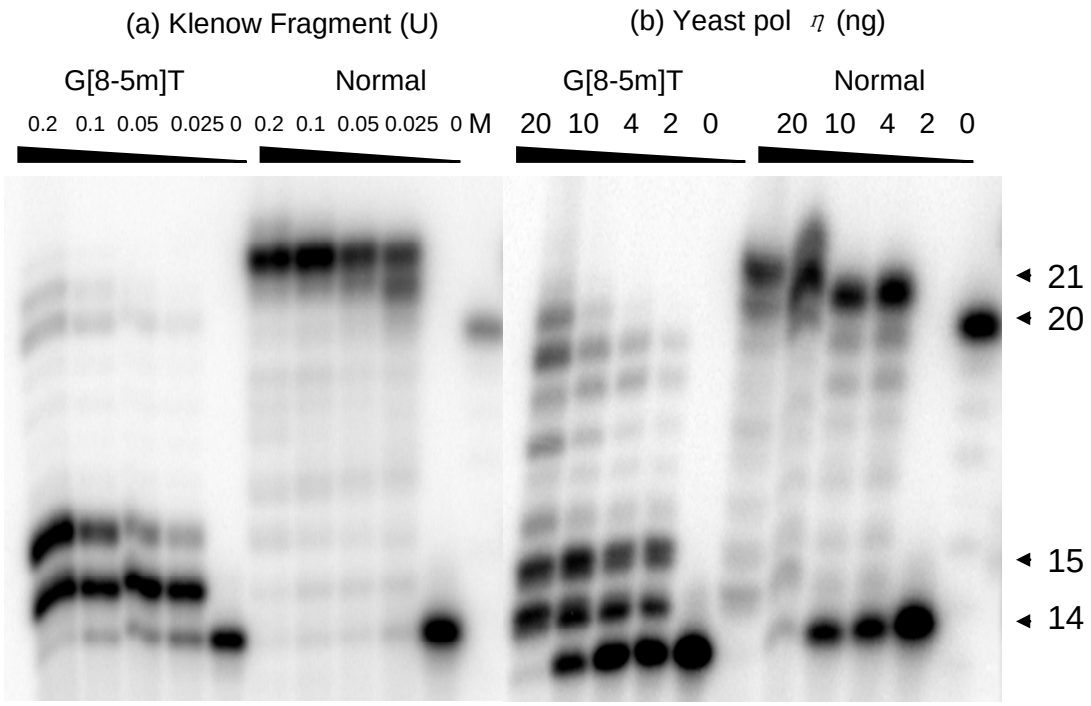

Figure 2-6. Primer extension assays for nucleotide incorporation opposite a G[8-5m]T-bearing substrate and its control undamaged substrate with exo$^-$-Klenow Fragment DNA polymerase (left two panels) and yeast pol η (right two panels). 5'-[^{32}P]-labeled d(GCTAGGATCATAGC) was used as primer. KF (exo-) and yeast pol η with the indicated concentrations was incubated with 10 nM substrate and 200 mM dNTPs at 37°C for 60 min.

Table 2-1. Fidelity of nucleotide incorporation by exo$^-$ Klenow fragment on a G[8-5m]T cross-link-containing substrate and the undamaged substrate as determined by steady-state kinetic measurements (K_m and V_{max} are average values based on three independent measurements).

dNTP	V_{max} *(nM/min)*	K_m *(nM)*	V_{max} / K_m	f_{inc}
G[8-5m]T-containing substrate (14mer Primer, 5'-GCTAGGATCATAGC-3')				
dATP	0.22±0.004	0.71±0.02	0.31	1.0
dGTP	0.29±0.02	$(6.0\pm1.0)\times10^{2}$	5.0×10^{-4}	2.0×10^{-3}
dCTP	0.28±0.01	$(4.0\pm0.4)\times10^{4}$	7.0×10^{-6}	2.3×10^{-5}
dTTP	0.24±0.004	$(1.07\pm0.05)\times10^{5}$	2.2×10^{-5}	7.1×10^{-5}
Undamaged DNA substrate (14mer Primer, 5'-GCTAGGATCATAGC-3')				
dATP	0.27±0.01	1.6±1.6	0.16	1.0
dGTP	0.17±0.04	$(4.0\pm1.0)\times10^{3}$	4.0×10^{-5}	2.0×10^{-4}
dCTP	0.16±0.01	$(5.2\pm0.5)\times10^{4}$	3.1×10^{-6}	1.9×10^{-5}
dTTP	0.10±0.001	$(3.0\pm0.3)\times10^{4}$	3.3×10^{-6}	2.0×10^{-5}

Table 2-2. Fidelity of nucleotide incorporation by yeast polymerase η on a G[8-5m]T cross-link-containing substrate and the undamaged substrate as determined by steady-state kinetic measurements (K_m and V_{max} are average values based on three independent measurements).

dNTP	V_{max} *(nM/min)*	K_m *(nM)*	V_{max}/K_m	f_{inc}
G[8-5m]T-containing substrate, 14mer primer (5'-GCTAGGATCATAGC-3')				
dATP	0.40±0.02	$(3.3\pm0.5)\times10^{2}$	1.2×10^{-3}	1.0
dGTP	0.45±0.06	$(1.7\pm0.3)\times10^{5}$	2.7×10^{-6}	2.3×10^{-3}
dCTP	0.20±0.01	$(8.0\pm2.0)\times10^{3}$	3.0×10^{-5}	2.0×10^{-2}
dTTP	0.38±0.07	$(1.2\pm0.4)\times10^{5}$	3.1×10^{-6}	2.6×10^{-3}
Undamaged substrates, 14mer primer (5'-GCTAGGATCATAGC-3')				
dATP	0.23±0.02	$(3.61\pm0.06)\times10$	6.4×10^{-3}	1.0
dGTP	0.33±0.02	$(5.9\pm0.5)\times10^{4}$	5.6×10^{-6}	8.8×10^{-4}
dCTP	0.32±0.04	$(4.1\pm0.1)\times10^{3}$	7.8×10^{-5}	1.2×10^{-2}
dTTP	0.53±0.01	$(1.1\pm0.9)\times10^{5}$	4.6×10^{-6}	7.2×10^{-4}
G[8-5m]T-containing substrate, 15mer primer (5'-GCTAGGATCATAGCA-3')				
dATP	0.48±0.03	$(5.0\pm0.6)\times10^{4}$	9.5×10^{-6}	1.0
dGTP	0.32±0.01	$(5.7\pm0.2)\times10^{4}$	5.6×10^{-6}	0.59
dCTP	0.47±0.05	$(2.3\pm0.2)\times10^{6}$	2.1×10^{-7}	2.2×10^{-2}
dTTP	0.33±0.02	$(6.2\pm0.4)\times10^{5}$	5.3×10^{-7}	5.6×10^{-2}
Undamaged substrate, 15mer primer (5'-GCTAGGATCATAGCA-3')				
dATP	0.97±0.08	$(5.2\pm0.3)\times10^{5}$	1.9×10^{-6}	4.8×10^{-5}
dGTP	1.57±0.01	$(5.8\pm0.1)\times10^{5}$	2.7×10^{-6}	7.0×10^{-5}
dCTP	0.36±0.04	9.2±2.5	3.9×10^{-2}	1.0
dTTP	0.36±0.04	$(1.8\pm0.3)\times10^{4}$	2.0×10^{-5}	5.1×10^{-4}

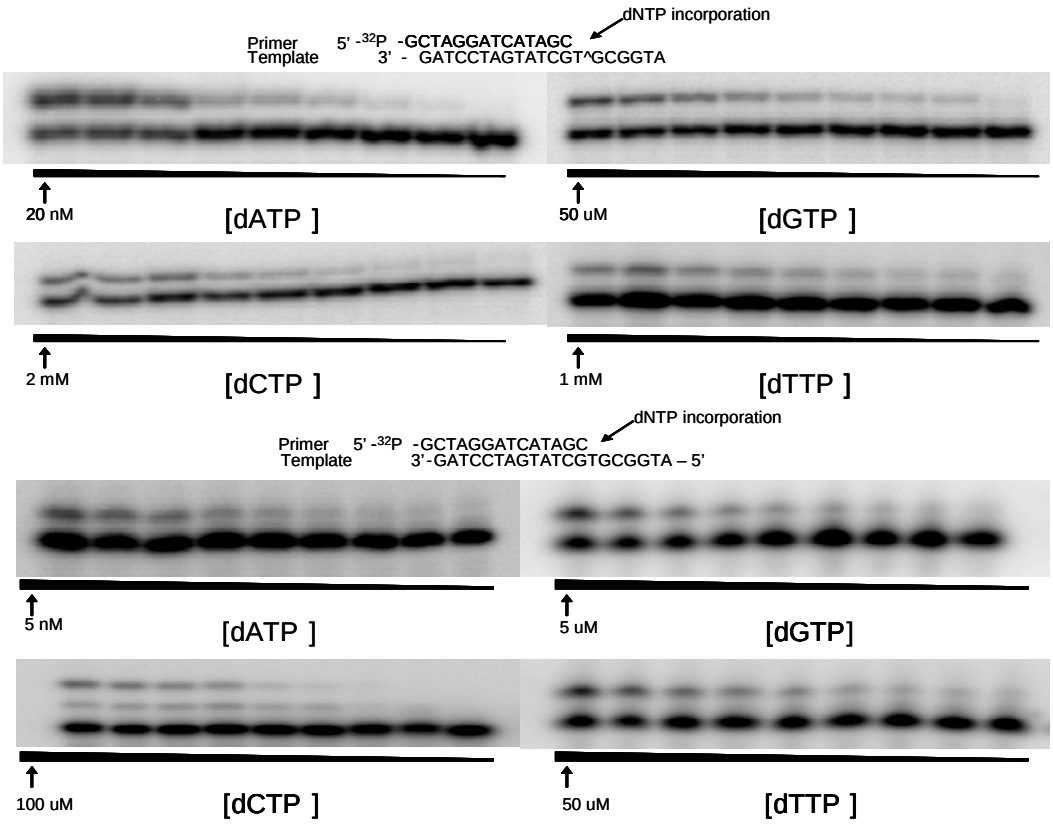

Figure 2-7. Steady-state kinetic measurements for the incorporation of dAMP, dGMP, dCMP and dTMP opposite the thymidine portion of G[8-5m]T (top panels) or the thymidine at an undamaged GT site (bottom panels). Exo$^-$-Klenow Fragment (0.1 U) was incubated with 10 nM DNA substrate at room temperature for 10 min. The highest dNTP concentration is shown in the figure, and the concentration ratio of dNTP between adjacent lanes was 0.5-0.6.

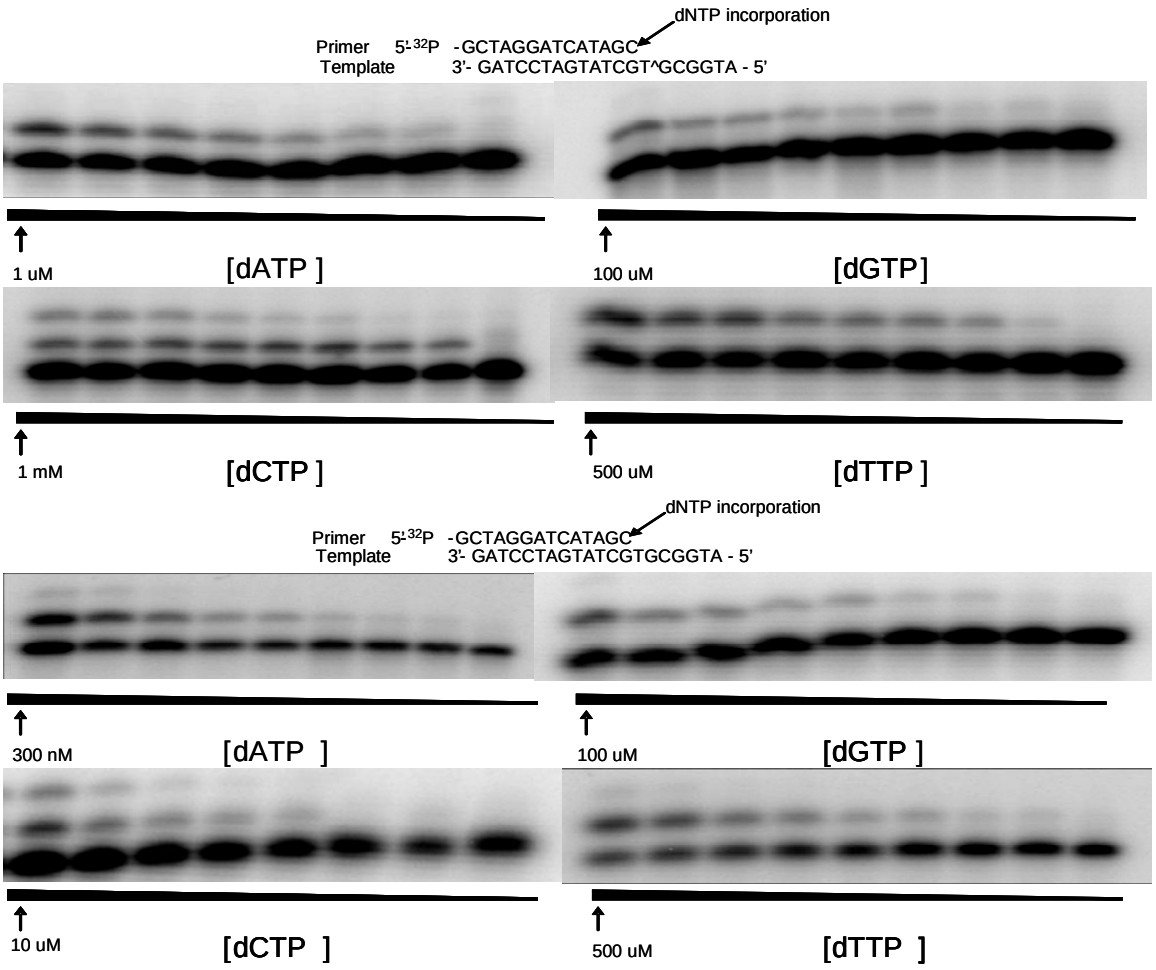

Figure 2-8. Steady-state kinetic measurements for incorporation of dAMP, dGMP, dCMP and dTMP opposite the thymidine portion of G[8-5m]T (top) or the thymidine at an undamaged GT site (bottom). Yeast pol*η* (5 ng) was incubated with 10 nM DNA substrate at room temperature for 10 minutes. The highest dNTP concentration is shown in the figure, and the concentration ratio of dNTP between adjacent lanes was 0.5 - 0.6.

dAMP is still much more preferred over those of the other three nucleotides in the presence of the lesion (Table 2-1). However, when we attempted to measure the steady-state kinetic parameters for nucleotide incorporation opposite the 5'-guanine moiety of the lesion with the Klenow fragment, we either could not detect any nucleotide incorporation or failed to derive valid kinetic parameters with applicable concentration range (< 2 mM) of dNTPs. It indicates that, even though one nucleotide can be incorporated opposite the 3'-T moiety, DNA synthesis is blocked mostly at the 5'-G moiety of the G[8-5m]T lesion. This result is consistent with results obtained from the primer extension assay (vide supra).

We further measured the steady-state kinetic parameters for nucleotide incorporation catalyzed by yeast pol η. When the data for the lesion-containing- and undamaged substrates were compared, we found that the presence of the cross-link lesion diminished the insertion efficiencies of all four dNTPs in the position opposite the 3'-T moiety of the lesion by nearly 1-5 times (Table 2-2). As a result, pol η still inserted dAMP opposite the 3'-T of the lesion most preferentially. The incorporation efficiency of the correct nucleotide, dCMP, opposite the 5'-G, however, is markedly reduced, by approximately 5 orders of magnitude, with the presence of the cross-link lesion (a 15mer primer with a dA at the 3' terminus was used for this measurement, Table 2-2). On the other hand, the efficiencies for the insertion of dAMP and dGMP opposite the 5'-G of the lesion became slightly higher than those for the incorporation of these two nucleotides opposite an unmodified guanine. Consequently, the fidelity of nucleotide incorporation opposite the 5'-G moiety of the lesion was significantly impaired. The insertion of dAMP

or dGMP was slightly favored over that of dCMP or dTMP. This result indicates that, during translesion synthesis by yeast pol *η,* the existence of G[8-5m]T intrastrand cross-link lesion in the template may lead to the incorporation of a dAMP or dGMP opposite the 5'-G moiety instead of the correct dCMP, thereby resulting in G → T and G → C transversions.

It is worth emphasizing that, even though yeast pol *η* can synthetically bypass both nucleobases of the cross-link lesion, in addition to the compromised fidelity, the efficiency for nucleotide incorporation opposite the 5'-G dropped by approximately 4000 times. Therefore, the presence of the G[8-5m]T cross-link lesion decreases both the efficiency and the fidelity of nucleotide incorporation mediated by yeast pol *η*.

Discussion

By using LC-MS/MS with the standard isotope dilution method, we demonstrated, for the first time, that the G[8-5m]T could be induced in Hela-S3 cells upon exposure to γ-rays. This result, combined with our previous finding that the lesion could be generated in calf thymus DNA upon treatment with Fenton reagents under aerobic conditions (*18*), underlies the biological significances of this type of lesions.

As we reported previously, a photochemical approach enabled us to obtain well-characterized intrastrand cross-link-containing ODNs (*29*). In this context, the use of ODN substrates bearing a structurally defined lesion for *in vitro* replication studies facilitates us to understand the biological implications of these lesions at the molecular level. Examining the behaviors of both a replicative polymerase and translesion synthesis

polymerase during DNA replication can provide us with a comprehensive view of the mutagenic properties of a DNA lesion. Our results revealed that both Klenow fragment and yeast pol *η* could incorporate the correct nucleotide, dAMP, opposite the 3'-T of the lesion with a relatively high efficiency. Thus, the hydrogen bonding properties of the 3'-T might be conferred during nucleotide incorporation by both polymerases, though Klenow fragment belongs to the high-fidelity A family of DNA polymerases, which adopt constrained active sites (*34, 35*). On the other hand, nucleotide incorporation by Klenow fragment opposite the 5'-G was completely abolished by the presence of the G[8-5m]T lesion. In addition, the 5'-G portion of the cross-link lesion conferred significant drop in efficiencies for nucleotide incorporation by yeast pol *η*. Moreover, yeast pol *η*-mediated nucleotide insertion opposite the 5'-G by yeast pol *η* was error-prone, with the dGMP and dAMP being incorporated much more efficiently than the correct nucleotide, dCMP. We reason that the presence of the cross-link lesion may lead to a structural distortion to duplex DNA, which may render the hydrogen-bonding property of the 5'-guanine portion not to be recognized by yeast pol *η* during nucleotide insertion. Indeed, molecular modeling results showed that the *N*-glycosidic linkage of the 3' nucleoside of the cross-link assumes an *anti* configuration, whereas that of the 5' nucleoside exhibits a *syn* configuration (Figure 2-9). Under such circumstances, purine nucleotides can conceivably be incorporated opposite the 5'-G more efficiently than pyrimidine nucleotides because the former nucleotides exhibit a stronger stacking interaction with the 3' nucleotide of the primer than the latter nucleotides (*36*). In this context, it is worth noting that the efficiencies and specificities of nucleotide

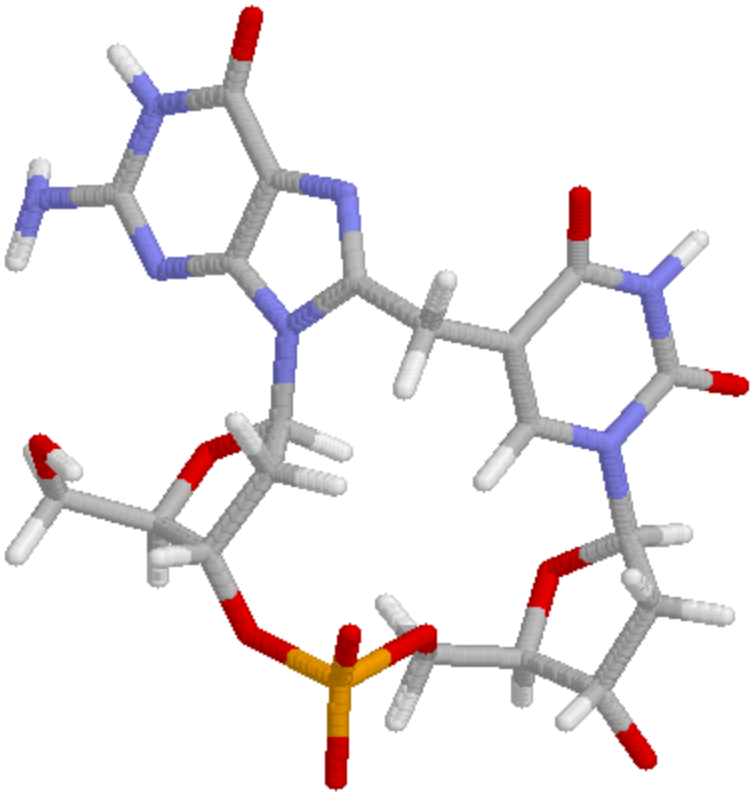

Figure 2-9. Optimized structure of G[8-5m]T obtained by the semi-empirical PM3 method.

incorporation opposite G[8-5m]T by yeast pol η are consistent with our previous observations with the G[8-5]C lesion (*17*).

Thermodynamic studies showed that the G[8-5m]T cross-link lesion could cause distortion to duplex DNA to an extent between two DNA photoproducts, i.e. T[6-4]T and T[c,s]T (*25*). G[8-5m]T can also be recognized by the *Escherichia coli* UvrABC nuclease, suggesting that this lesion may be a good substrate for the NER pathway (*29, 37*). Therefore, the presence of the lesion is expected to have significant biological consequences, especially for people suffering from genetic diseases associated with deficiency in NER, i.e. *Xeroderma pigmentosum* (XP) (*38*). XP patients usually exhibit a progressive, yet massive, neuron loss with accompanying mental deterioration over (*39*). The accumulation of oxidative intrastrand cross-link lesions may contribute to the pathophysiological symptoms of XP patients.

The intracellular concentrations of iron and copper ions can be dramatically elevated under oxidative stress conditions via the release of these ions from iron- or copper-storage proteins (*40, 41*). In humans, genetic hemochromatosis and Wilson's disease induce abnormal accumulation of iron and copper, respectively, in various organs. Bulky DNA lesions were found in the liver of patients with Wilson's disease and primary hemochromatosis (*42*). On the grounds that oxidative intrastrand cross-link lesions could be induced in DNA by iron- or copper-mediated Fenton-type reactions (*18, 43*), we reason that this type of lesion may also play a role in the pathological conditions associated with high intracellular concentrations of these transition metal ions.

References:

(1) Lindahl, T. (1999) DNA lesions generated in vivo by reactive oxygen species, their accumulation and repair. *NATO ASI Ser., Ser. A 302*, 251-257.

(2) Finkel, T., and Holbrook, N. J. (2000) Oxidants, oxidative stress and the biology of ageing. *Nature 408*, 239-47.

(3) Marnett, L. J. (2000) Oxyradicals and DNA damage. *Carcinogenesis 21*, 361-70.

(4) Dizdaroglu, M., Jaruga, P., Birincioglu, M., and Rodriguez, H. (2002) Free radical-induced damage to DNA: mechanisms and measurement. *Free Radic. Biol. Med. 32*, 1102-15.

(5) Box, H. C., Budzinski, E. E., Dawidzik, J. D., Wallace, J. C., Evans, M. S., and Gobey, J. S. (1996) Radiation-induced formation of a crosslink between base moieties of deoxyguanosine and thymidine in deoxygenated solutions of d(CpGpTpA). *Radiat. Res. 145*, 641-3.

(6) Box, H. C., Budzinski, E. E., Dawidzik, J. B., Gobey, J. S., and Freund, H. G. (1997) Free radical-induced tandem base damage in DNA oligomers. *Free Radic. Biol. Med. 23*, 1021-30.

(7) Box, H. C., Budzinski, E. E., Dawidzik, J. B., Wallace, J. C., and Iijima, H. (1998) Tandem lesions and other products in X-irradiated DNA oligomers. *Radiat. Res. 149*, 433-9.

(8) Budzinski, E. E., Dawidzik, J. B., Rajecki, M. J., Wallace, J. C., Schroder, E. A., and Box, H. C. (1997) Isolation and characterization of the products of anoxic irradiation of d(CpGpTpA). *Int. J. Radiat. Biol. 71*, 327-36.

(9) Romieu, A., Bellon, S., Gasparutto, D., and Cadet, J. (2000) Synthesis and UV photolysis of oligodeoxynucleotides that contain 5- (phenylthiomethyl)-2'-deoxyuridine: a specific photolabile precursor of 5-(2'-deoxyuridilyl)methyl radical. *Org. Lett. 2*, 1085-8.

(10) Bellon, S., Ravanat, J. L., Gasparutto, D., and Cadet, J. (2002) Cross-linked thymine-purine base tandem lesions: synthesis, characterization, and measurement in gamma-irradiated isolated DNA. *Chem. Res. Toxicol. 15*, 598-606.

(11) Zeng, Y., and Wang, Y. (2004) Facile formation of an intrastrand cross-link lesion between cytosine and guanine upon Pyrex-filtered UV light irradiation of d(^{Br}CG) and duplex DNA containing 5-bromocytosine. *J. Am. Chem. Soc. 126*, 6552-6553.

(12) Zhang, Q., and Wang, Y. (2003) Independent generation of 5-(2'-deoxycytidinyl)methyl radical and the formation of a novel crosslink lesion between 5-methylcytosine and guanine. *J. Am. Chem. Soc. 125*, 12795-802.

(13) Zhang, Q., and Wang, Y. (2004) Independent generation of the 5-hydroxy-5,6-dihydrothymidin-6-yl radical and its reactivity in dinucleoside monophosphates. *J. Am. Chem. Soc. 126*, 13287-97.

(14) Zhang, Q., and Wang, Y. (2005) Generation of 5-(2'-deoxycytidyl)methyl radical and the formation of intrastrand cross-link lesions in oligodeoxyribonucleotides. *Nucleic Acids Res. 33*, 1593-1603.

(15) Liu, Z. J., Gao, Y., and Wang, Y. S. (2003) Identification and characterization of a novel cross-link lesion in d(CpC) upon 365-nm irradiation in the presence of 2-methyl-1,4-naphthoquinone. *Nucleic Acids Research 31*, 5413-5424.

(16) Liu, Z. J., Gao, Y., Zeng, Y., Fang, F., Chi, D., and Wang, Y. S. (2004) Isolation and characterization of a novel cross-link lesion in d(CpC) induced by one-electron photooxidation. *Photochemistry and Photobiology 80*, 209-215.

(17) Gu, C., and Wang, Y. (2004) LC-MS/MS identification and yeast polymerase eta bypass of a novel gamma-irradiation-induced intrastrand cross-link lesion G[8-5]C. *Biochemistry 43*, 6745-50.

(18) Hong, H., Cao, H., Wang, Y., and Wang, Y. (2006) Identification and quantification of a guanine-thymine intrastrand cross-link lesion induced by Cu(II)/H_2O_2/ascorbate. *Chem. Res. Toxicol. 19*, 614-621.

(19) von Sonntag, C. (1987) *The Chemical Basis of Radiation Biology*, Taylor & Francis, London.

(20) Friedberg, E. C., Walker, G. C., and Siede, W. (1995) *DNA Repair and Mutagenesis*, ASM Press, Washington, D.C.

(21) Feig, D. I., Reid, T. M., and Loeb, L. A. (1994) Reactive oxygen species in tumorigenesis. *Cancer Res. 54*, 1890s-1894s.

(22) Lee, D. H., O'Connor, T. R., and Pfeifer, G. P. (2002) Oxidative DNA damage induced by copper and hydrogen peroxide promotes CG-->TT tandem mutations at methylated CpG dinucleotides in nucleotide excision repair-deficient cells. *Nucleic Acids Res. 30*, 3566-73.

(23) Reid, T. M., and Loeb, L. A. (1993) Tandem double CC-->TT mutations are produced by reactive oxygen species. *Proc. Natl. Acad. Sci. USA 90*, 3904-7.

(24) Newcomb, T. G., Allen, K. J., Tkeshelashvili, L., and Loeb, L. A. (1999) Detection of tandem CC-->TT mutations induced by oxygen radicals using mutation-specific PCR. *Mutat Res. 427*, 21-30.

(25) Gu, C., and Wang, Y. (2005) Thermodynamic and in-vitro replication studies of an intrastrand crosslink lesion G[8-5]C. *Biochemistry 44*, 8883-8889.

(26) Johnson, R. E., Prakash, S., and Prakash, L. (1999) Efficient bypass of a thymine-thymine dimer by yeast DNA polymerase, Poleta. *Science 283*, 1001-4.

(27) Masutani, C., Kusumoto, R., Yamada, A., Dohmae, N., Yokoi, M., Yuasa, M., Araki, M., Iwai, S., Takio, K., and Hanaoka, F. (1999) The *XPV* (xeroderma pigmentosum variant) gene encodes human DNA polymerase eta. *Nature 399*, 700-4.

(28) Hong, H., and Wang, Y. (2005) Formation of intrastrand cross-link products between cytosine and adenine from UV irradiation of d(^{Br}CA) and duplex DNA containing a 5-bromocytosine. *J. Am. Chem. Soc. 127*, 13969-77.

(29) Gu, C., Zhang, Q., Yang, Z., Wang, Y., Zou, Y., and Wang, Y. (2006) Recognition and incision of oxidative intrastrand cross-link lesions by UvrABC nuclease. *Biochemistry 45*, 10739-46.

(30) Goodman, M. F., Creighton, S., Bloom, L. B., and Petruska, J. (1993) Biochemical basis of DNA replication fidelity. *Crit. Rev. Biochem. Mol. Biol. 28*, 83-126.

(31) Creighton, S., Bloom, L. B., and Goodman, M. F. (1995) Gel fidelity assay measuring nucleotide misinsertion, exonucleolytic proofreading, and lesion bypass efficiencies. *Methods Enzymol. 262*, 232-56.

(32) Hong, H., and Wang, Y. (2007) Derivatization with Girard reagent T combined with LC-MS/MS for the sensitive detection of 5-formyl-2'-deoxyuridine in cellular DNA. *Anal. Chem. 79*, 322-6.

(33) Bellon, S., Gasparutto, D., Saint-Pierre, C., and Cadet, J. (2006) Guanine-thymine intrastrand cross-linked lesion containing oligonucleotides: from chemical synthesis to in vitro enzymatic replication. *Org. Biomol. Chem. 4*, 3831-3837.

(34) Ito, J., and Braithwaite, D. K. (1991) Compilation and alignment of DNA polymerase sequences. *Nucleic Acids Res. 19*, 4045-57.

(35) Li, Y., Dutta, S., Doublie, S., Bdour, H. M. d., Taylor, J.-S., and Ellenberger, T. (2004) Nucleotide insertion opposite a *cis-syn* thymine dimer by a replicative DNA polymerase from bacteriophage T7. *Nat. Struct. Mol. Biol. 11*, 784-790.

(36) Saenger, W. (1984) *Principles of Nucleic Acid Structure*, Springer-Verlag New York Inc., New York.

(37) Yang, Z., Colis, L. C., Basu, A. K., and Zou, Y. (2005) Recognition and incision of gamma-radiation-induced cross-linked guanine-thymine tandem lesion G[8,5-Me]T by UvrABC nuclease. *Chem. Res. Toxicol. 18*, 1339-46.

(38) Berneburg, M., and Lehmann, A. R. (2001) Xeroderma pigmentosum and related disorders: defects in DNA repair and transcription. *Adv Genet 43*, 71-102.

(39) Cleaver, J. E., and Kraemer, K. H. (1989) in *The Metabolic Basis of Inherited Disease* (Scriver, C., Beaudet, A. L., Sly, W. S., and Vale, D., Eds.) pp 2949-2971, McGraw-Hill, New York.

(40) Reif, D. W. (1992) Ferritin as a source of iron for oxidative damage. *Free Radic. Biol. Med. 12*, 417-427.

(41) Calderaro, M., Martins, E. A. L., and Meneghini, R. (1993) Oxidative stress by menadione affects cellular copper and iron homeostasis. *Mol. Cell. Biochem. 126*, 17-23.

(42) Carmichael, P. L., Hewer, A., Osborne, M. R., Strain, A. J., and Phillips, D. H. (1995) Detection of bulky DNA lesions in the liver of patients with Wilson's disease and primary hemochromatosis. *Mutat. Res. 326*, 235-243.

(43) Cao, H., and Wang, Y. (2007) Quantification of oxidative single-base and intrastrand cross-link lesions in unmethylated and CpG-methylated DNA induced by Fenton-type reagents. *Nucleic Acids Res. 35*, in press (DOI: 10.1093/nar/gkm497).

CHAPTER 3

In-vitro Replication and Repair Studies of Tandem Lesions Containing Neighboring Thymidine Glycol and 8-Oxo-7,8-dihydro-2'-deoxyguanosine

Introduction

It has been demonstrated that other than single-nucleobase lesions, clustered DNA lesions, where two or more damaged nucleosides are located within 1-2 helical turns of DNA, can form upon interaction with ROS, particularly those formed upon exposure to ionizing radiation (*1-3*). In addition, complex lesions are often more difficult to repair than when they are present alone (*4-11*). Among the complex DNA lesions, tandem lesions, consisting of two neighboring damaged nucleotides on the same DNA strand, could be initiated from a single hydroxyl radical attack and, depending on the nature of the tandem lesions, molecular oxygen may or may not be involved in their formation (*12-20*).

Some lesions, when present in replicating DNA, can lead to replication fork stalling and/or give rise to mutations. Thymidine glycol blocks effectively DNA replication, but is not mutagenic under most conditions (*21*); on the other hand, 8-oxodG does not block appreciably the DNA replication and it can result in significant frequencies of G→T transversion mutation (*22, 23*). Tg could also arise from the deamination of 5-methylcytosine glycol (*24*), an oxidative lesion formed on 5-methylcytosine (*25*). In this respect, cytosine at a CpG dinucleotide site can be methylated, and approximately 5% cytosine residues are methylated in the human genome (*26*). The methylated CpGs are

mutational hot spots in the human *p53* tumor suppressor gene (*27*). Previously we found that oxidative intrastrand cross-link lesions could form at methylated CpG sites, which may account for the mCG→TT tandem double mutations induced by Fenton type reagents (*28*). The 5'-Tg-(8-oxodG)-3' tandem lesion may also emanate from ROS attack at methylated CpG site thereby contributing to CpG mutagenesis. Along this line, a relatively high frequency of mCG→TT mutation was observed after the Cu^{2+}/H_2O_2/ascorbate-treated pSP189 shuttle vector was propagated in nucleotide excision repair (NER)-deficient human XPA cells (*27*).

Several studies have been carried out to assess the cytotoxic and mutagenic properties of clustered DNA lesions. Our previous *in-vitro* replication studies on several intrastrand cross-link lesions, i.e. G[8-5]C, and G[8-5m]T (In Chapter 2), showed that they can either stall DNA replication performed by high-fidelity replicative polymerases or give rise to mutations by a translesion synthesis polymerase, yeast polymerase η (*29-31*). In addition, altered mutagenic potential was found for 8-oxodG when it is present in a clustered DNA damage site (*11, 32, 33*).

The base excision repair (BER) pathway can allow for the efficient and accurate repair of ROS-induced single-nucleobase lesions (*34*). However, when these lesions are present as components of complex lesions, the repair by the BER enzymes becomes difficult. A number of studies showed that the excision, by purified BER enzymes or by cell extracts, of clustered DNA lesions is indeed compromised, and the effects vary with the types of lesions involved and their spatial distribution (*5-8, 11, 35*).

Building upon our successful synthesis of oligodeoxyribonucleotides (ODNs) containing neighboring Tg and 8-oxodG (*36*), here we examined how the presence of the 5'-Tg-(8-oxodG)-3' and 5'-(8-oxodG)-Tg-3' tandem lesions in template DNA perturbs nucleotide incorporation by two DNA polymerases. One is a replicative DNA polymerase, the exonuclease-free Klenow fragment of *E. coli* DNA polymerase I, and the other is a member of the "Y" superfamily polymerases, *Sacchramyces cerevisiae* DNA polymerase η (pol η). Pol η was reported to bypass efficiently many DNA lesions, including 8-oxodG and Tg (*37, 38*). We also assessed how these two types of tandem lesions are recognized by human 8-oxoguanine-DNA glycosylase (hOGG1) and *E. coli* endonuclease III.

Experimental

Materials

All unmodified ODNs used in this study were purchased from Integrated DNA Technologies (Coralville, IA). [γ-^{32}P]ATP was obtained from Amersham Biosciences (Piscataway, NJ). The Klenow fragment (3'→5' exo$^-$) of *E. coli* DNA polymerase I and endonuclease III were from New England Biolabs (Ipswich, MA). One unit of Endonuclease III is defined as the amount of enzyme required to cleave 1 pmol of a 34-mer ODN duplex containing a single abasic site in a total reaction volume of 10 μl in 1 hour at 37°C in the Endonuclease III reaction buffer containing 10 pmol of fluorescently labeled ODN duplex. Human AP endonuclease 1 (APE1) was purchased from Enzymax (Lexington, KY). Yeast pol η and hOGG1 were expressed and purified following previously published procedures (*39, 40*).

Preparation of Substrates for In-vitro Replication and Repair Studies

The ODNs containing the *cis*-(*5R,6S*) diastereomer of Tg, an 8-oxodG, or both were synthesized previously (sequences shown in Table 3-1) (*36*). The dodecameric lesion-bearing substrate, e.g., d(ATGGCTgG*GCTAT) ("G*" represents 8-oxodG), was ligated with the 5'-phosphorylated d(GATCCTAG) in the presence of a template ODN, d(CCGCTCCCTAGGATCATAGCCAGCCAT), following previously described procedures (*29*). The desired lesion-containing 20-mer ODN was purified by using 20% denaturing polyacrylamide gel electrophoresis (PAGE) and desalted by ethanol precipitation. The purity of the product was further confirmed by PAGE analysis.

Primer Extension Assays

The 20-mer lesion-containing ODNs or the unmodified template (20 nM) were annealed with a 5' ^{32}P-labeled 14- or 15-mer primer (10 nM). To the duplex mixture were added all four dNTPs at a concentration of 200 μM each and a DNA polymerase. The reaction was carried out in a buffer containing 10 mM Tris-HCl (pH 7.5), 50 mM NaCl, 10 mM $MgCl_2$, and 1 mM dithiothreitol (DTT) at 37 °C for 60 min. The amounts of the polymerases are indicated in the figures. The reaction was terminated by adding a 2 volume excess of formamide gel-loading buffer [80% formamide, 10 mM EDTA (pH 8.0), 1 mg/mL xylene cyanol, and 1 mg/mL bromophenol blue]. The products were resolved on 20% (29:1) cross-linked polyacrylamide gels containing 8 M urea. Gel band intensities for the substrates and products were quantified by using a Typhoon 9410 variable-mode imager (Amersham Biosciences Co.).

Table 3-1. The sequences of ODNs used for enzymatic ligation ("G*" represents an 8-oxodG).

ODNs	Sequences
1, 5'-Tg-(8-oxodG)-3'	5'-ATG GCTg G*GC TAT-3'
2, 5'-(8-oxodG)-Tg-3'	5'-ATG GCG* TgGC TAT-3'
3, 5'-(8-oxodG)-dT-3'	5'-ATG GCG* TGC TAT-3'
4, 5'-Tg-dG-3'	5'-ATG GCG TgGC TAT-3'
5, control	5'-ATG GCG TGC TAT-3'

Steady-state Kinetic Measurements

The steady-state kinetic analyses were performed as described previously (*41*). In this measurement, the primer-template complex (10 nM) was incubated with either Klenow fragment (5 ng) or yeast pol η (5 ng) in the presence of an individual dNTP at various concentrations as indicated in the figures. The reaction was carried out at room temperature with the same reaction buffer as described for the primer extension assays. The dNTP concentration was optimized for different insertion reactions to allow for less than 20% primer extension. The observed rate of nucleotide incorporation (V_{obs}) was plotted as a function of dNTP concentration, and the apparent K_m and V_{max} steady-state kinetic parameters for the incorporation of both the correct and incorrect nucleotides were determined by fitting the rate data with the Michaelis-Menten equation:

$$V_{obs} = \frac{V_{max} \times [dNTP]}{K_m + [dNTP]}$$

The k_{cat} values were then calculated by dividing the V_{max} values with the concentration of the polymerase used. The efficiency of nucleotide incorporation was determined by the ratio of k_{cat}/K_m, and the fidelity of nucleotide incorporation was calculated by the frequency of misincorporation (f_{inc}) with the following equation:

$$f_{inc} = \frac{(k_{cat} / K_m)_{incorrect}}{(k_{cat} / K_m)_{correct}}$$

BER Assays

The 20mer 5' ^{32}P-labeled lesion-containing ODNs or a control substrate were annealed with their respective complementary strands by heating the mixture to 90 °C

and cooling slowly to room temperature in a solution containing 10 mM Tris-HCl (pH 7.5), 100 mM NaCl, and 1 mM EDTA. The duplex (10 nM) was incubated with either hOGG1 or endonuclease III in a 10-μL buffer solution at 37 °C for 30 min. The amounts of enzyme are shown in the figures. A buffer containing 10 mM Tris-HCl (pH 7.5), 50 mM NaCl, 10 mM $MgCl_2$ and 1 mM DTT, along with 1 ng of APE1, was used for the hOGG1 cleavage assays, and a buffer bearing 20 mM Tris-HCl (pH 8.0), 1 mM EDTA, and 1 mM DTT was employed for endonuclease III reactions. The reaction products were mixed with formamide gel-loading buffer, heated at 90 °C for 20 min to cleave the apurinic/apyrimidinic sites (AP sites), and the resulting products were resolved by 20% denaturing polyacrylamide gels. The level of the BER enzyme-induced cleavage was quantified based on the gel band intensities for the substrates and products by phosphorimaging analysis.

Results

To assess how the tandem 5'-Tg-(8-oxodG)-3' and 5'-(8-oxodG)-Tg-3' lesions perturb DNA replication and how they are recognized by BER enzymes, we first constructed 12-mer ODN substrates carrying the *cis*-(*5R,6S*) diastereomer of Tg, an 8-oxodG, or both (Table 3-1) (*36*). These lesion-containing ODNs were further ligated with a 5'-phosphorylated 8-mer ODN to afford 20-mer lesion-containing substrates for *in-vitro* replication and repair studies (Figure 3-1).

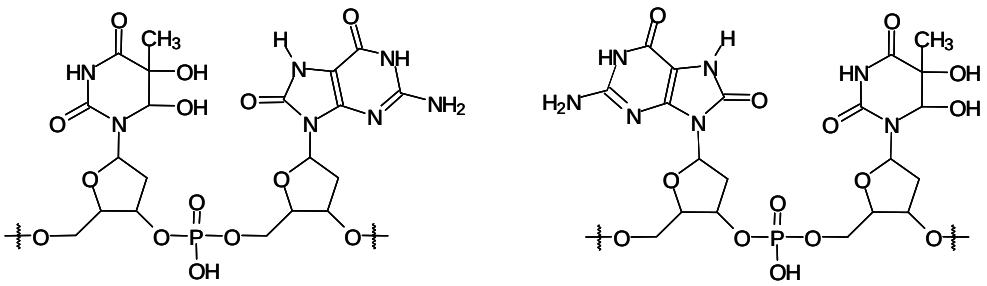

5'- ATG GC*X* *Y*GC TAT GAT CCT AG – 3'

XY = Tg-(8-oxodG), (8-oxodG)-Tg, dG-Tg, (8-oxodG)-dT or dG-dT

Figure 3-1. The structures of the 5'-Tg-(8-oxodG)-3' and 5'-(8-oxodG)-Tg-3' tandem lesions, and the sequences of the 20-mer lesion-containing substrates used in the present *in-vitro* replication and repair studies.

Increased Blocking Effects Induced by Tandem Lesions during DNA Replication in vitro

First, we performed primer extension assays on the four lesion-bearing substrates and an undamaged control substrate with Klenow fragment and yeast pol η. The results with the Klenow fragment showed that, in the presence of all four dNTPs, the synthesis catalyzed by the Klenow fragment stopped mostly after incorporating one or two nucleotides opposite the tandem lesions (Figure 3-2a). In addition, the Tg moiety of the tandem lesions could lead to a greater blocking effect than 8-oxodG on the Klenow fragment-mediated bypass of the tandem lesions. For instance, when the polymerase encounters the Tg first, i.e, for the 5'-(8-oxodG)-Tg-3' tandem lesion, some of the primers remain unextended; only a trace amount of full-length product was detected (Figure 3-2a). This observation is in keeping with the fact that Tg is a replication-blocking lesion (*21*), whereas 8-oxodG does not block appreciably the DNA replication (*22, 23*). Together, the two tandem lesions block the Klenow fragment-mediated primer extension more readily than the two composing single-nucleobase lesions when present alone.

The primer extension assay with yeast pol η showed that this polymerase could bypass both tandem and isolated single-nucleobase lesions, and generate full-length replication products in the presence of all four dNTPs (Figure 3-2b). However, similar to what we found for the Klenow fragment, both tandem lesions were somewhat more difficult for yeast pol η to bypass than either single-nucleobase lesion.

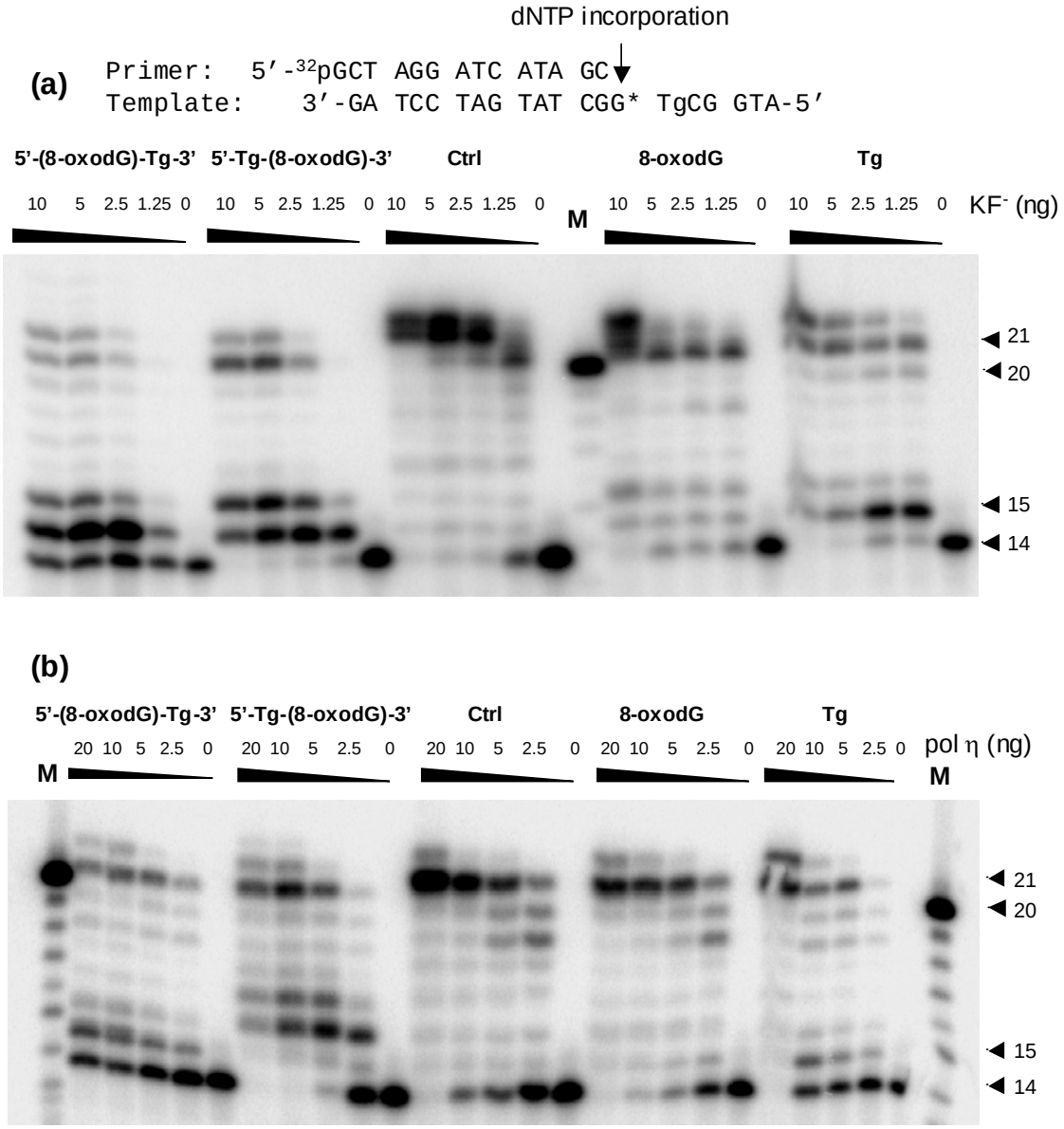

Figure 3-2. Primer extension assays for nucleotide incorporation opposite tandem lesions, i.e., 5'-(8-oxodG)-Tg-3' and 5'-Tg-(8-oxodG)-3', a single 8-oxodG or Tg, and the undamaged control, with exo$^-$ Klenow fragment (a) and yeast pol η (b). 5'-[^{32}P]-labeled d(GCTAGGATCATAGC) was used as the primer. Klenow fragment or yeast pol η at the indicated units/concentrations was incubated with 10 nM substrate and 200 μM dNTPs at 37 °C for 60 min. The products were subsequently resolved by using 20% denaturing polyacrylamide gels. The 21-mer was observed due to the presence of a 1-base overhang in the primer, and the 22-mer primer extension products were originated from the terminal transferase activity of the polymerase.

We next determined the steady-state kinetic parameters for nucleotide incorporation opposite both moieties of the tandem lesions, opposite an isolated 8-oxodG or Tg, or across an unmodified dG or dT by Klenow fragment and yeast pol η (Figure 3-3, and the steady-state kinetic parameters for nucleotide incorporation are summarized in Tables 3-2 to 3-4). It turned out that the Klenow fragment incorporated preferentially the correct nucleotide opposite the 3' modified nucleoside in both tandem lesions, namely, dAMP and dCMP were the most favored nucleotides inserted opposite the Tg in the 5'-(8-oxodG)-Tg-3' tandem lesion and the 8-oxodG in the 5'-Tg-(8-oxodG)-3' tandem lesion, respectively. The presence of a 5' neighboring 8-oxodG does not affect the efficiency of dAMP incorporation opposite Tg. Likewise, an adjacent 5' Tg does not confer compromised efficiency in nucleotide incorporation opposite 8-oxodG. The nucleotide insertion opposite the 5' component of the tandem lesion by Klenow fragment, however, became much more difficult; only little incorporation of dAMP opposite the Tg was observed when it lies on the 5' side of the 8-oxodG (Tables 3-2 & 3-4).

Unlike the nucleotide incorporation with the Klenow fragment, yeast pol η could insert nucleotides opposite both moieties of the tandem lesions. The efficiencies for the incorporation of the most favorable nucleotide, dCMP, opposite the 8-oxodG that is isolated, in 5'-Tg-(8-oxodG)-3', or in 5'-(8-oxodG)-Tg-3' are 3.7×10^{-3}, 2.9×10^{-3} and 1.1×10^{-4} $nM^{-1}min^{-1}$, respectively (Tables 3-3 & 3-4). Thus, the presence of Tg as the 5' neighboring nucleotide only resulted in marginal decrease (i.e., 22%) in efficiency of nucleotide incorporation; the existence of Tg as the 3' adjoining nucleotide, however, led

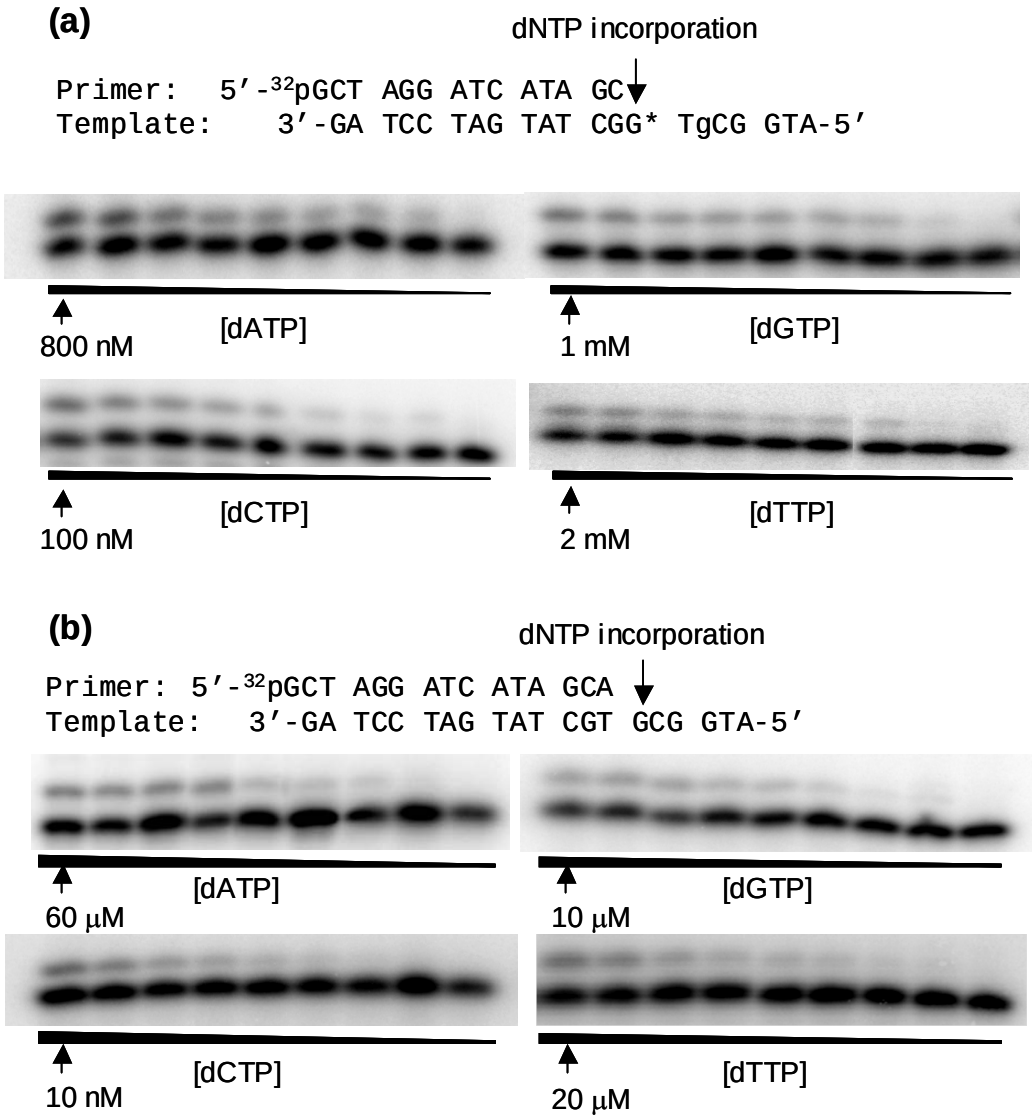

Figure 3-3. Example gel images for the steady-state kinetic measurements for the nucleotide incorporation opposite the 8-oxodG portion of the 5'-Tg-(8-oxodG)-3' tandem lesion (a) or the corresponding dG site for the undamaged substrate. (b). Klenow fragment (5 ng) was incubated with 10 nM DNA substrate at room temperature for 10 min. The highest dNTP concentration is shown in the figure, and the ratio of dNTP concentrations between adjacent lanes was 0.5-0.6.

Table 3-2. Steady-state kinetic parameters for Exo$^-$ Klenow fragment-mediated nucleotide incorporation opposite Tg and 8-oxodG in tandem lesion-containing substrates and opposite undamaged dG or dT in the control substrate.[a]

Substrates	*dNTP*	k_{cat} *(min^{-1})*	K_m *(nM)*	k_{cat}/K_m *(nM^{-1} min^{-1})*	f_{inc}
5'-Tg-(8-oxodG)-3'	14 mer Primer: 5' - GCTAGGATCATAGC - 3'				
	dATP	0.10 ± 0.01	$(2.9 \pm 0.6) \times 10^2$	3.4×10^{-4}	5.2×10^{-2}
	dGTP	0.057 ± 0.003	$(1.4 \pm 0.2) \times 10^5$	3.8×10^{-7}	5.8×10^{-5}
	dCTP	0.073 ± 0.008	11 ± 1	6.6×10^{-3}	1.0
	dTTP	0.090 ± 0.008	$(1.5 \pm 0.2) \times 10^6$	6.0×10^{-8}	9.1×10^{-6}
	15 mer Primer: 5' - GCTAGGATCATAGCC - 3'				
	dATP	0.098 ± 0.001	$(3.1 \pm 0.3) \times 10^4$	3.2×10^{-6}	1.0
5'-(8-oxodG)-Tg-3'	14 mer Primer: 5' - GCTAGGATCATAGC - 3'				
	dATP	0.21 ± 0.01	16 ± 0.75	1.3×10^{-3}	1.0
	dGTP	0.065 ± 0.001	$(2.4 \pm 0.1) \times 10^4$	2.7×10^{-6}	2.1×10^{-3}
	dCTP	0.049 ± 0.02	$(2.7 \pm 1.2) \times 10^5$	1.8×10^{-7}	1.4×10^{-4}
	dTTP	0.030 ± 0.0003	$(2.2 \pm 0.1) \times 10^5$	1.4×10^{-7}	1.1×10^{-4}
Undamaged 5'-dG-dT-3'	14 mer Primer: 5' - GCTAGGATCATAGC – 3'				
	dATP	0.060 ± 0.001	0.71 ± 0.02	0.085	1.0
	dGTP	0.079 ± 0.005	$(6.0 \pm 1.1) \times 10^2$	1.3×10^{-4}	1.5×10^{-3}
	dCTP	0.076 ± 0.003	$(4.0 \pm 0.4) \times 10^4$	1.9×10^{-6}	2.2×10^{-5}
	dTTP	0.063 ± 0.001	$(1.1 \pm 0.1) \times 10^5$	5.7×10^{-6}	6.7×10^{-5}
	15 mer Primer: 5' – GCTAGGATCATAGCA - 3'				
	dATP	0.057 ± 0.001	$(2.2 \pm 0.2) \times 10^4$	2.6×10^{-6}	2.8×10^{-4}
	dGTP	0.076 ± 0.003	$(4.6 \pm 0.4) \times 10^3$	1.7×10^{-5}	1.8×10^{-3}
	dCTP	0.079 ± 0.008	8.5 ± 3.4	9.3×10^{-3}	1.0
	dTTP	0.11 ± 0.01	$(2.1 \pm 0.3) \times 10^4$	5.2×10^{-6}	5.6×10^{-4}

[a] k_{cat} and K_m are average values based on three independent measurements

Table 3-3. Steady-state kinetic parameters for nucleotide incorporation mediated by yeast pol η opposite Tg and 8-oxodG in tandem lesion-containing substrates and opposite undamaged dG and dT in the control substrate.[a]

Substrates	*dNTP*	k_{cat} *(min^{-1})*	K_m *(nM)*	k_{cat} / K_m *(nM^{-1} min^{-1})*	f_{inc}
5'-Tg-(8-oxodG)-3'	14 mer Primer: 5' - GCTAGGATCATAGC - 3'				
	dATP	0.29 ± 0.02	(2.3 ± 0.3) × 10^3	1.3 × 10^{-4}	4.5 × 10^{-2}
	dGTP	0.060 ± 0.005	(4.9 ± 0.9) × 10^3	1.2 × 10^{-5}	4.1 × 10^{-3}
	dCTP	0.099 ± 0.029	34 ± 16	2.9 × 10^{-3}	1.0
	dTTP	0.060 ± 0.005	(5.8 ± 0.7) × 10^3	1.0 × 10^{-5}	3.4 × 10^{-3}
	15 mer Primer: 5' – GCTAGGATCATAGCC - 3'				
	dATP	0.063 ± 0.001	(2.9 ± 0.7) × 10^2	2.2 × 10^{-4}	1.0
	dGTP	0.16 ± 0.01	(6.3 ± 0.4) × 10^4	2.5 × 10^{-6}	1.1 × 10^{-2}
	dCTP	0.11 ± 0.002	(6.3 ± 0.5) × 10^5	1.7 × 10^{-7}	7.7 × 10^{-4}
	dTTP	0.13 ± 0.01	(2.7 ± 0.7) × 10^5	4.8 × 10^{-6}	2.2 × 10^{-3}
5'-(8-oxodG)-Tg-3'	14 mer Primer: 5' - GCTAGGATCATAGC - 3'				
	dATP	0.12 ± 0.002	(3.3 ± 0.1) × 10^2	3.6 × 10^{-4}	1.0
	dGTP	0.048 ± 0.002	(1.4 ± 0.1) × 10^4	3.4 × 10^{-6}	9.4 × 10^{-3}
	dCTP	0.063 ± 0.005	(2.5 ± 0.4) × 10^3	2.5 × 10^{-5}	6.9 × 10^{-2}
	dTTP	0.080 ± 0.002	(5.3 ± 0.5) × 10^4	1.5 × 10^{-6}	4.2 × 10^{-3}
	15 mer Primer: 5' - GCTAGGATCATAGCA - 3'				
	dATP	0.084 ± 0.002	(1.1 ± 0.1) × 10^5	7.6 × 10^{-7}	6.9 × 10^{-3}
	dGTP	0.15 ± 0.01	(9.6 ± 0.5) × 10^5	1.6 × 10^{-7}	1.5 × 10^{-3}
	dCTP	0.046 ± 0.005	(4.1 ± 0.6) × 10^2	1.1 × 10^{-4}	1.0
	dTTP	0.17 ± 0.02	(6.4 ± 0.5) × 10^5	2.7 × 10^{-7}	2.5 × 10^{-3}
5'-dG-dT-3'	14 mer Primer: 5' - GCTAGGATCATAGC - 3'				
	dATP	0.055 ± 0.005	36 ± 1	1.5 × 10^{-3}	1.0
	dGTP	0.080 ± 0.005	(5.9 ± 0.5) × 10^4	1.4 × 10^{-6}	9.3 × 10^{-4}
	dCTP	0.077 ± 0.010	(4.1 ± 0.1) × 10^3	1.9 × 10^{-5}	1.3 × 10^{-2}
	dTTP	0.13 ± 0.003	(1.1 ± 0.9) × 10^5	1.2 × 10^{-6}	8.0 × 10^{-4}
	15 mer Primer: 5' - GCTAGGATCATAGCA - 3'				
	dATP	0.23 ± 0.02	(5.2 ± 0.3) × 10^5	4.4 × 10^{-7}	4.6 × 10^{-5}
	dGTP	0.38 ± 0.01	(5.8 ± 0.07) × 10^5	6.7 × 10^{-7}	7.1 × 10^{-5}
	dCTP	0.087 ± 0.010	9.2 ± 2.5	9.5 × 10^{-3}	1.0
	dTTP	0.087 ± 0.010	(1.8 ± 0.3) × 10^4	4.8 × 10^{-6}	5.1 × 10^{-4}

[a] k_{cat} and K_m are average values based on three independent measurements

Table 3-4. Steady-state kinetic parameters for nucleotide incorporation by Exo$^-$ Klenow fragment and yeast polymerase η on 8-oxodG- and Tg-containing substrates.[a]

Substrates	*dNTP*	k_{cat} *(min^{-1})*	K_m *(nM)*	k_{cat}/K_m *(nM^{-1} min^{-1})*	f_{inc}
5'-(8-oxodG)-dT-3'	By Exo- Klenow fragment with 15 mer Primer: 5' – GCTAGGATCATAGCA - 3'				
	dATP	0.082 ± 0.005	$(9.7 \pm 0.2) \times 10^2$	8.5×10^{-5}	5.7×10^{-2}
	dGTP	0.082 ± 0.001	$(3.7 \pm 0.2) \times 10^4$	2.2×10^{-7}	1.5×10^{-4}
	dCTP	0.038 ± 0.003	26 ± 7	1.5×10^{-3}	1.0
	dTTP	0.016 ± 0.001	$(4.8 \pm 0.7) \times 10^5$	3.3×10^{-8}	2.2×10^{-5}
	By yeast polymerase *η* with 15 mer Primer: 5' – GCTAGGATCATAGCA - 3'				
	dATP	0.13 ± 0.01	$(6.9 \pm 1.3) \times 10^2$	1.9×10^{-4}	5.1×10^{-2}
	dGTP	0.065 ± 0.010	$(4.0 \pm 0.9) \times 10^3$	1.6×10^{-5}	4.3×10^{-3}
	dCTP	0.063 ± 0.005	17 ± 4	3.7×10^{-3}	1.0
	dTTP	0.041 ± 0.005	$(1.3 \pm 0.04) \times 10^3$	3.2×10^{-5}	8.6×10^{-3}
5'-dG-Tg-3'	By Exo- Klenow fragment with 14 mer Primer: 5' - GCTAGGATCATAGC - 3'				
	dATP	0.057 ± 0.005	36 ± 3	1.6×10^{-3}	1.0
	dGTP	0.087 ± 0.014	$(2.1 \pm 0.4) \times 10^4$	4.1×10^{-6}	2.6×10^{-3}
	dCTP	0.052 ± 0.005	$(1.1 \pm 0.2) \times 10^5$	4.7×10^{-7}	2.9×10^{-4}
	dTTP	0.030 ± 0.003	$(2.0 \pm 0.2) \times 10^5$	1.5×10^{-6}	9.4×10^{-4}
	By yeast polymerase *η* with 14 mer Primer: 5' - GCTAGGATCATAGC – 3'				
	dATP	0.053 ± 0.001	71.1 ± 0.2	7.5×10^{-4}	1.0
	dGTP	0.070 ± 0.005	$(6.0 \pm 1.0) \times 10^3$	1.2×10^{-6}	1.6×10^{-3}
	dCTP	0.067 ± 0.002	$(4.0 \pm 0.4) \times 10^5$	1.7×10^{-7}	2.3×10^{-4}
	dTTP	0.058 ± 0.001	$(1.1 \pm 0.1) \times 10^5$	5.3×10^{-7}	7.1×10^{-4}

[a] k_{cat} and K_m are average values based on three independent measurements

to a pronounced drop in efficiency for dCMP insertion, i.e., by ~34 fold. This large drop is mainly due to the increase in K_m, i.e., by ~24 fold, for the 5'-(8-oxodG)-Tg-3' lesion relative to the isolated 8-oxodG lesion (Tables 3-3 & 3-4). The latter compromised efficiency for dCMP incorporation reflects the difficulty experienced by the polymerase in extending the Tg:A base pair at the primer-template junction.

The efficiencies for the insertion of the most favorable nucleotide, i.e., dAMP, opposite the Tg that is alone, in 5'-Tg-(8-oxodG)-3', or in 5'-(8-oxodG)-Tg-3' were 7.5×10^{-4}, 2.2×10^{-4}, and 3.6×10^{-4} $nM^{-1}min^{-1}$, respectively (Tables 3-3 & 3-4). The 5' and 3' adjacent 8-oxodG, therefore, led to the decreases in nucleotide incorporation efficiency by ~2.1 and ~3.4 fold, respectively, and the decrease arises again from the increase in K_m (Tables 3-3 & 3-4). This result revealed that pol η encounters greater difficulty in extending the 8-oxoG:C base pair than a G:C base pair. The extent of decrease, however, is much less drastic than what we found for the 8-oxodG in the tandem lesions where Tg is the neighboring lesion (*vide supra*).

The Presence of Single-nucleobase Lesions in Tandem Affects their Mutagenic Potential

The steady-state kinetic parameters for yeast pol η-mediated nucleotide incorporation also revealed some notable differences in mutagenicity for the two single-nucleobase lesions while they are present alone or in tandem. In addition, the fidelity for nucleotide insertion is different for the tandem lesions with the Tg and 8-oxodG being in the opposite orientation. In this regard, the frequency of misincorporation of dAMP opposite 8-oxodG in the 5'-Tg-(8-oxodG)-3' (4.5%) was similar as that opposite an

isolated 8-oxodG (5.1%). However, the frequency for the misinsertion of dAMP opposite the 8-oxodG in 5'-(8-oxodG)-Tg-3' was only 0.69% (Tables 3-3 & 3-4). The Tg component, however, exhibits greater mutagenic potential for both orientations of the tandem lesions than when it is present alone; the misinsertion of dGMP occurred at frequencies of 1.1% and 0.16% for the 5'-Tg-(8-oxodG)-3' and isolated Tg, respectively (Tables 3-3 & 3-4). By contrast, dCMP was inserted opposite the Tg moiety of the 5'-(8-oxodG)-Tg-3' tandem lesion at a relatively high frequency, i.e., 6.7% (Tables 3-3 & 3-4).

Very limited differences were found for the fidelity of Klenow fragment-mediated nucleotide incorporation opposite the Tg and 8-oxodG while they are isolated or neighboring to each other. The frequencies for the misincorporation of dAMP opposite 8-oxodG by Klenow fragment were similar, namely, 5.7% and 5.2% for isolated 8-oxodG and 5'-Tg-(8-oxodG)-3' tandem lesion, respectively (Tables 3-2 & 3-4). In addition, the frequencies for the misinsertion of dGMP opposite the Tg were comparable, i.e., 0.21% and 0.26% for substrates containing 5'-(8-oxodG)-Tg-3' tandem lesion and isolated Tg, respectively (Tables 3-2 & 3-4).

The Recognition of Tandem Lesions by BER Enzymes

We next investigated how efficiently the two tandem lesions can be recognized by two BER enzymes, i.e., hOGG1 and *E. coli* endonuclease III. Although hOGG1 is a bifunctional glycosylase harboring both glycosylase and AP lyase activities (*42*), previous kinetic studies showed that the hOGG1-mediated strand cleavage at 8-oxodG site is not very efficient, and the k_{cat} values indicated that the purified protein may take more than 20 min to perform a single repair event *in vitro* (*43*). Human AP endonuclease

1 (APE1), however, can stimulate the DNA glycosylase activity of hOGG1 by cleaving the AP site produced by the latter (*44*). Thus, we employed APE1 to induce cleavage at the hOGG1-produced AP sites.

It turned out that the 8-oxodG in the two tandem lesions could be cleaved by hOGG1 (Figure 3-4); the efficiencies for the cleavage of 8-oxodG in the two tandem lesions are, however, considerably different from each other and from the hOGG1-mediated cleavage of an isolated 8-oxodG. In this respect, hOGG1 could remove 8-oxoguanine from the 5'-(8-oxodG)-Tg-3' tandem lesion-bearing substrate more efficiently than from the substrate housing an isolated 8-oxodG (Figure 3-4). By contrast, the cleavage of 8-oxoguanine from the 5'-Tg-(8-oxodG)-3' tandem lesion-carrying substrate is much less efficient than that from the substrate containing 8-oxodG alone; the cleavage of the former substrate was almost completely abolished at the lowest level of the enzyme used (Figure 3-4b). This result revealed that the presence of a vicinal Tg can perturb significantly the hOGG1-mediated cleavage of 8-oxodG, and this perturbation is dependent on the spatial arrangement of the two single-nucleobase lesions.

We next examined whether the presence of an adjoining 8-oxodG can affect the endonuclease III-mediated cleavage of Tg. Since endonuclease III has both glycosylase activity and a relatively robust AP lyase activity (*45*), no AP endonuclease was added for the endonuclease III-mediated cleavage reactions. In contrast to what we observed for hOGG1, the Tg in both tandem lesions could be cleaved by endonuclease III at comparable efficiencies as an isolated Tg (Figure 3-5).

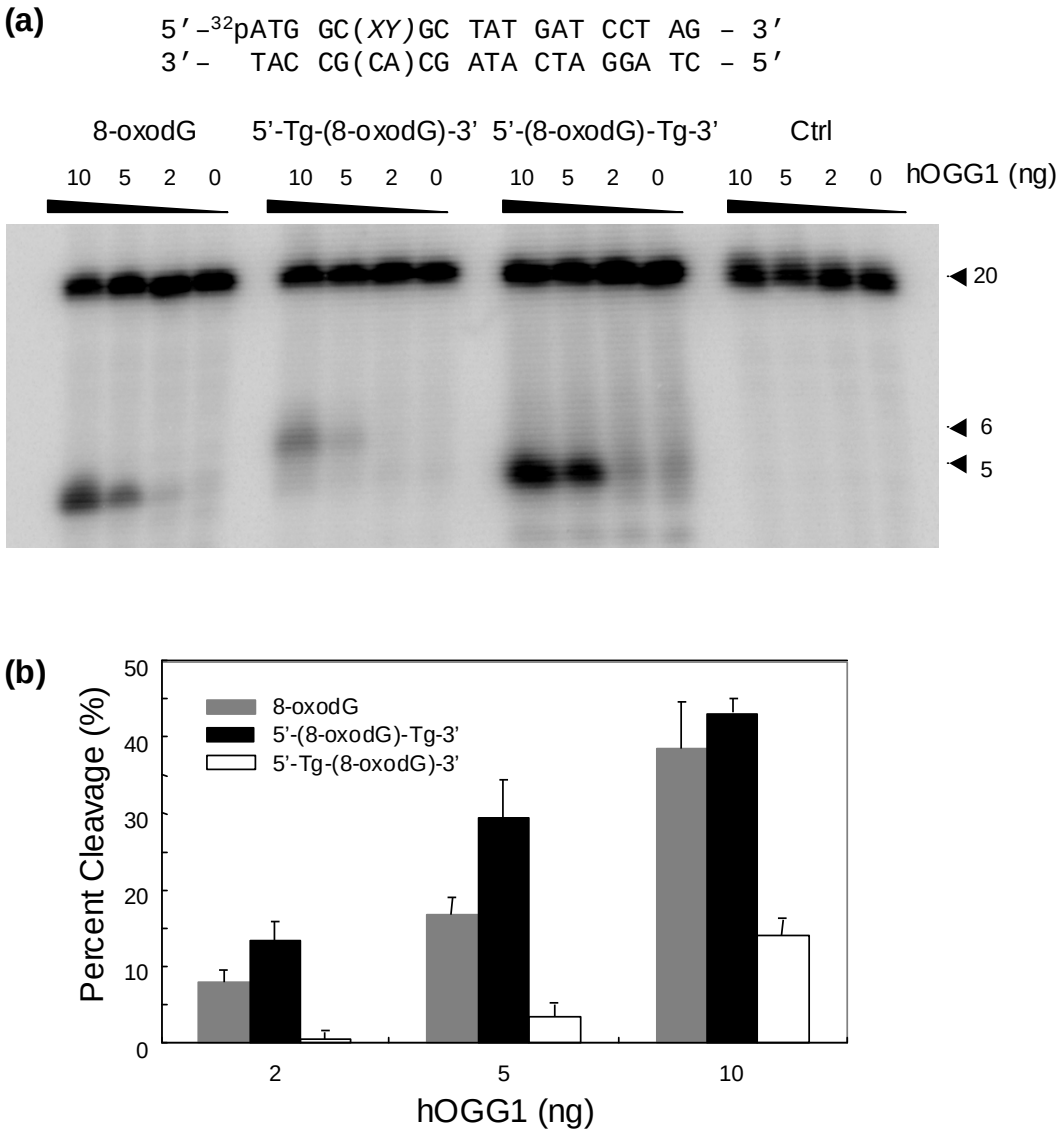

Figure 3-4. (a) PAGE analysis of the hOGG1-mediated cleavage products of the substrates containing an 8-oxodG, the two tandem lesions, and unmodified GT. "XY" represents different lesions, and the 20 mer 5'-(CA)-3'- and 5'-(AC)-3'-containing complementary strands were used for the repair studies of the 5'-Tg-(8-oxodG)-3'- and 5'-(8-oxodG)-Tg-3'-containing substrates, respectively. (b) A summary of the quantification results of the percent cleavage products for different substrates. The values represent the mean ± standard deviation from three independent treatments and quantification experiments.

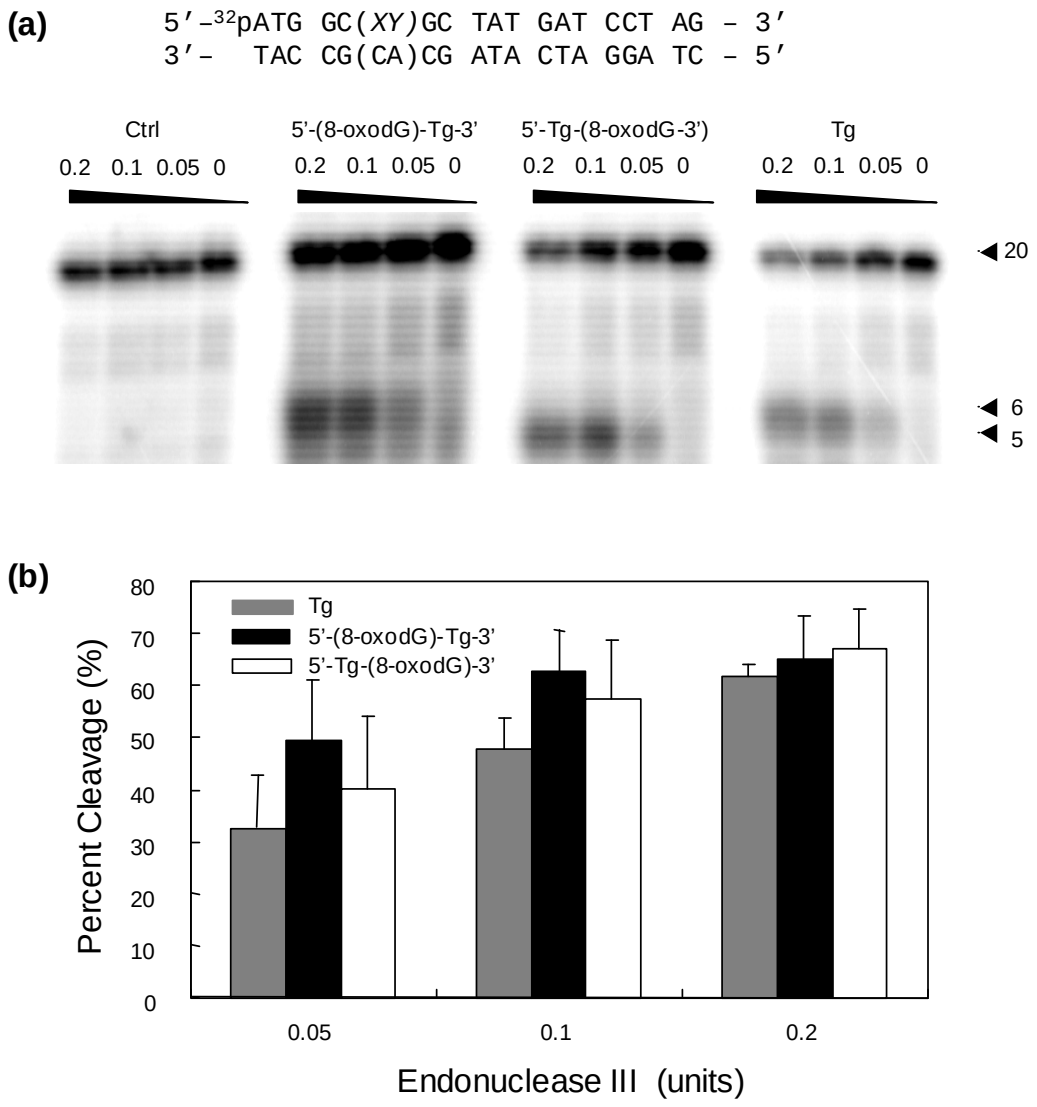

Figure 3-5. (a) PAGE analysis of the products arising from the endonuclease III-mediated cleavage of substrates housing Tg, 5'-Tg-(8-oxodG)-3', 5'-(8-oxodG)-Tg-3' and unmodified GT. (b) The quantification results of percent cleavage products for different substrates. The values represent the mean ± standard deviation from three independent treatments and quantification experiments.

Discussion

In this chapter, we employed the ODN substrates containing Tg and 8-oxodG, either alone or neighboring each other, and examined how these lesions perturb DNA replication by using purified DNA polymerases and how efficiently they are recognized by two BER enzymes, hOGG1 and *E. coli* endonuclease III.

Our primer extension assay results revealed that the tandem lesions blocked DNA replication more effectively than the two isolated single-nucleobase lesions. In addition, the miscoding potentials of Tg and 8-oxodG, as revealed by steady-state kinetic measurements, are different while these lesions are present alone or in tandem. Our observation is consistent with previous findings that the tandem lesions, where an 8-oxodG is vicinal to an abasic site or a formylamine, can perturb differently the fidelity and efficiency of nucleotide incorporation opposite the lesion site from the situations where the composing lesions are present alone (*32, 33*). The alteration in the fidelity of nucleotide incorporation might be attributed to the local structure change imposed by the neighboring lesion.

BER assay results showed that Endonuclease III recognizes and cleaves the thymine glycol in the two tandem lesion-containing substrates at a similar efficiency as the substrate housing an isolated thymine glycol. On the other hand, the 8-oxodG in the two tandem lesions could be recognized differently by hOGG1; whereas the lesion with an adjacent 5' Tg could be cleaved much less efficiently than an isolated 8-oxodG, the lesion with a neighboring 3' Tg could be cleaved more readily than when the 8-oxodG was present alone.

Thermodynamic measurements revealed that the 5'-Tg-(8-oxodG)-3' and 5'-(8-oxodG)-Tg-3' tandem lesions destabilized duplex DNA to a similar extent, which is represented by a 5.1 kcal/mol increase in Gibbs free energy for duplex formation at 37 °C (*36*). Thus, the difference in recognition of the two tandem lesions by hOGG1 is not due to difference in overall destabilization to duplex DNA induced by the two tandem lesions. However, the above differential cleavage efficiencies for the three substrates can be rationalized from the nature of hOGG1-DNA interaction based on the X-ray structure of the hOGG1-DNA complex (*46*) and the structural perturbation to duplex DNA introduced by thymidine glycol (*47, 48*).

The X-ray co-crystal structure of hOGG1 and 8-oxodG-bearing duplex DNA revealed a marked structure alteration of the lesion-containing DNA (*46*). The modified nucleobase, 8-oxo-7,8-dihydroguanine (8-oxoGua) is extruded from the helix and is inserted deeply into an extrahelical active-site pocket of the enzyme. In addition, the X-ray structure showed the hydrogen bonding interaction between the nucleobase on the 5' side of 8-oxoGua and Asn151 in the protein (*46*). The lack of aromaticity of Tg may compromise this interaction thereby resulting in decreased binding of the 5'-Tg-(8-oxodG)-3'-bearing substrate toward hOGG1. Furthermore, the structure showed that the formation of a catalytically competent protein-DNA complex necessitates significant bond rotation of the flanking 5' phosphate so that its non-bridging oxygen atoms point inward towards the helix axis. The presence of Tg as the 5' neighboring nucleoside may also perturb this bond rotation thereby decreasing the catalytic proficiency of the enzyme. The above factors together may contribute to the poorer hOGG1-mediated cleavage of 5'-

Tg-(8-oxodG)-3' than an isolated 8-oxodG.

The X-ray structure showed no direct contact between the protein and the 3' flanking nucleobase and no significant bond rotation in the phosphate group on the 3' side of 8-oxodG (*46*). On the other hand, previous molecular modeling studies showed that the methyl group in the *cis*-(5R,6S) isomer of Tg favors an axial conformation, which results in a steric clash between the methyl group and the 5' neighboring nucleobase thereby destabilizing the 5' base pair (*47, 48*). Therefore, the destabilization of the 8-oxoGua:Cyt ("Cyt" represents cytosine) base pair induced by the 3' vicinal Tg may result in the facile extrusion of 8-oxoGua from the helix thereby enhancing the cleavage efficiency of the enzyme toward the 5'-(8-oxodG)-Tg-3' substrate.

The relatively poor cleavage of 8-oxodG from the 5'-Tg-(8-oxodG)-3'-tandem lesion-containing substrate may render this lesion a substrate for the NER pathway. In this regard, both Tg and 8-oxodG can be recognized by mammalian NER machinery (*49*). The formation of this tandem lesion at methylated CpG site, therefore, may account for the occurrence of high frequency of mCG→TT mutation while CpG-methylated pSP189 shuttle vector was replicated in NER-deficient XPA cells (*27*).

Together, the above results revealed that when the two commonly observed ROS-induced lesions, i.e., Tg and 8-oxodG, are neighboring to each other, they impose greater challenges to DNA replication apparatus and confer different mutagenic properties than when these lesions are present alone. Moreover, the 5'-Tg-(8-oxodG)-3' tandem lesion can be recognized by hOGG1 much less efficiently than an isolated 8-oxodG. Therefore, the efficient formation of the 5'-Tg-(8-oxodG)-3' tandem lesion, coupled with the

elevated difficulty in the hOGG1-mediated repair of its 8-oxodG component, underscores the biological significance of this tandem lesion. To our knowledge, this represents the first replication and repair study on a tandem single-nucleobase lesion [i.e., 5'-Tg-(8-oxodG)-3'] whose efficient formation in isolated DNA has been demonstrated.

References:

(1) Gulston, M., Fulford, J., Jenner, T., de Lara, C., and O'Neill, P. (2002) Clustered DNA damage induced by radiation in human fibroblasts (HF19), hamster (V79-4) cells and plasmid DNA is revealed as Fpg and Nth sensitive sites. *Nucleic Acids Research 30*, 3464-3472.

(2) Nikjoo, H., O'Neill, P., Wilson, W. E., and Goodhead, D. T. (2001) Computational approach for determining the spectrum of DNA damage induced by ionizing radiation. *Radiation Research 156*, 577-583.

(3) Sutherland, B. M., Bennett, P. V., Sutherland, J. C., and Laval, J. (2002) Clustered DNA damages induced by X rays in human cells. *Radiation Research 157*, 611-616.

(4) Budworth, H., and Dianov, G. L. (2003) Mode of inhibition of short-patch base excision repair by thymine glycol within clustered DNA lesions. *Journal of Biological Chemistry 278*, 9378-9381.

(5) Budworth, H., Dianova, I. I., Podust, V. N., and Dianov, G. L. (2002) Repair of clustered DNA lesions - Sequence-specific inhibition of long-patch base excision repair by 8-oxoguanine. *J. Biol. Chem. 277*, 21300-21305.

(6) Yang, N., Chaudhry, M. A., and Wallace, S. S. (2006) Base excision repair by hNTH1 and hOGG1: A two edged sword in the processing of DNA damage in gamma-irradiated human cells. *DNA Repair 5*, 43-51.

(7) David-Cordonnier, M. H., Cunniffe, S. M. T., Hickson, I. D., and O'Neill, P. (2002) Efficiency of incision of an AP site within clustered DNA damage by the major human AP endonuclease. *Biochemistry 41*, 634-642.

(8) David-Cordonnier, M. H., Laval, J., and O'Neill, P. (2000) Clustered DNA damage, influence on damage excision by XRS5 nuclear extracts and Escherichia coli Nth and Fpg proteins. *J. Biol. Chem. 275*, 11865-11873.

(9) Harrison, L., Hatahet, Z., and Wallace, S. S. (1999) In vitro repair of synthetic ionizing radiation-induced multiply damaged DNA sites. *J. Mol. Biol. 290*, 667-684.

(10) Lomax, M. E., Cunniffe, S., and O'Neill, P. (2004) 8-oxoG retards the activity of the ligase III/XRCC1 complex during the repair of a single-strand break, when present within a clustered DNA damage site. *DNA Repair 3*, 289-299.

(11) Pearson, C. G., Shikazono, N., Thacker, J., and O'Neill, P. (2004) Enhanced mutagenic potential of 8-oxo-7,8-dihydroguanine when present within a clustered DNA damage site. *Nucleic Acids Res. 32*, 263-270.

(12) Bellon, S., Ravanat, J. L., Gasparutto, D., and Cadet, J. (2002) Cross-linked thymine-purine base tandem lesions: synthesis, characterization, and measurement in gamma-irradiated isolated DNA. *Chem. Res. Toxicol. 15*, 598-606.

(13) Box, H. C., Budzinski, E. E., Dawidzik, J. B., Gobey, J. S., and Freund, H. G. (1997) Free radical-induced tandem base damage in DNA oligomers. *Free Radic. Biol. Med. 23*, 1021-1030.

(14) Box, H. C., Budzinski, E. E., Dawidzik, J. B., Wallace, J. C., and Iijima, H. (1998) Tandem lesions and other products in X-irradiated DNA oligomers. *Radiat. Res. 149*, 433-9.

(15) Hong, H., Cao, H., Wang, Y., and Wang, Y. (2006) Identification and quantification of a guanine-thymine intrastrand cross-link lesion induced by Cu(II)/H_2O_2/ascorbate. *Chem. Res. Toxicol. 19*, 614-621.

(16) Hong, I. S., Carter, K. N., Sato, K., and Greenberg, M. M. (2007) Characterization and mechanism of formation of tandem lesions in DNA by a nucleobase peroxyl radical. *J. Am. Chem. Soc. 129*, 4089-4098.

(17) Zhang, Q., and Wang, Y. (2003) Independent generation of 5-(2 '-deoxycytidinyl)methyl radical and the formation of a novel cross-link lesion between 5-methylcytosine and guanine. *J. Am. Chem. Soc. 125*, 12795-12802.

(18) Zhang, Q., and Wang, Y. (2005) Generation of 5-(2 '-deoxycytidyl)methyl radical and the formation of intrastrand cross-link lesions in oligodeoxyribonucleotides. *Nucleic Acids Res. 33*, 1593-1603.

(19) Wang, Y. (2008) Bulky DNA lesions induced by reactive oxygen species. *Chem. Res. Toxicol. 21*, 276-81.

(20) Hong, H., Cao, H., and Wang, Y. (2007) Formation and genotoxicity of a guanine cytosine intrastrand cross-link lesion in vivo. *Nucleic Acids Res. 35*, 7118-7127.

(21) Aller, P., Rould, M. A., Hogg, M., Wallace, S. S., and Doublie, S. (2007) A structural rationale for stalling of a replicative DNA polymerase at the most

common oxidative thymine lesion, thymine glycol. *Proc. Natl. Acad. Sci. USA 104*, 814-8.

(22) Suzuki, N., Ohashi, E., Kolbanovskiy, A., Geacintov, N. E., Grollman, A. P., Ohmori, H., and Shibutani, S. (2002) Translesion synthesis by human DNA polymerase kappa on a DNA template containing a single stereoisomer of dG-(+)- or dG-(-)-anti-N-2-BPDE (7,8-dihydroxy-anti-9,10-epoxy-7,8,9,10-tetrahydrobenzo[a]pyrene). *Biochemistry 41*, 6100-6106.

(23) Cheng, K. C., Cahill, D. S., Kasai, H., Nishimura, S., and Loeb, L. A. (1992) 8-Hydroxyguanine, an abundant form of oxidative DNA damage, causes G----T and A----C substitutions. *J Biol Chem 267*, 166-72.

(24) Bienvenu, C., and Cadet, J. (1996) Synthesis and kinetic study of the deamination of the cis diastereomers of 5,6-dihydroxy-5,6-dihydro-5-methyl-2'-deoxycytidine. *J. Org. Chem. 61*, 2632-7.

(25) Zuo, S., Boorstein, R. J., and Teebor, G. W. (1995) Oxidative damage to 5-methylcytosine in DNA. *Nucleic Acids Res. 23*, 3239-43.

(26) Ehrlich, M., Gama-Sosa, M. A., Huang, L. H., Midgett, R. M., Kuo, K. C., McCune, R. A., and Gehrke, C. (1982) Amount and Distribution of 5-Methylcytosine in Human DNA from Different Types of Tissues or Cells. *Nucleic Acids Res. 10*, 2709-2721.

(27) Lee, D. H., O'Connor, T. R., and Pfeifer, G. P. (2002) Oxidative DNA damage induced by copper and hydrogen peroxide promotes CG-->TT tandem mutations

at methylated CpG dinucleotides in nucleotide excision repair-deficient cells. *Nucleic Acids Res. 30*, 3566-73.

(28) Cao, H., and Wang, Y. (2007) Quantification of oxidative single-base and intrastrand cross-link lesions in unmethylated and CpG-methylated DNA induced by Fenton-type reagents. *Nucleic Acids Res 35*, 4833-44.

(29) Gu, C., and Wang, Y. (2004) LC-MS/MS identification and yeast polymerase η bypass of a novel γ-irradiation-induced intrastrand cross-link lesion G[8-5]C. *Biochemistry 43*, 6745-6750.

(30) Gu, C., and Wang, Y. (2005) Thermodynamic and in vitro replication studies of an intrastrand G[8-5]C cross-link lesion. *Biochemistry 44*, 8883-8889.

(31) Jiang, Y., Hong, H., Cao, H., and Wang, Y. (2007) In vivo formation and in vitro replication of a guanine-thymine intrastrand cross-link lesion. *Biochemistry 46*, 12757-12763.

(32) Gentil, A., Le Page, F., Cadet, J., and Sarasin, A. (2000) Mutation spectra induced by replication of two vicinal oxidative DNA lesions in mammalian cells. *Mutat. Res. 452*, 51-6.

(33) Kalam, M. A., and Basu, A. K. (2005) Mutagenesis of 8-oxoguanine adjacent to an abasic site in simian kidney cells: tandem mutations and enhancement of G-->T transversions. *Chem. Res. Toxicol. 18*, 1187-92.

(34) David, S. S., O'Shea, V. L., and Kundu, S. (2007) Base-excision repair of oxidative DNA damage. *Nature 447*, 941-50.

(35) Imoto, S., Bransfield, L. A., Croteau, D. L., Van Houten, B., and Greenberg, M. M. (2008) DNA tandem lesion repair by strand displacement synthesis and nucleotide excision repair. *Biochemistry 47*, 4306-4316.

(36) Wang, Y., and Wang, Y. (2006) Synthesis and thermodynamic studies of oligodeoxyribonucleotides containing tandem lesions of thymidine glycol and 8-oxo-2 '-deoxyguanosine. *Chem. Res. Toxicol. 19*, 837-843.

(37) Kusumoto, R., Masutani, C., Iwai, S., and Hanaoka, F. (2002) Translesion synthesis by human DNA polymerase eta across thymine glycol lesions. *Biochemistry 41*, 6090-6099.

(38) Zhang, Y., Yuan, F., Wu, X., Rechkoblit, O., Taylor, J. S., Geacintov, N. E., and Wang, Z. (2000) Error-prone lesion bypass by human DNA polymerase η. *Nucleic Acids Res. 28*, 4717-24.

(39) Cannistraro, V. J., and Taylor, J. S. (2004) DNA-thumb interactions and processivity of T7 DNA polymerase in comparison to yeast polymerase eta. *J. Biol. Chem. 279*, 18288-95.

(40) Kuznetsov, N. A., Koval, V. V., Zharkov, D. O., Nevinsky, G. A., Douglas, K. T., and Fedorova, O. S. (2005) Kinetics of substrate recognition and cleavage by human 8-oxoguanine-DNA glycosylase. *Nucleic Acids Res. 33*, 3919-31.

(41) Goodman, M. F., Creighton, S., Bloom, L. B., and Petruska, J. (1993) Biochemical basis of DNA replication fidelity. *Crit. Rev. Biochem. Mol. Biol. 28*, 83-126.

(42) Shinmura, K., Kasai, H., Sasaki, A., Sugimura, H., and Yokota, J. (1997) 8-hydroxyguanine (7,8-dihydro-8-oxoguanine) DNA glycosylase and AP lyase activities of hOGG1 protein and their substrate specificity. *Mutat. Res. 385*, 75-82.

(43) Asagoshi, K., Yamada, T., Terato, H., Ohyama, Y., Monden, Y., Arai, T., Nishimura, S., Aburatani, H., Lindahl, T., and Ide, H. (2000) Distinct repair activities of human 7,8-dihydro-8-oxoguanine DNA glycosylase and formamidopyrimidine DNA glycosylase for formamidopyrimidine and 7,8-dihydro-8-oxoguanine. *J Biol Chem 275*, 4956-64.

(44) Vidal, A. E., Hickson, I. D., Boiteux, S., and Radicella, J. P. (2001) Mechanism of stimulation of the DNA glycosylase activity of hOGG1 by the major human AP endonuclease: bypass of the AP lyase activity step. *Nucleic Acids Res. 29*, 1285-92.

(45) Warner, H. R., Demple, B. F., Deutsch, W. A., Kane, C. M., and Linn, S. (1980) Apurinic/apyrimidinic endonucleases in repair of pyrimidine dimers and other lesions in DNA. *Proc. Natl. Acad. Sci. USA 77*, 4602-6.

(46) Bruner, S. D., Norman, D. P., and Verdine, G. L. (2000) Structural basis for recognition and repair of the endogenous mutagen 8-oxoguanine in DNA. *Nature 403*, 859-66.

(47) Clark, J. M., Pattabiraman, N., Jarvis, W., and Beardsley, G. P. (1987) Modeling and molecular mechanical studies of the *cis*-thymine glycol radiation damage lesion in DNA. *Biochemistry 26*, 5404-9.

(48) Brown, K. L., Adams, T., Jasti, V. P., Basu, A. K., and Stone, M. P. (2008) Interconversion of the *cis*-5R,6S- and *trans*-5R,6R-thymine glycol lesions in duplex DNA. *J. Am. Chem. Soc. 130*, 11701-10.

(49) Reardon, J. T., Bessho, T., Kung, H. C., Bolton, P. H., and Sancar, A. (1997) In vitro repair of oxidative DNA damage by human nucleotide excision repair system: possible explanation for neurodegeneration in xeroderma pigmentosum patients. *Proc. Natl. Acad. Sci. USA 94*, 9463-8.

CHAPTER 4

Efficient Formation of the Tandem Thymine Glycol/8-oxo-7,8-dihydroguanine Lesion in Isolated DNA and the Mutagenic and Cytotoxic Properties of the Tandem Lesions in *Escherichia coli* Cells

Introduction

The integrity of human genome is constantly challenged by endogenous and exogenous ROS and other reactive agents. In this regard, ROS include hydroxyl radical, superoxide radical, hydrogen peroxide, and singlet oxygen; they can react directly with DNA (i.e., hydroxyl radical and singlet oxygen) or modify DNA when in the presence of transition metal ions (i.e., hydrogen peroxide and superoxide radical) (*1, 2*).

Copper is an important structural metal in chromatin (*3*) and it can form stable complexes with DNA (*4-6*). Studies showed that copper plays a significant role in H_2O_2-mediated DNA damage (*7-10*). *In-vitro* studies showed that Cu(II) and H_2O_2, frequently together with the presence of ascorbate, induce DNA strand breaks as well as many types of single-nucleobase and intrastrand crosslink lesions (*8, 9, 11-13*).

Due to the intrinsic chemical and structural properties of different lesions and their close proximity, complex or clustered DNA lesions often display altered mutagenic potential (*14, 15*) and are more difficult to repair than when they are present alone (*16-21*). As a subset of clustered lesions, tandem lesions, comprising of two contiguously damaged nucleotides, can emanate from ROS attack (*8, 9, 22-31*). One type of tandem lesion, with an 8-oxo-7,8-dihydro-2'-deoxyguanosine (8-oxodG) and a formamido (dβF) moiety being

neighboring each other, was first found to form in short ODNs upon exposure to γ-rays or Fenton-type reagents under aerobic conditions (*32, 33*). Later it was observed that the amounts of these tandem lesions, with dβF being adjacent to 8-oxodG, formed in isolated DNA upon γ-ray exposure cannot account for the total amount of tandem lesions involving 8-oxodG (*27*). It was, thus, concluded that other tandem lesions involving 8-oxodG may exist (*27*). Since 5,6-dihydroxy-5,6-dihydrothymidine (or thymidine glycol, Tg) and 8-oxodG are major single-nucleobase lesions induced by ROS from thymidine and 2'-deoxyguanosine, respectively (*18, 34, 35*), we reasoned that tandem lesions with an 8-oxodG being adjacent to a Tg might be induced in DNA by ROS.

Tg can block effectively DNA replication *in vitro* (*36, 37*) and exhibits a low mutagenic potential (*34*). The 8-oxodG, on the other hand, does not block DNA replication, but is highly mutagenic, which can result in both G→T and G→C mutations, with the former being more prevalent (*38, 39*). Thymidine glycol could also arise from the deamination of 5-methylcytosine glycol, a common oxidatively induced lesion of 5-methylcytosine (Figure 4-1) (*40*). Thus, the 5'-Tg-(8-oxodG)-3' tandem lesion may also form from ROS attack at methylated CpG site and contribute to CpG mutagenesis (*41*).

In Chapter 3, our data showed that the tandem lesions composing of Tg and 8-oxodG exhibit stronger blocking effects toward DNA replication mediated by purified DNA polymerases *in vitro* than when either lesion is present on its own. In addition, steady-state kinetic studies revealed that the mutagenic properties of isolated Tg or 8-oxodG are different from when they are neighbors to each other. However, it has not been assessed whether the above findings can be extended to cells.

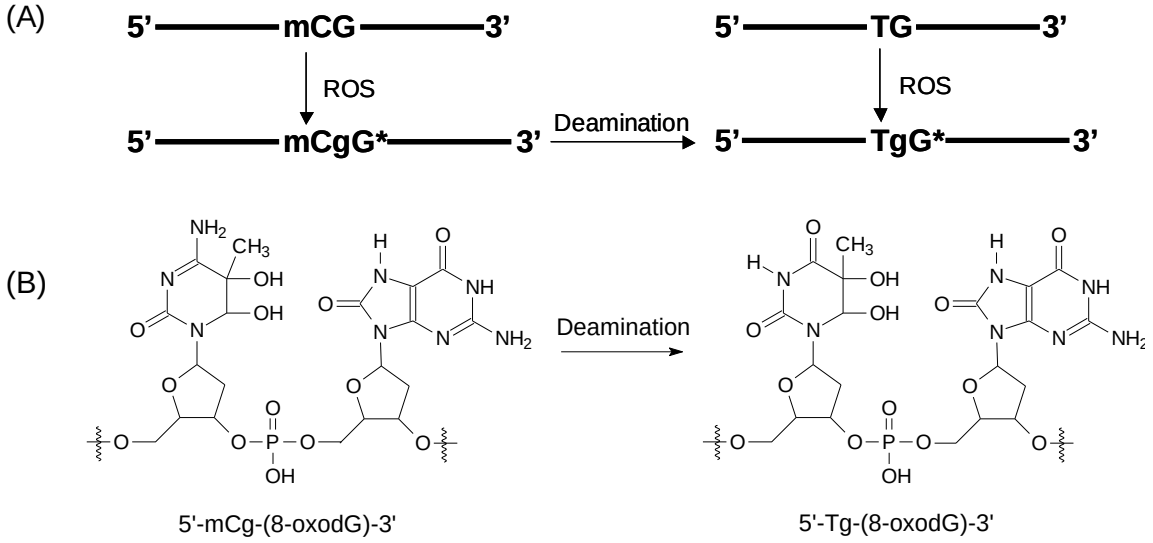

Figure 4-1. The formation of the 5’-Tg-(8-oxodG)-3’ tandem lesion. G*, mC, and mCg represent 8-oxoGua, 5-methylcytosine and 5-methylcytosine glycol, respectively.

In this chapter, we will assess quantitatively the formation of the tandem lesion 5'-Tg-(8-oxodG)-3' in isolated DNA. We also prepared single-stranded pYMV1 shuttle vectors containing a 5'-(8-oxodG)-Tg-3', 5'-Tg-(8-oxodG)-3', or an isolated Tg or 8-oxodG at a defined site and assessed how these lesions compromise the efficiency and fidelity of DNA replication in *E. coli* cells.

Experimental

Materials

Copper (II) chloride, L-methionine, L-ascorbic acid and calf thymus DNA were from Sigma-Aldrich (St. Louis, MO). Hydrogen peroxide (30%) and nuclease P1 were purchased from Fisher Scientific (Fair Lawn, NJ) and MP Biomedicals (Aurora, OH), respectively. Unmodified ODNs used in this study were purchased from Integrated DNA Technologies (Coralville, IA), and [γ-^{32}P]ATP was obtained from Perkin Elmer (Piscataway, NJ). 1,1,1,3,3,3-hexafluoro-2-propanol (HFIP) was purchased from TCI America (Portland, OR). Shrimp alkaline phosphatase was obtained from USB Corporation (Cleveland, OH); all other enzymes were from New England Biolabs (Ipswich, MA). The single-stranded pYMV1 vector and the wild-type AB1157 *E. coli* strain were kindly provided by Prof. Peter E.M. Gibbs (*42*) and Prof. John M. Essigmann, respectively. The polymerase-deficient AB1157 strains [Δ*pol B1*::spec (pol II-deficient), *ΔdinB* (pol IV-deficient), *ΔumuC*::kan (pol V-deficient) and *ΔumuC*::kan *ΔdinB* (pol IV, pol V-double knockout)] were generously provided by Prof. Graham C. Walker (*43*).

Treatment of calf thymus DNA

Calf thymus DNA was desalted by ethanol precipitation. The DNA pellet was redissolved in a solution containing 100 mM NaCl, 1 mM EDTA and 10 mM Tris-HCl (pH 7.5), and the DNA was annealed by heating the solution to 90 °C and cooling slowly to room temperature. Aliquots of DNA (150 μg) were incubated with $CuCl_2$ (12.5-200 μM), H_2O_2 (0.1-1.6 mM), and ascorbate (1-16 mM) in a 0.5-mL solution at room temperature for 50 min (The concentrations of individual Fenton reagents are shown in Table 4-1). In this respect, chemicals used in Fenton-type reaction were freshly dissolved in doubly distilled water and the reactions were carried out under aerobic conditions. The reactions were terminated by adding an excess amount of L-methionine, and the resulting DNA samples were desalted by ethanol precipitation and quantified by measuring the UV absorbance at 260 nm.

For the treatment with γ rays, calf thymus DNA (50 μg) was first dissolved in a 250 μL solution containing 50 mM NaCl and 10 mM phosphate (pH 7.0), Cu(II), and ascorbate at concentrations shown in Table 4-1. The resulting solution was exposed to γ rays delivered by a Mark I ^{137}Cs irradiator (JL Shepherd and Associates, San Fernando, CA). The samples were exposed to γ rays at a total dose of 50 Gy over a period of 20 min. The γ ray-exposure experiments were also carried out in the presence of 50 μM of Cu(II), 4 mM of ascorbate, or both. After the γ-ray exposure, the DNA samples were desalted by ethanol precipitation and quantified.

Table 4-1. Concentrations of Fenton-type reagents employed for the treatment of calf thymus DNA[a]

	Control	A	B	C	D	E
$CuCl_2$ (μM)	0	12.5	25.0	50.0	100	200
H_2O_2 (μM)	0	100	200	400	800	1600
Ascorbate (mM)	0	1.0	2.0	4.0	8.0	16

a, All reactions were carried out in a 500 μL solution containing 150 μg of calf thymus DNA.

Enzymatic digestion of calf thymus DNA

To the above treated DNA (20 μg) were added 2 units of nuclease P1 and a 30-μL buffer solution containing 300 mM sodium acetate (pH 5.0) and 10 mM zinc acetate. The digestion was continued at 37 °C for 4 hrs, and the enzyme in the resulting digestion mixtures was removed by chloroform extraction. The amount of nucleosides in the mixture was quantified by UV absorbance measurements, and aliquots of the nucleoside mixture were subjected directly to LC-MS/MS analysis.

Quantitative LC-MS/MS analysis

LC-MS/MS quantification was performed by using an Agilent 1100 capillary HPLC pump (Agilent Technologies, Santa Clara, CA) interfaced with an LTQ linear ion-trap mass spectrometer (Thermo Fisher Scientific, San Jose, CA). A 0.5×250 mm Zorbax SB-C18 column (5 μm in particle size, Agilent Technologies) was used for the separation of the DNA hydrolysates, and the flow rate was 7.0 μL/min. A 10-min gradient of 0-20% methanol in 400 mM HFIP (pH was adjusted to 7.0 by addition of triethylamine), followed by a 30-min gradient of 20-50% methanol in 400 mM HFIP, was used for the separation. The mass spectrometer was set up for monitoring the fragmentation of the $[M - H]^-$ ions of 2'-deoxyadenosine-5'-phosphate (pdA) and dinucleotides pTg-p(8-oxodG) and pTg-pdG. The capillary temperature for the electrospray source of the mass spectrometer was maintained at 300 °C to minimize the formation of the HFIP adducts of nucleotides.

Construction of calibration curves for the quantifications of the 5'-Tg-(8-oxodG)-3' tandem lesion and an isolated Tg lesion

Certain amounts of tandem lesion-containing dodecameric standard, d(ATGGCTgG*GCTAT) [G* represents an 8-oxodG, and Tg represents the *cis*-(*5R,6S*) diastereomer of Tg], or single Tg lesion-bearing dodecameric standard, d(ATGGCTgGGCTAT) (*44*), were mixed with 20 μg of untreated calf thymus DNA. The resulting DNA was enzymatically digested following the same methods as described above and the samples were subjected to LC-MS/MS analysis.

Preparation of lesion-bearing ODN substrates

The above described 12mer lesion-bearing substrates were 5'-phosphorylated firstly, then ligated with a d(GTATCCTCC) in the presence of a template ODN, d(TTTTATAGCACGCCATGGAGGATACTTTT), following previously described procedures (*28*). The resulting lesion-containing 21-mer ODNs (sequences shown in Table 4-2) were purified by using 20% denaturing polyacrylamide gel electrophoresis (PAGE) and desalted by ethanol precipitation. The integrity and purity of the ligation products were further confirmed by LC-MS/MS and PAGE analysis.

Construction of ss-pYMV1 genomes harboring a site-specifically inserted 8-oxodG, Tg, 5'-(8-oxodG)-Tg-3', or 5'- Tg-(8-oxodG)-3'

The lesion-containing single-stranded pYMV1 viral genomes and the control lesion-free genome were prepared following the previously described procedures (*45*). Briefly, 20 pmol of pYMV1 vector was digested with 40 U EcoRI at 23°C for 8 hrs to

Table 4-2. The sequences of ligated ODNs for *in vivo* replication ("G*" and "Tg" represent an 8-oxodG and thymidine glycol, respectively).

ODNs	Sequences
Control	5'-GTATCCTCCATGGCGTGCTAT-3'
5'-(8-oxodG)-dT-3'	5'-GTATCCTCCATGGC**G***TGCTAT-3'
5'-Tg-dG-3'	5'-GTATCCTCCATGGCG**Tg**GCTAT-3'
5'-(8-oxodG)-Tg-3'	5'-GTATCCTCCATGGC**G*Tg**GCTAT-3'
5'-Tg-(8-oxodG)-3'	5'-GTATCCTCCATGGC**TgG***GCTAT-3'

linearize the vector. Two scaffolds:

5'-ATGGAGGATACCACTGAATCATGGTCATAGC-3'

and 5'-AAAACGACGGCCAGTGAATTATAGC-3' (25 pmol), each spanning one end of the linearized vector and the modified ODN insert, were annealed with the linearized pYMV1 vector. The 21mer control or lesion-containing inserts were 5'-phosphorylated with T4 polynucleotide kinase and subsequently ligated to the above vector by using T4 DNA ligase at 16°C for 8 hrs. T4 DNA polymerase (22.5 U) was subsequently added and the solution was incubated at 37°C for 4 hrs to digest the scaffolds and residual unligated pYMV1 vector. The constructed genomes were normalized against a lesion-free competitor genome (*45, 46*), which was prepared by inserting a 24mer unmodified ODN, 5'-GTATCCTCCATGGCACAGCGCTAT-3', to the EcoRI-linearized genome.

Transfection of E. coli cells with ss-pYMV1 vectors containing an 8-oxodG, Tg, 5'-(8-oxodG)-Tg-3' or 5'- Tg-(8-oxodG)-3'

Purified control or lesion-containing genome (150 fmol) was mixed with the competitor genome at a molar ratio of 6:1 (lesion/competitor) and transfected into the AB1157 *E. coli* cells by electroporation. The *E. coli* cells were then grown in 3-mL LB medium at 37°C for 6 hrs and the phage was recovered from the supernatant by centrifugation at 13,000 rpm for 5 min. The resulting phage was further amplified in SCS110 *E. coli* cells to increase the progeny/lesion-genome ratio (*45, 46*). After the phage was recovered from the supernatant, the progenies of the pYMV1 vector were isolated using QIAprep Spin M13 kit (Qiagen, Valencia, CA).

Determination of the bypass efficiency and mutation frequency using competitive replication and adduct bypass (CRAB) and restriction endonuclease and post-labeling (REAP) assays

CRAB and REAP assays were carried out to examine the bypass efficiency and mutation frequency according to the previously described procedures (*45-47*) with some modifications (*48*). PCR amplification of the region of interest in the resulting isolated progeny genome was performed by using Phusion high-fidelity DNA polymerase. The primers were 5'-YCAGCTATGACCATGATTCAGTGGTATCCTCC-3' and 5'-Y TCGGTGCGGGCCTCTTCGCTATTAC-3' (Y is an amino group), and the amplification conditions consisted of 10 s at 98°C, 30 s at 62°C, 15 s at 72°C for 30 cycles, followed by a final extension at 72°C for 5 min. The PCR products were purified by using QIAquick PCR purification kit (Qiagen, Valencia, CA).

For the bypass efficiency assay, 5% of the above PCR products was treated with 10 U NcoI and 1 U shrimp alkaline phosphatase in a 10-μL NEB buffer 2 at 37°C for 2 hrs, followed by heating at 65°C for 20 min to deactivate the phosphatase. The mixture was then treated in a 15-μL NEB buffer 2 containing 5 mM DTT, ATP (50 pmol cold, premixed with 1.66 pmol [γ-^{32}P] ATP) and 10 U polynucleotide kinase. The reaction was continued at 37°C for 1 hr, followed by heating at 65°C for 20 min to deactivate the polynucleotide kinase. To the above reaction mixture was added Tsp509I (10 U) and the solution was incubated at 65°C for 1 hr, followed by quenching with 15 μL formamide gel loading buffer containing xylene cyanol FF and bromophenol blue dyes. The mixture was resolved by using 30% native polyacrylamide gels (acrylamide:bis-acrylamide=19:1)

and quantified by phosphorimager analysis. After the restriction enzyme cleavages, the DNA fragment of interest from the full-length replication product was liberated as an 13mer ODN, d(p*CATGGC**MN**GCTAT), where "MN" designates the nucleobases present at the original 5'-(8-oxodG)-dT-3', 5'-Tg-dG-3', 5'-(8-oxodG)-Tg-3' or 5'-Tg-(8-oxodG)-3' site after *in vivo* DNA replication and "p*" represents the 5'-radiolabeled phosphate. The 13mer with a single-nucleotide difference could be resolved by 30% native polyacrylamide gels except that the 13mer-GT and 13mer-CT exhibited similar mobility. On the other hand, the corresponding DNA fragment released from the competitor genome was a 16mer ODN, d(p*CATGGCACAGCGCTAT). The mutation frequencies were determined from the relative amounts of different 13mer products from the gel band intensities except for the G→C mutation arising from 8-oxodG, which was calculated by combining LC-MS/MS analysis with gel assay. Briefly, we first measured the ratio of 13mer-CT/13mer-TT (ratio A) by LC-MS/MS and quantified the ratio (ratio B) of 13mer-TT over the total amount of all 13mer bypass products (i.e., 13mer-GT, 13mer-CT and 13mer-GT) by gel electrophoresis, and we then obtained the frequency of the G→C mutation by multiplying the ratios A and B. The bypass efficiency was calculated using the following formula, %bypass= (lesion signal/competitor signal)/(non-lesion control signal/its competitor signal) (*45*).

Identification of replication products by using LC-MS/MS

In order to identify the replication products using LC-MS/MS, 80% of the above PCR products were treated with 50 U NcoI and 20 U shrimp alkaline phosphatase in 200-μL NEB buffer 2 at 37°C for 2 hrs, followed by heating at 65°C for 20 min. To the

resulting solution was added Tsp509I (50 U), and the reaction mixture was incubated at 65°C for 1 hr followed by extraction with phenol/chloroform/isoamyl alcohol (25:24:1, v/v), and the aqueous portion was dried with Speed-vac and dissolved in water. The resulting mixture was subjected to LC-MS/MS analysis. A 0.5×150 mm Zorbax SB-C18 column (Agilent Technologies) was used for the separation, the flow rate was 8.0 μL/min, and a 5-min gradient of 0-20% methanol followed by a 35-min of 20-50% methanol in 400 mM HFIP was employed for the separation. The LTQ linear ion trap mass spectrometer was set up for monitoring the fragmentation of the $[M-3H]^{3-}$ ions of the 13mer [d(CATGGC**MN**GCTAT), where "**MN**" designates GT, TT, CT, or TG] and 16mer [i.e., d(CATGGCACAGCGCTAT)] ODNs.

Results

Quantitative measurement of the formation of tandem single-nucleobase lesions in DNA by LC-MS/MS necessitates the development of enzymatic digestion procedures for the selective release of the tandem lesion as a unique chemical entity. To this end, we took advantage of the previous observation that thymidine glycol prohibits the cleavage of its 3' phosphodiester linkage by nuclease P1 (*49*), and employed this enzyme to liberate the tandem 5'-Tg-(8-oxodG)-3' lesion from DNA as a dinucleotide. Under this digestion condition, an isolated Tg is also released along with its 3' flanking undamaged nucleoside as a dinucleotide.

We supplemented calf thymus DNA with different amounts of an authentic dodecameric ODN carrying an isolated thymidine glycol (5'-Tg-dG-3') or the 5'-Tg-(8-oxodG)-3' tandem lesion. We then digested the DNA mixture with nuclease P1,

removed the enzyme, and subjected it to LC-MS/MS analysis, where we monitored specifically the fragmentation of the $[M - H]^-$ ions of 2'-deoxyadenosine-5'-phosphate (pdA) and Tg-carrying dinucleotide, namely, 5'-pTg-p(8-oxodG)-3' (Figure 4-2), for the tandem lesion-carrying substrate, or 5'-pTg-pdG-3', for the substrate containing a Tg situating on the 5' side of an unmodified dG. The ratio for the peak areas found in the extracted-ion chromatogram for monitoring the fragmentation of the dinucleotide over that for pdA was then plotted against the amount of Tg- or 5'-Tg-8-oxodG-3'-bearing substrate that we added, which afforded straight lines for both types of lesion-containing substrates (Figure 4-3). These results support that nuclease P1 digestion combined with LC-MS/MS analysis can allow for a reliable quantification of the thymidine glycol lesion, which is present on the 5' side of an unmodified nucleoside or 8-oxodG. In this respect, we normalized the ion currents of the analytes to that of pdA to correct for the variation in sample loading and analyte loss during the sample preparation.

After having established an analytical method for monitoring the formation of the tandem 5'-Tg-(8-oxodG)-3' lesion and Tg followed by an unmodified dG, we demonstrated the formation of these two types of lesions in calf thymus DNA treated with Cu(II)/H_2O_2/ascorbate (Figure 4-2). Quantification of the results revealed the dose-responsive formation of both lesions (Figure 4-4a). To our surprise, we observed that the yield of the tandem lesion, 5'-Tg-(8-oxodG)-3', was merely 5-6 fold lower than what was found for the Tg that is situated on the 5' side of an unmodified dG (Figure 4-4a).

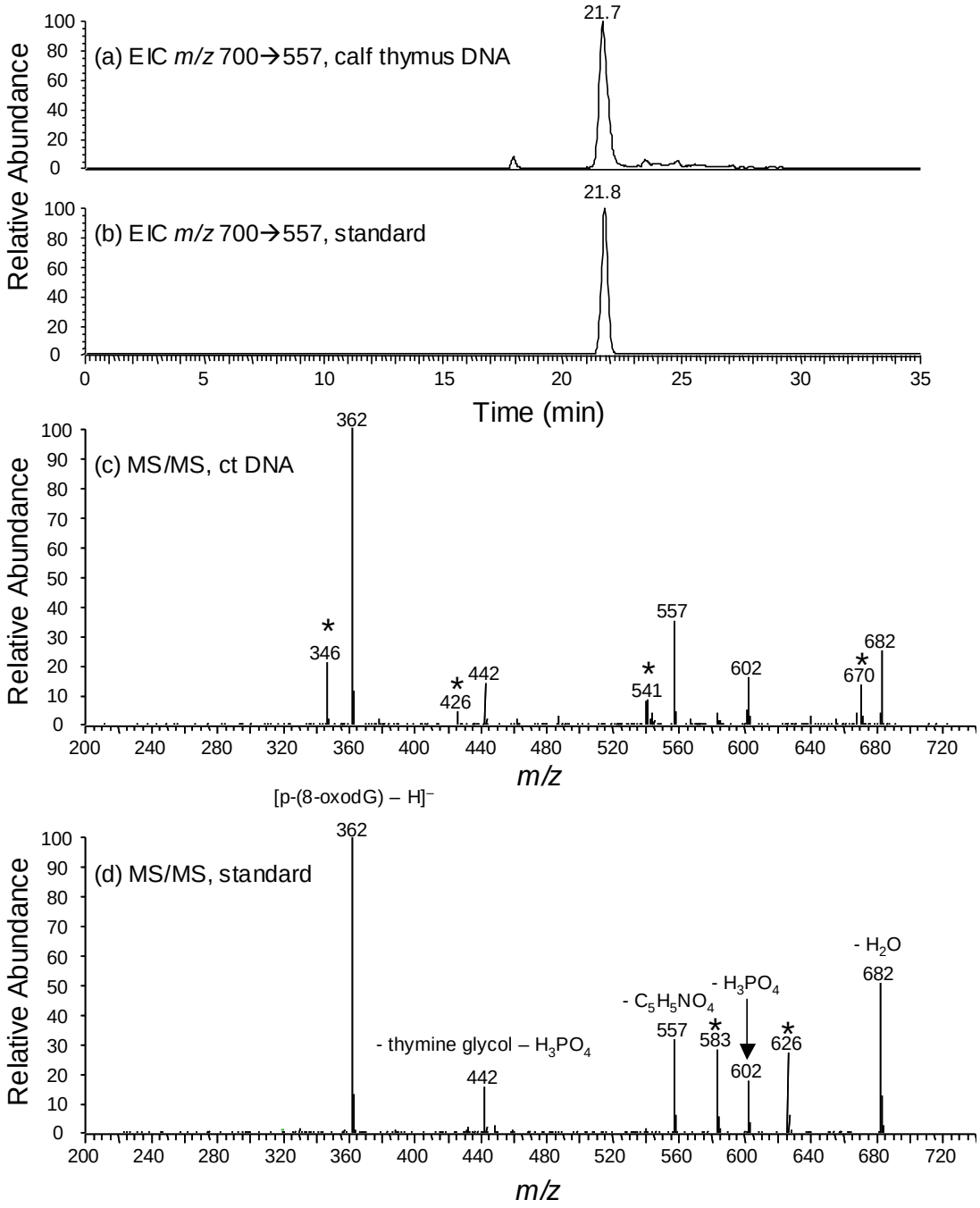

Figure 4-2. LC-MS/MS identification of 5'-Tg-(8-oxodG)-3' tandem lesion formation in calf thymus DNA treated with Cu(II)/H_2O_2/ascorbate. Extracted-ion chromatograms (EICs) for monitoring the *m/z* 700 → 557 transitions for pTg-p(8-oxodG) in Fenton reagent-treated calf thymus DNA (under reaction condition D described in Table 4-1, a) and calf thymus DNA doped with authentic tandem lesion-containing ODN (b). Shown in (c) and (d) are the MS/MS averaged from the 21.7-min peak in (a) and the 21.8-min peak in (b). Ions labeled with "*" are due to the fragmentation of other co-eluting species.

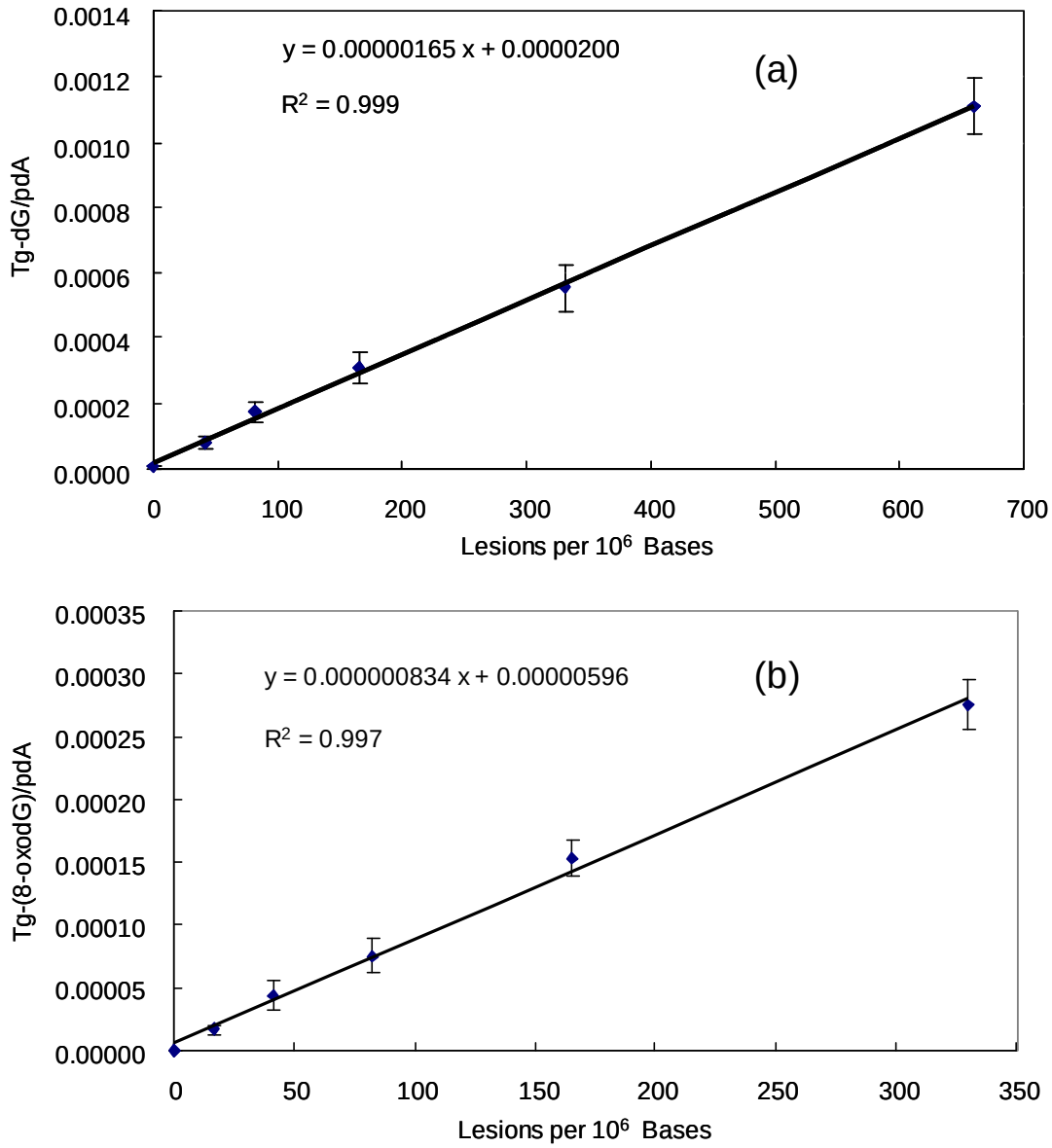

Figure 4-3. Calibration curves for the quantification of pTg-dG (a) and pTg-p(8-oxodG) (b). Plotted in (a) is the ratio of peak area found in the extracted-ion chromatogram (EIC) for the *m/z* 684→541 transition for the loss of the $C_5H_5NO_4$ from the modified thymine glycol moiety in pTg-pdG (see ref. 9) over the peak area found in the EIC for the $[M - H]^-$ ion of pdA (*m/z* 330) versus the amount of the lesion (in lesions per 10^6 nucleobases). Plotted in (b) is the ratio of peak area found in the EIC for the *m/z* 700→557 transition for the loss of the $C_5H_5NO_4$ from the modified thymine glycol moiety (see ref. 9) in pTg-p(8-oxodG) over the peak are found in the EIC for the $[M - H]^-$ ion of pdA (*m/z* 330) versus the amount of lesion, in lesions per 10^6 nucleobases.

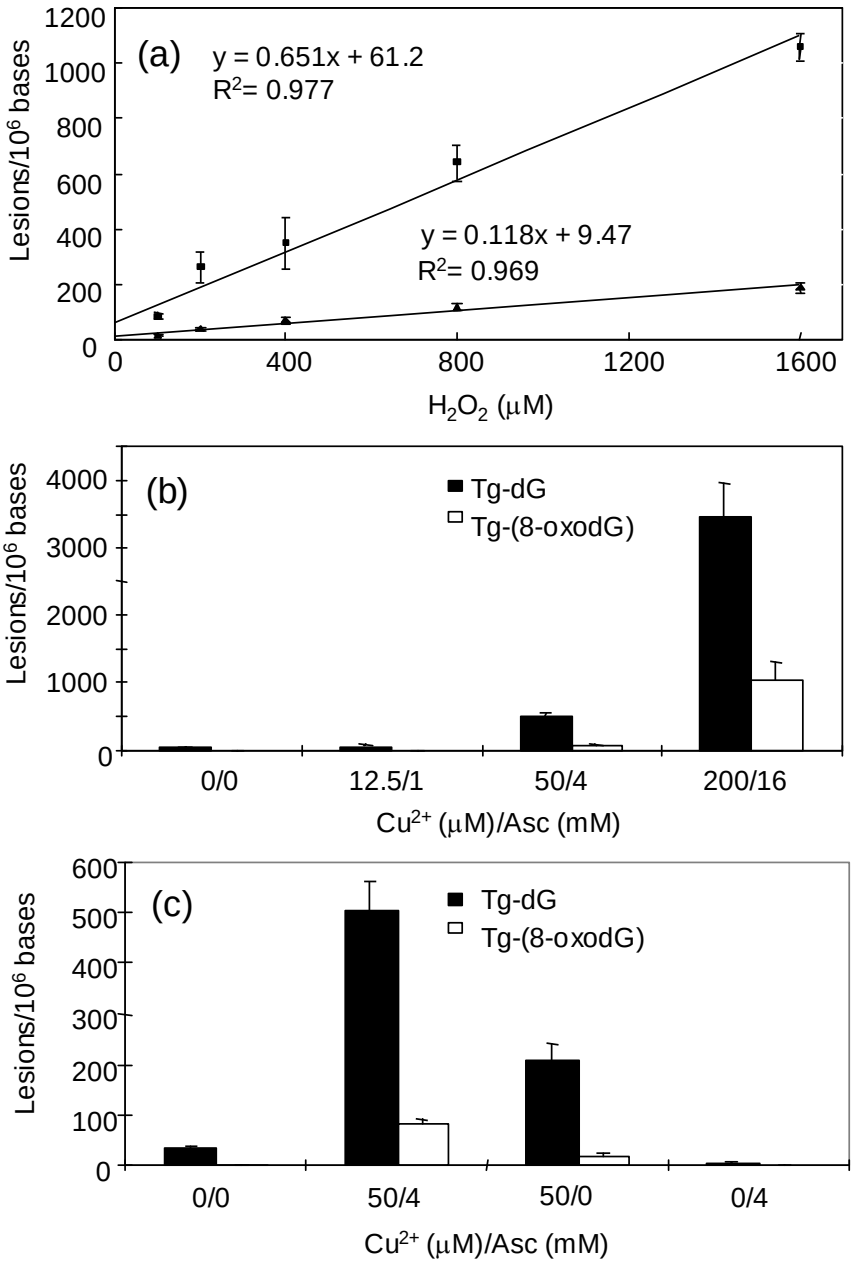

Figure 4-4. The quantitative formation of the 5'-Tg-dG-3' and 5'-Tg-(8-oxodG)-3' lesions in calf thymus DNA exposed with Cu(II) and ascorbate along with H_2O_2 or γ rays. (a) Dose-dependent induction of the 5'-Tg-dG-3' and 5'-Tg-(8-oxodG)-3' lesions in calf thymus DNA by Cu(II)/H_2O_2/Ascorbate. (b) The induction of 5'-Tg-dG-3' and 5'-Tg-(8-oxodG)-3' lesions in calf-thymus DNA upon exposure to 50 Gy of γ rays in combination with Cu(II) and ascorbate at the indicated concentrations. (c) The induction of 5'-Tg-dG-3' and 5'-Tg-(8-oxodG)-3' lesions in calf thymus DNA upon treatment with 50 Gy of γ rays, alone or in combination with 50 μM Cu(II), 4 mM ascorbic acid, or both. The data represent the means ± S.D. of results from three independent treatments and LC-MS/MS quantification experiments.

Our experimental results also revealed that copper ions, especially Cu(I), can stimulate the γ ray-induced formation of the 5'-Tg-(8-oxodG)-3' tandem lesion (Figure 4-4b&c). In this regard, we exposed calf thymus DNA to 50 Gy of γ-rays in the presence of increasing concentrations of Cu(II) and ascorbate, and quantified the Tg and Tg-(8-oxodG) lesions by LC-MS/MS. The presence of Cu(II) and ascorbate enhanced markedly the γ ray-mediated formation of both types of lesions. For instance, the amount of the 5'-Tg-(8-oxodG)-3' formed in the presence of 200 μM of Cu(II) and 16 mM of ascorbate is approximately 400 times higher than that induced by γ-rays alone (Figure 4-4b). To gain further insights into the Cu(II)/ascorbate-enhanced formation of these lesions, we also compared the formation of lesions in calf thymus DNA upon treatment with 50 Gy of γ-rays in the presence of 50 μM of Cu(II) or 4 mM of ascorbate, or both. It turned out that, while the presence of ascorbate inhibited considerably the formation of both types of lesions, the existence of Cu(II) stimulated significantly the formation of these lesions. The presence of both Cu(II) and ascorbate further enhanced the formation of both types of lesions (Figure 4-4c). These results support without ambiguity the role of Cu(I) in enhancing the γ ray-mediated formation of these lesions.

We next investigated the mutagenic and cytotoxic properties of the tandem lesions, where the Tg and 8-oxodG are neighboring to each other, as well as the isolated Tg and 8-oxodG in *E. coli* cells. To this end, we prepared the lesion-carrying 21-mer substrates by enzymatic ligation (Table 4-2), confirmed the identities of the 21-mer ODNs by ESI-MS and MS/MS (Figures 4-5 to 4-8), and inserted the above 21mer lesion-containing ODNs into the single-stranded pYMV1 genome. We then assessed the bypass

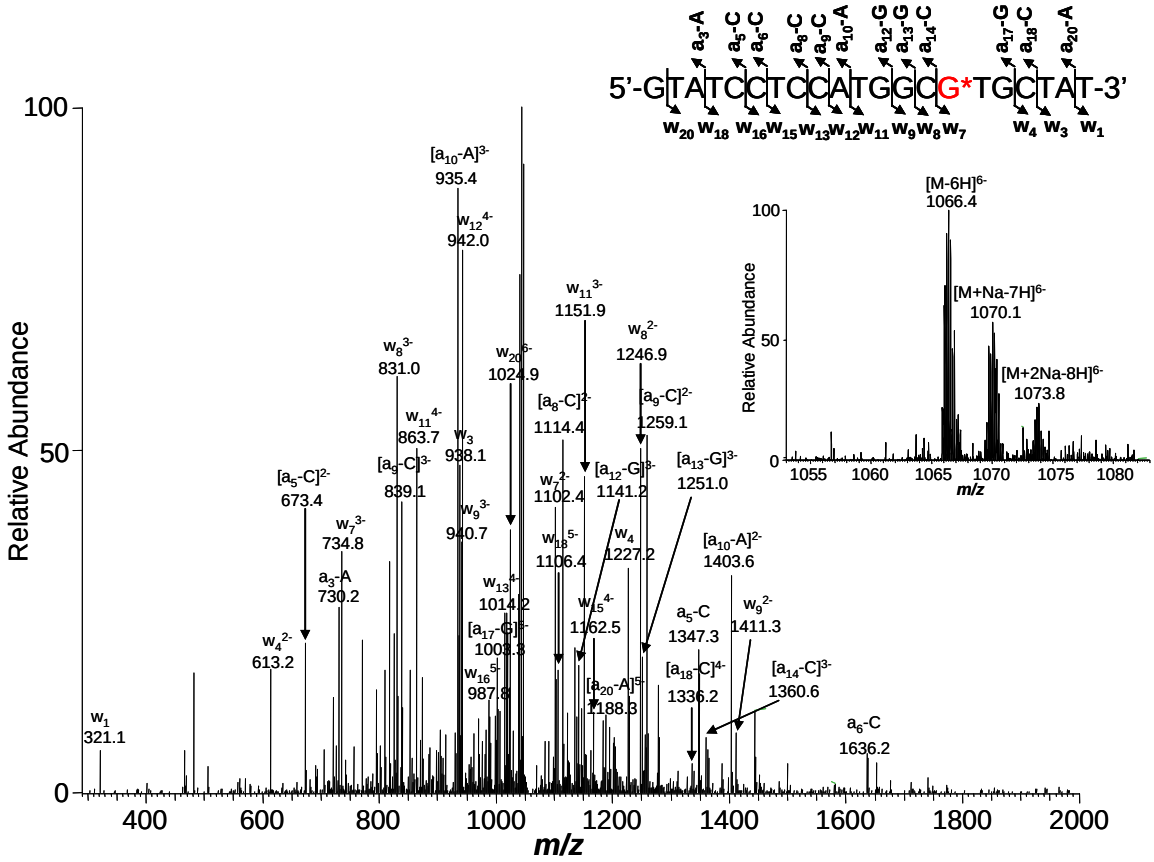

Figure 4-5. The product-ion spectrum of the ESI-produced $[M-6H]^{6-}$ ion (*m/z* 1065.8) of d(GTATCCTCCATGGC**G***TGCTAT). Shown in the inset are the zoom-scan negative-ion ESI-MS for the ODN and a scheme summarizing the observed fragment ions.

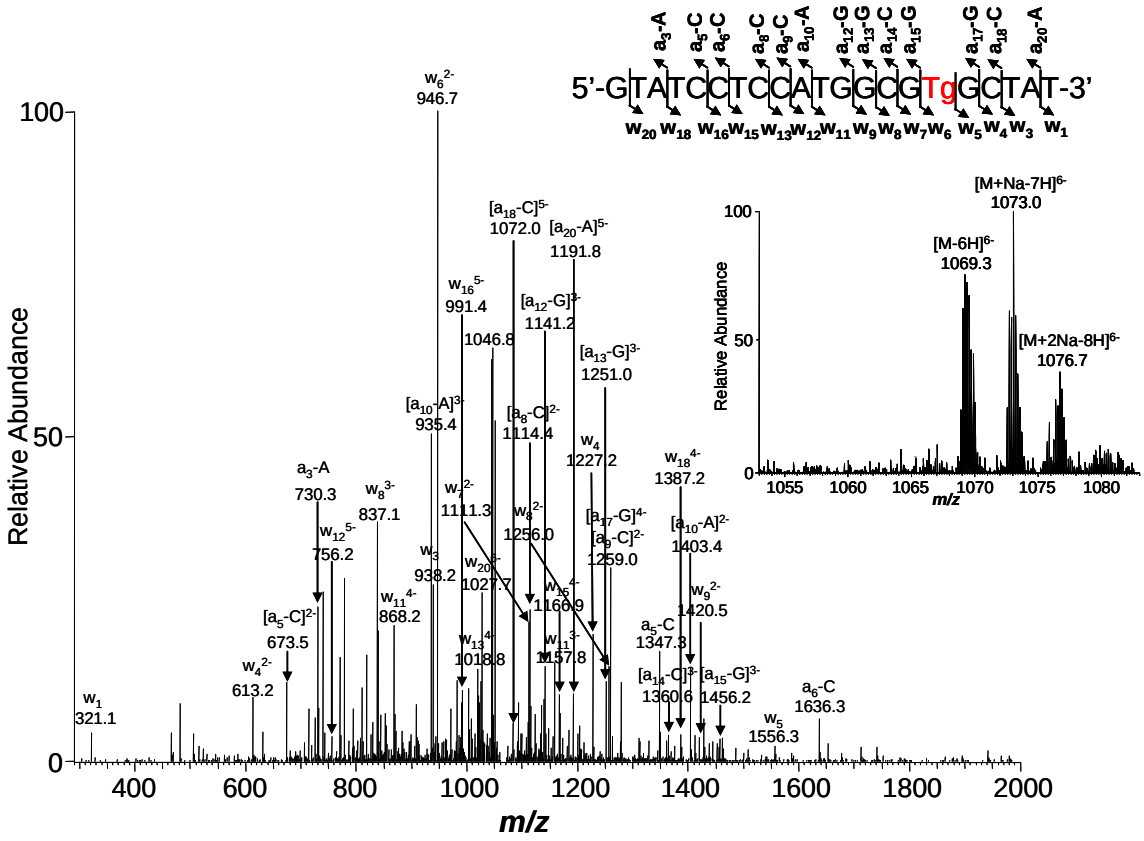

Figure 4-6. The product-ion spectrum of the ESI-produced $[M-6H]^{6-}$ ion (*m/z* 1068.8) of d(GTATCCTCCATGGCG**Tg**GCTAT). Shown in the inset are the zoom-scan negative-ion ESI-MS for the ODN and a scheme summarizing the observed fragment ions.

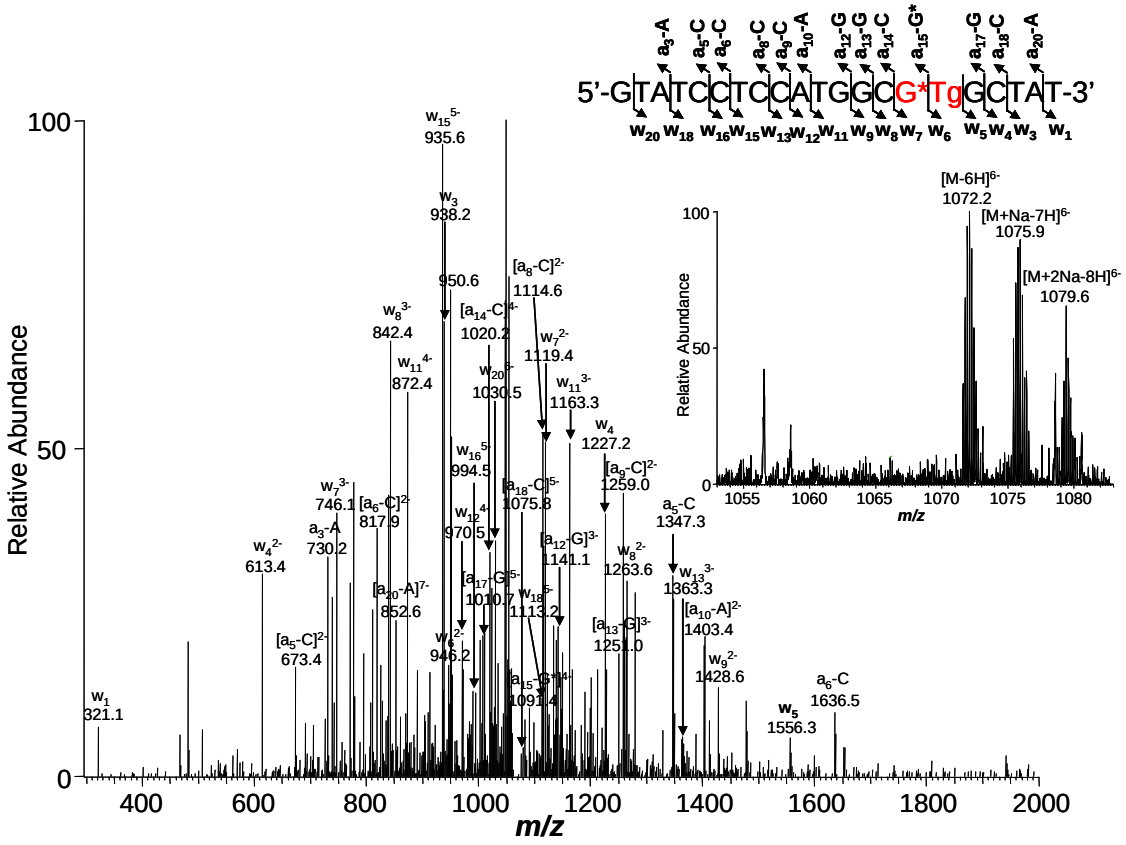

Figure 4-7. The product-ion spectrum of the ESI-produced $[M-6H]^{6-}$ ion (*m/z* 1071.5) of d(GTATCCTCCATGGC**G*Tg**GCTAT). Shown in the inset are the zoom-scan negative-ion ESI-MS for the ODN and a scheme summarizing the observed fragment ions.

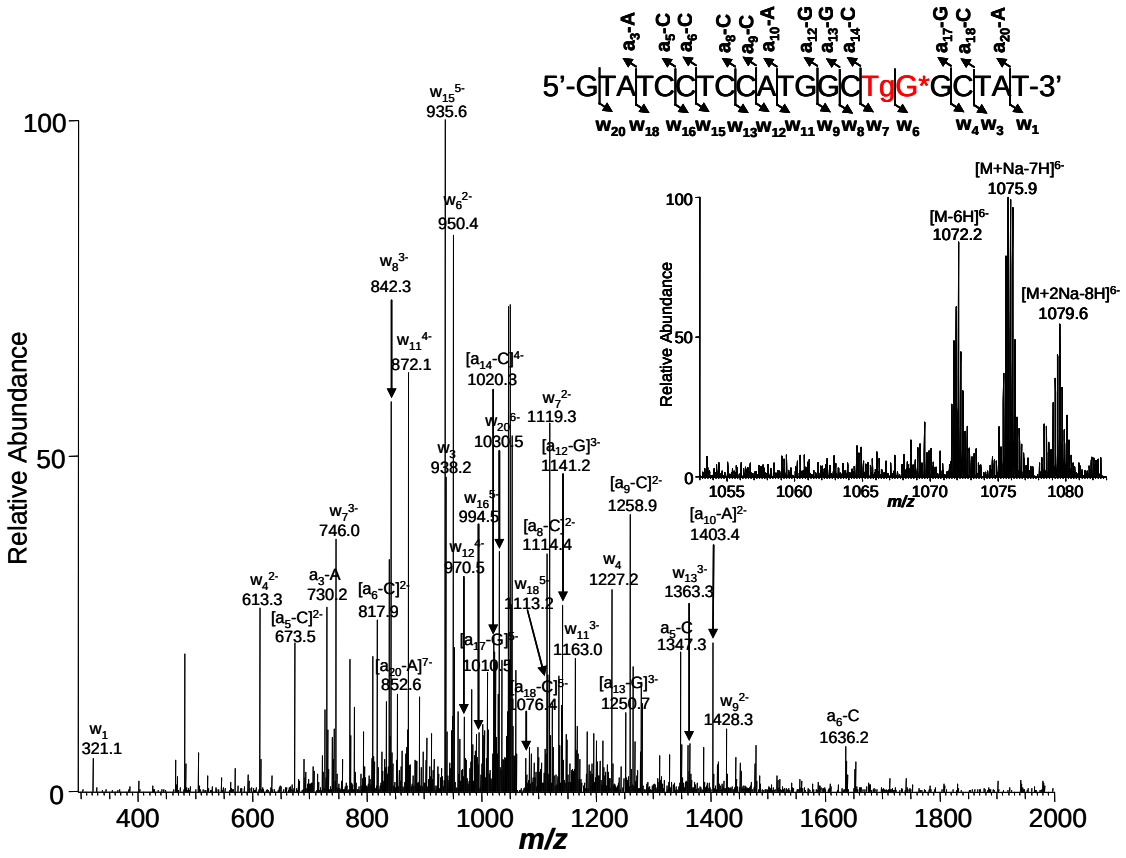

Figure 4-8. The product-ion spectrum of the ESI-produced $[M-6H]^{6-}$ ion (*m/z* 1071.5) of d(GTATCCTCCATGGC**TgG***GCTAT). Shown in the inset are the zoom-scan negative-ion ESI-MS for the ODN and a scheme summarizing the observed fragment ions.

efficiencies and mutation frequencies of these DNA lesions by using the CRAB and REAP assays introduced by Essigmann and coworkers (Figure 4-9) (*45*-*47*). A unique feature of these assays lies in that the entire progeny population was used for determining the mutation frequency and bypass efficiency, thereby affording statistically sound conclusions (*45*). Additionally, the methods do not require phenotypic selection (*45*).

Restriction digestion of the PCR products of the progeny pYMV1 genome resulting from *in-vivo* replication renders 13mer fragment(s) harboring the site where the single or tandem lesions were initially incorporated. The corresponding digestion of PCR products of the progeny of the competitor genome gives a 16mer fragment (Figure 4-9). The failure to detect radio-labeled fragments with lengths shorter than 13mer supports that none of the single or tandem lesions gives rise to deletion mutations (Figure 4-10). In this context, we employed 30% (19:1, acrylamide:bisacrylamide) non-denaturing polyacrylamide gels to resolve the ^{32}P-labeled fragments; the 13mers with a single nucleotide difference can be resolved from each other except that 13mer-GT and 13mer-CT exhibit very similar mobility (Figure 4-10).

It is worth noting that the identities of the above restriction fragments were confirmed by LC-MS/MS analyses (*48*). In this context, we were able to detect the 13mer ODNs d(CATGGC**MN**GCTAT) ["**MN**" is GT, TT or CT for the isolated 8-oxodG-bearing substrate; GT for the isolated Tg-bearing substrate; GT or TT for 5'-(8-oxodG)-Tg-3'; and TG, GT or TT for 5'-Tg-(8-oxodG)-3'] in the restriction digestion mixtures (Some example LC-MS and MS/MS results are depicted in Figures 4-11 to 4-13), which is consistent with the findings made from native PAGE analysis.

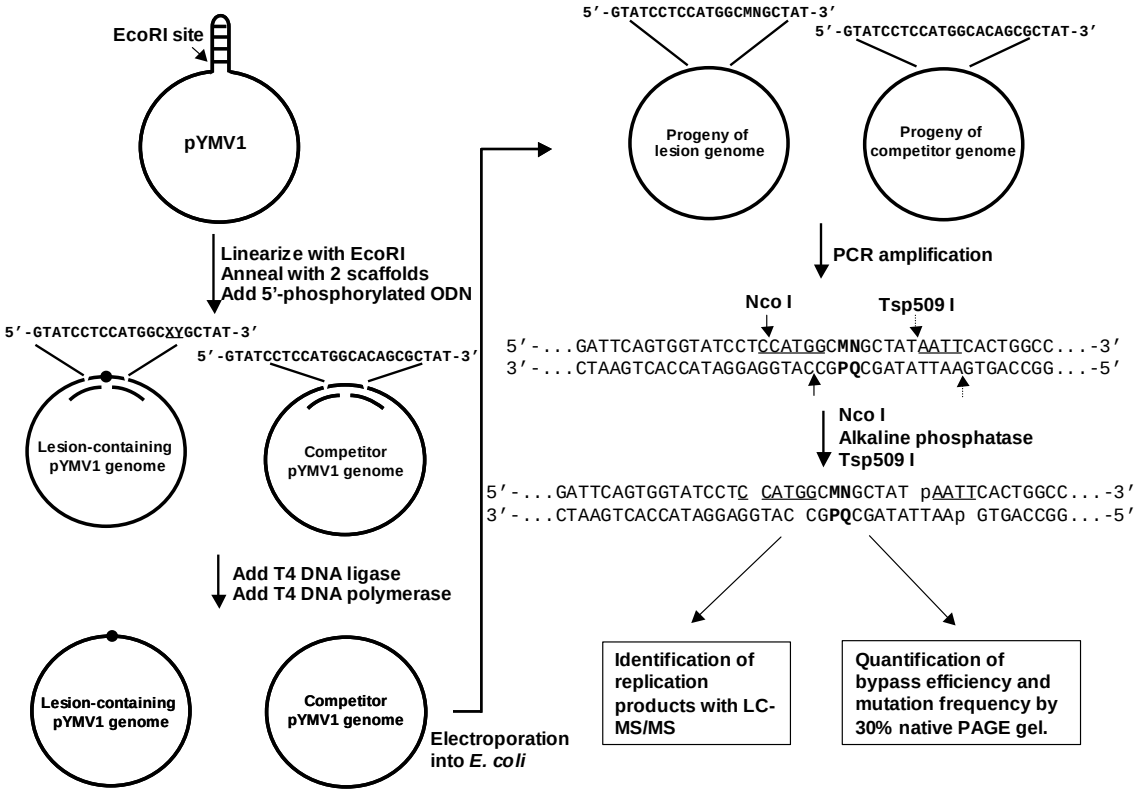

Figure 4-9. The method for the determination of the cytotoxicity and mutagenicity of DNA lesions in *E. coli* cells. "XY" in the 16mer ODN represents 5'-(8-oxodG)-dT-3' (G*T), 5'-Tg-dG-3' (TgG), 5'-(8-oxodG)-Tg-3' (G*Tg) and 5'-Tg-(8-oxodG)-3' (TgG*). "MN" in the progeny of the lesion genome represents the nucleotides inserted at the above dinucleotide site. NcoI and Tsp509I restriction endonuclease recognition sites are underlined and the cleavage sites induced by the two enzymes are designated by solid and broken arrows, respectively. Only partial sequence of PCR products for the lesion genome is shown, and the PCR products of the competitor genome are not shown.

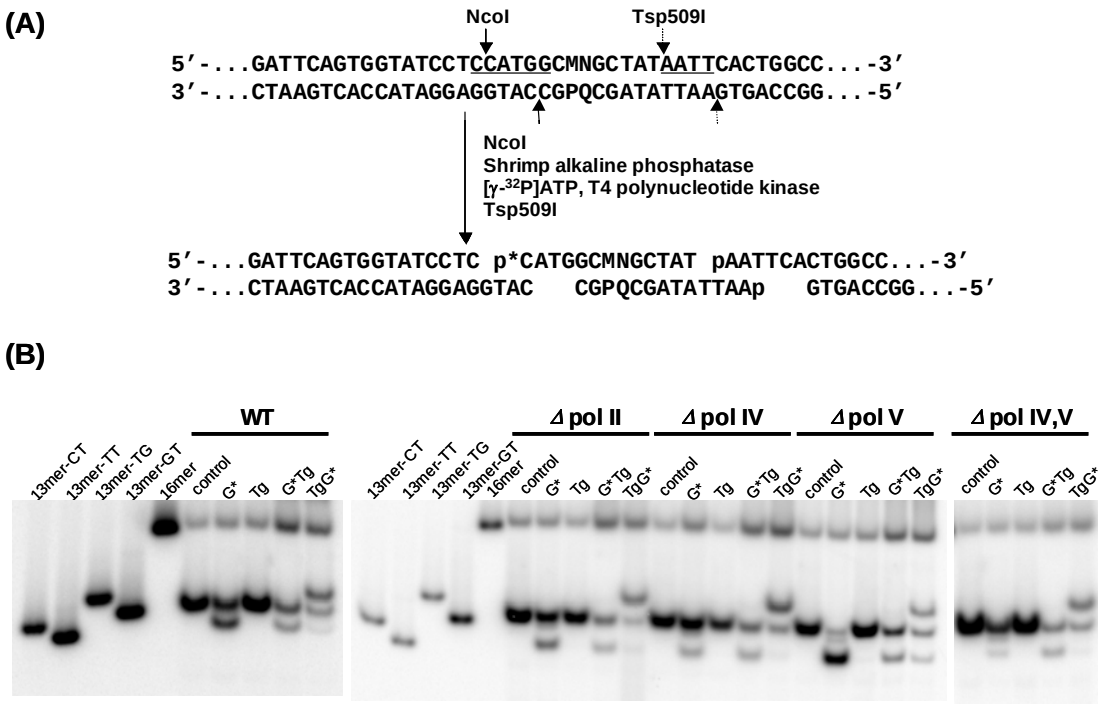

Figure 4-10. Measurement of the *in vivo* bypass efficiencies and mutation frequencies by the CRAB and REAP assay. (A) Sample processing ("p*" represents the ^{32}P-labeled phosphate group); (B) gel image showing the 16mer and 13mer ODNs released from the PCR products of the progeny resulting from the replication of the competitor genome and the control or lesion-carrying genome in wild-type and the isogenic AB1157 cells deficient in pol II, pol IV, pol V, or both pol IV and pol V. The restriction fragment arising from the competitor genome, i.e., d(CATGGCACAGCGCTAT), is designated with "16mer"; "13mer-GT", "13mer-TT", "13mer-CT" and "13mer-TG" represent standard ODNs d(CATGGC**MN**GCTAT), where "MN" are "GT", "TT", "CT" and "TG", respectively. G* represents 8-oxodG.

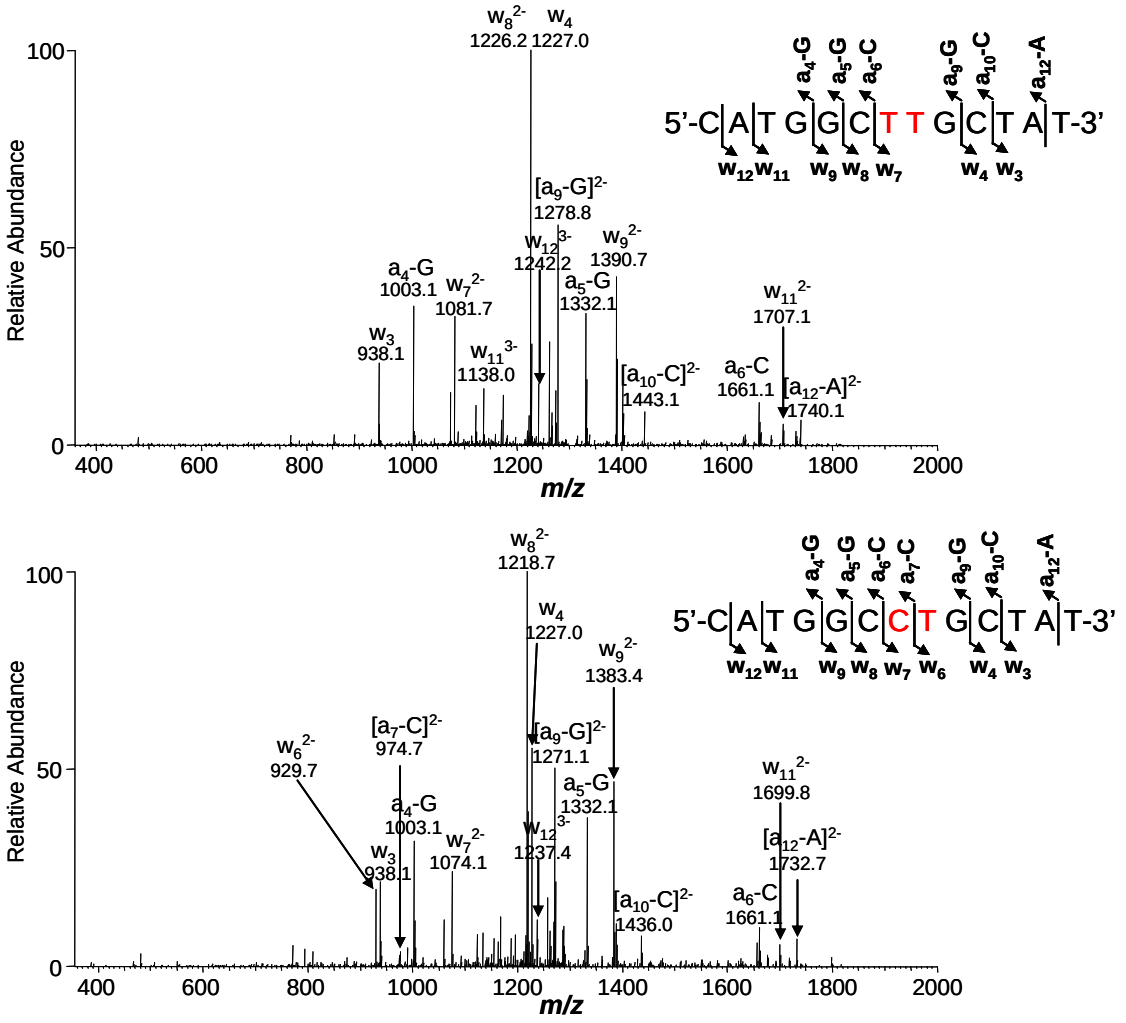

Figure 4-11. MS/MS for monitoring the restriction fragments arising from the replication, in wild-type AB1157 cells, of the isolated 8-oxodG-containing substrate. Shown are the MS/MS for the 13mer fragments with a G→T or G→C mutation at the original 8-oxodG site [i.e., d(CATGGC***T***TGCTAT) (A) and d(CATGGC***C***TGCTAT) (B)]. Depicted in the insets are schemes summarizing the observed fragment ions.

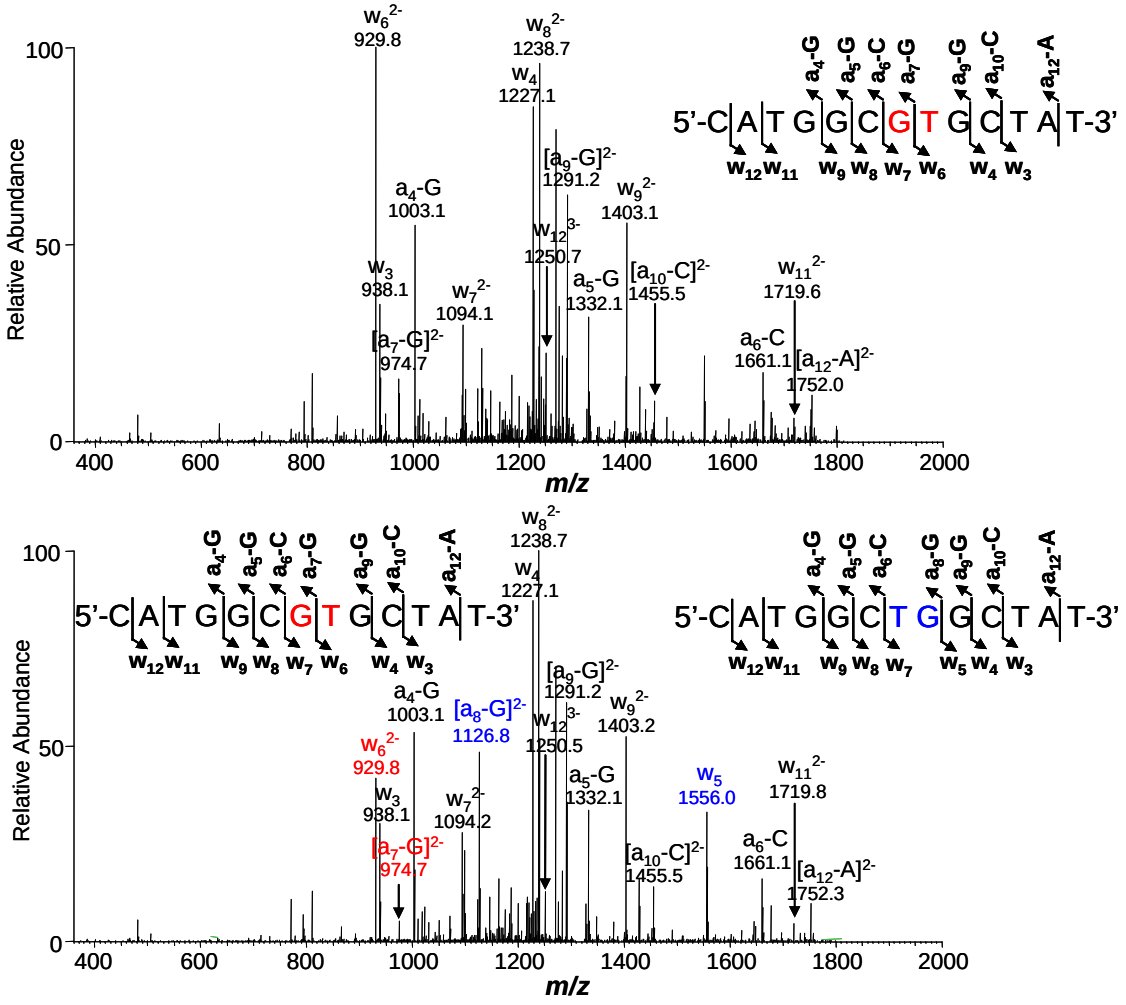

Figure 4-12. (A) MS/MS for monitoring the restriction fragment arising from the replication, in wild-type AB1157 cells, of the isolated 8-oxodG-containing substrate where there is no mutation [i.e., d(CATGGC***TG***GCTAT)]. (B) LC-MS/MS for monitoring the restriction fragments arising from the replication, in wild-type AB1157 cells, of the 5'-Tg-(8-oxodG)-3'-containing substrate where there is no mutation [i.e., d(CATGGC***TG***GCTAT)] or there is TG→GT tandem mutation [i.e., d(CATGGC***GT***GCTAT)]. Depicted in the insets are schemes summarizing the observed fragment ions. The unique fragment ions for d(CATGGC***GT***GCTAT) and d(CATGGC***TG***GCTAT) found in panel (B) are w_6^{2-}, $[a_7\text{-G}]^{2-}$ and w_5, $[a_8\text{-G}]^{2-}$, respectively.

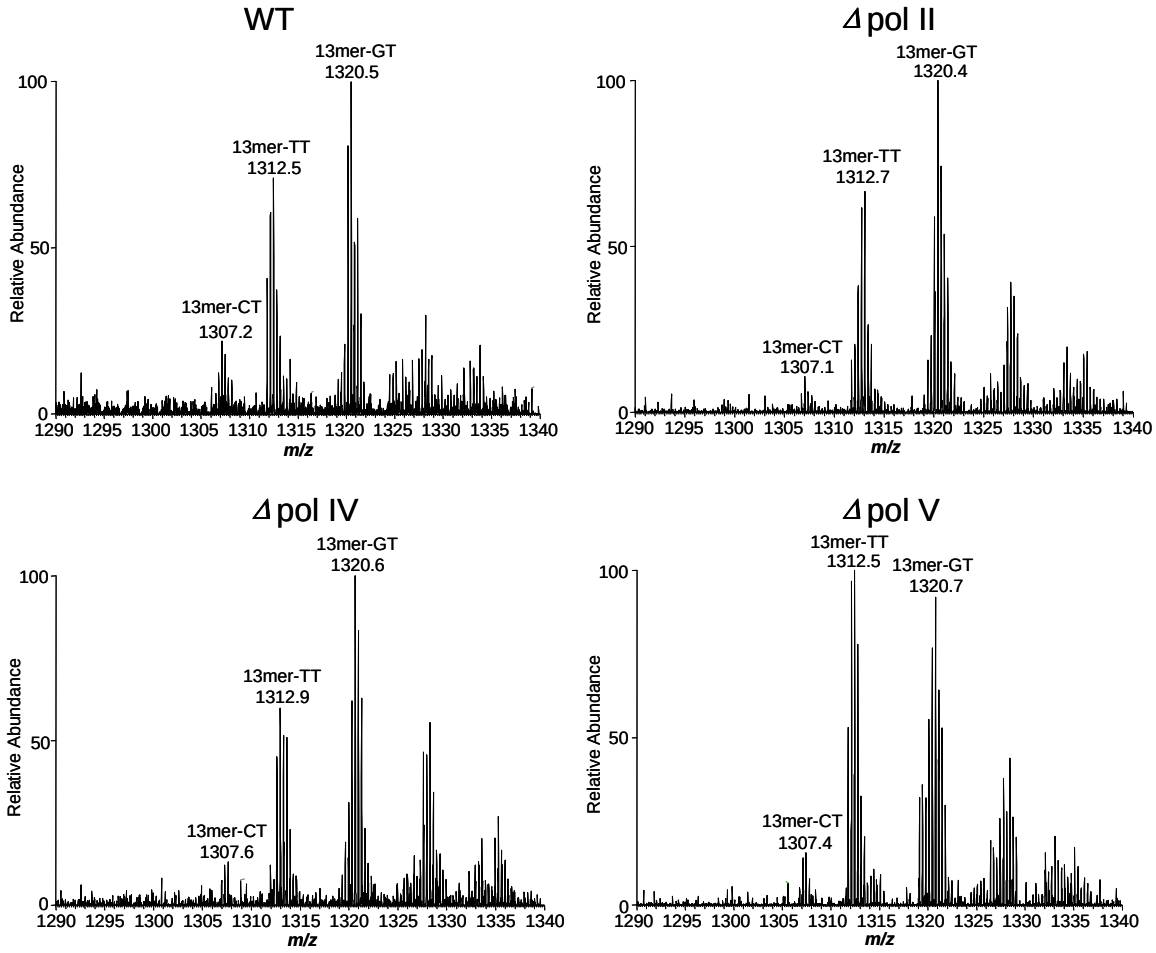

Figure 4-13. The zoom-scan negative-ion ESI-MS for monitoring the restriction fragments of interest without mutation [i.e., d(CATGGC***G***TGCTAT)] or with a G→T or G→C mutation at the original 8-oxodG site [i.e., d(CATGGC***T***TGCTAT) and d(CATGGC***C***TGCTAT)] in wild-type AB1157 cells (A) as well as in the isogenic cells deficient in pol II (B), pol IV (C) or pol V (D).

The bypass efficiencies were calculated from the ratio of the combined intensities of bands observed for the 13mer products, which were from the replication of the lesion genome, over the intensity of the 16mer band, from the replication of the competitor genome, with the consideration of the ratio of the lesion over competitor genomes employed during the initial transfection. The bypass efficiencies for the lesion-carrying genomes were then normalized against that for the control lesion-free genome.

The results showed that the bypass efficiencies for the tandem lesions are about one half of that for the isolated Tg or 8-oxodG in all AB1157 strains that we examined (Figure 4-14A). The bypass efficiencies for the isolated 8-oxodG, isolated Tg, 5'-(8-oxodG)-Tg-3' and 5'-Tg-(8-oxodG)-3' in wild-type AB1157 cells were ~102%, 90%, 46% and 56%, respectively (Figure 5-14A). However, the bypass efficiencies for all lesion-containing substrates dropped in the isogenic AB1157 cells deficient in pol IV, pol V, or both. Deficiency in pol II in the isogenic AB1157 background does not affect appreciably the bypass efficiencies of Tg or 8-oxodG, either present alone or in tandem (Figure 4-14A). These data support that both pol IV and pol V are involved partially in the bypass of Tg and 8-oxodG in *E. coli* cells, regardless of whether the two lesions are present alone or adjacent to each other.

The results from native PAGE analysis also allowed us to measure the mutation frequencies of these lesions in wild-type and DNA polymerase-deficient AB1157 *E. coli* strains (*43*). The quantification data showed that the 8-oxodG, when isolated or present in the 5'-(8-oxodG)-Tg-3' or 5-Tg-(8-oxodG)-3', is mutagenic in wild-type AB1157 cells, with G→T transversion occurring at frequencies of 38%, 32% and 7%, respectively.

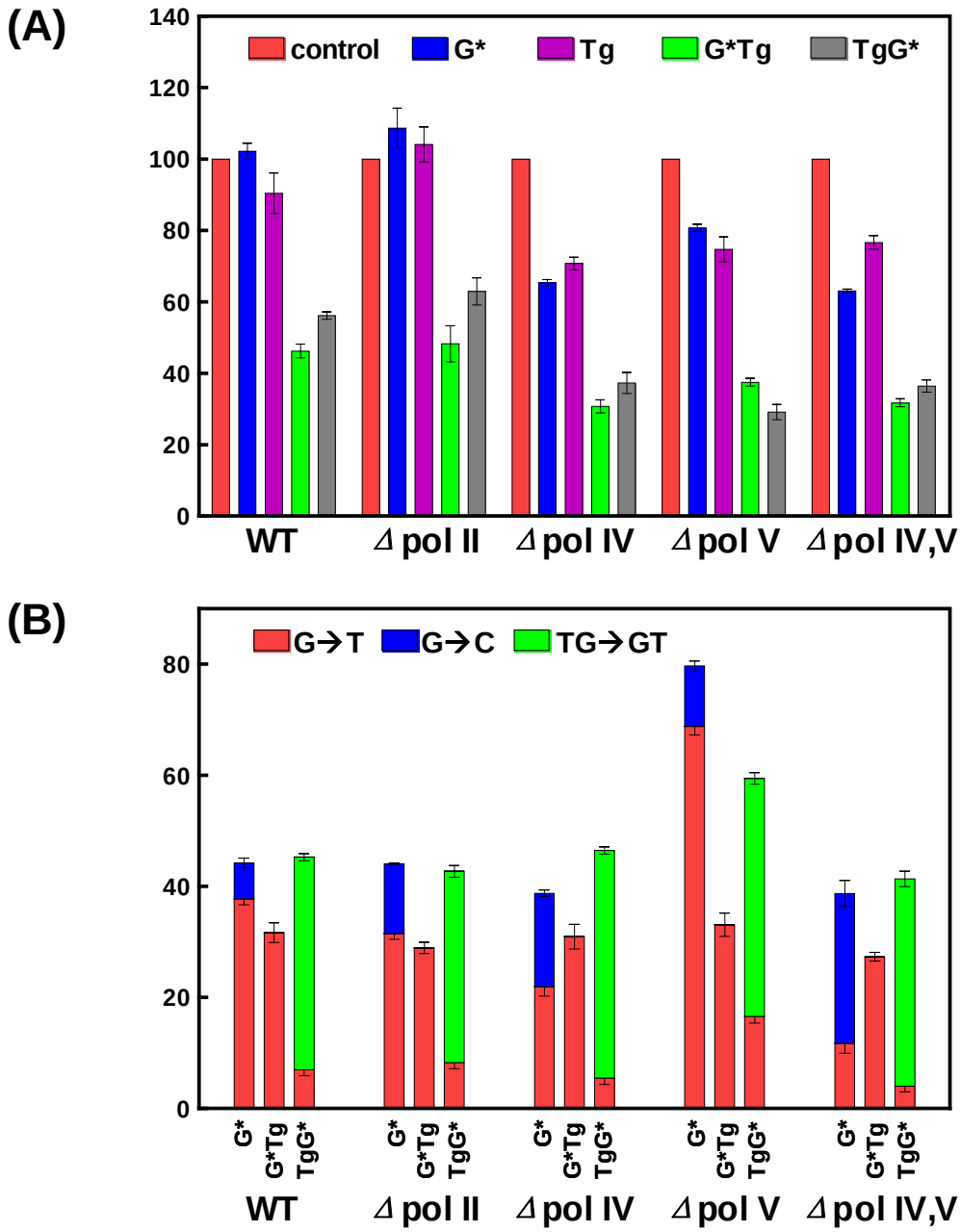

Figure 4-14. Bypass efficiencies (A) and mutation frequencies (B) of 8-oxodG and Tg, present alone or in tandem, in wild-type and polymerase-deficient AB1157 *E. coli* cells. Shown are the results for the substrates carrying unmodified GT, an isolated 8-oxodG (G*), an isolated Tg (Tg), 5'-(8-oxodG)-Tg-3' (G*Tg) and 5'-Tg-(8-oxodG)-3' (TgG*), respectively. "Ctrl" designates the control substrate. The data represent the means and standard deviations of results from three independent experiments.

Interestingly, the G→T mutation for the 8-oxodG that was isolated or situated on the 3' side of Tg was found to be decreased in pol IV-deficient cells and increased in pol V-deficient cells. However, deficiency in SOS-induced polymerases does not result in significant change in G→T mutation induced by 5'-(8-oxodG)-Tg-3' (Figure 4-14B). In addition, G→C mutation was found for 8-oxodG after it was replicated in all *E. coli* strains. To our surprise, we also observed a TG→GT tandem mutation at a frequency of approximately 40% in the replication of 5'-Tg-(8-oxodG)-3' in each strain we studied.

Discussion

The availability of ODNs containing both Tg and 8-oxodG (*44*) facilitated us to develop an LC-MS/MS method to quantify the formation of the tandem lesion where a Tg lies on the 5' side of an 8-oxodG and allowed us to assess the mutagenicity and cytotoxicity of the tandem lesions composed of Tg and 8-oxodG. We found that the tandem lesion, where a Tg lies on the 5' side of an 8-oxodG, could be induced, at a relatively high yield (i.e., about 5-6 fold less than an isolated Tg situated on the 5' side of an unmodified dG), in calf thymus DNA upon exposure to Cu(II)/ascorbate along with H_2O_2 or γ-rays. In this context, an electron transfer mechanism, which was initiated from a single radical attack, was proposed for the formation of the 5'-dβF-(8-oxodG)-3' tandem lesion (*27, 50*). By employing isotope-labeling and using dinucleoside monophosphate as a substrate, Cadet et al. (*50*) later argued that the tandem lesion may arise from the intramolecular addition of thymine peroxyl radical to guanine. Our preliminary ^{18}O incorporation experiment suggested that neither electron transfer

pathway nor the peroxyl radical addition constitutes the major mechanism for the formation of this 5'-Tg-(8-oxodG)-3' tandem lesion (data not shown).

Copper is known to associate with chromatin (*3*), and the binding constants of Cu(I) and Cu(II) with DNA are 10^9 and 10^4 M (*11, 51*), respectively, with the N^7 of guanine being the most favorable binding site (*52*). We observed that Cu(II), and more substantially Cu(I), can enhance markedly the γ-ray induced formation of both single and the tandem lesions in calf thymus DNA (Figure 4-4c). We speculate that the DNA-bound Cu(I) may reduce H_2O_2 to release hydroxyl radicals or similar oxidizing species, which may attack its complexed guanine and the neighboring thymine to give 8-oxodG and thymidine glycol, respectively. Additionally, copper may induce significant conformational change to DNA (*53*), which may also render the neighboring thymine residue more susceptible to damage by the ROS formed from the reaction of H_2O_2 with the DNA-bound Cu(I) or γ-rays. Indeed copper binding was found to enhance the formation of radiation-induced strand breaks, and the conformational change induced by metal binding was proposed to be a mechanism for the elevated formation of the strand breaks (*54*). Therefore, it can be envisaged that Cu(I) may also enhance the formation of other tandem lesions in DNA exposed with H_2O_2 or γ-rays.

Thymidine glycol and 8-oxodG are two major DNA lesions induced by ROS. In Chapter 3, our *In-vitro* primer extension assay with exonuclease-free Klenow fragment and yeast polymerase η showed that the presence of the tandem lesion containing both Tg and 8-oxodG in template DNA blocks the progression of DNA replication more readily than when the two lesions were present alone (*55*). The mutagenic properties of the

tandem lesions, as revealed by steady-state kinetic assay, also differ from the two composing lesions when exist on their own (*55*). Moreover, it was found that the cleavage of 8-oxodG by hOGG1 was inhibited substantially by the presence of a neighboring 5' Tg (*55*), indicating that the tandem lesion might be more resistant to repair. In the present Chapter, we investigated the mutagenic and cytotoxic properties of the tandem lesions in *E. coli* cells by using single-stranded pYMV1 shuttle vectors containing an isolated 8-oxodG, Tg, or both of them being adjacent to each other.

Our data revealed that the isolated and tandem single-nucleobase lesions exhibited considerably different bypass efficiencies in *E. coli* cells. The tandem lesions are twice as effective as single lesions in blocking DNA replication in AB1157 *E. coli* cells. In addition, the absence of pol IV and pol V, either alone or in combination, results in an appreciable drop in bypass efficiency (Figure 4-14A). In this context, it is worth noting that Tg does not constitute a replication block in wild-type *E. coli* cells (bypass efficiency ~90%, Figure 4-14A), which is considerably different from the observation that this lesion inhibits appreciably the DNA replication *in vitro* (*36, 37*). Our results, however, are in line with the report by Essigmann et al. (*56*), where no decrease in bypass efficiency was observed for Tg as assessed by using a survival assay with a Tg-bearing single-stranded M13 shuttle vector. Different from the DNA replication *in vitro*, the replication in *E. coli* cells may involve more than one DNA polymerases and the participation of other protein factors (*57, 58*), which may render a more efficient bypass of the lesion.

The 8-oxodG is mutagenic in all AB1157 strains that we examined. The frequency of G→T transversion mutation is approximately 38%, which is relatively high when compared with the results from recent *in-vivo* replication studies (*29, 59*). However, Basu et al. (*15, 60*) observed that, when the 8-oxodG-bearing shuttle vectors were replicated in COS-7 cells, the lesion induced G→T transversion mutation at frequencies of 23-24% and 6% in 5'-TG*T-3' and 5'-TG*A-3' sequence contexts, respectively. Furthermore, molecular modeling results predict that the 8-oxoGua:Ade ("8-oxoGua" and "Ade" are 8-oxo-7,8-dihydroguanine and adenine, respectively) base pair stacked relatively poorly with the neighboring 3' base pair in a 5'-TG*A-3' sequence when compared with a 5'-TG*T-3' sequence (*60*). Therefore, the placement of an 8-oxodG on the 5' side of thymine could confer an increased mutation frequency for 8-oxodG, which may account for a relatively high frequency of G→T mutation for 8-oxodG in the 5'-CG*T-3' sequence context used in the present study.

The frequency of the 8-oxodG-induced G→T transversion mutation was reduced in pol IV-deficient background, supporting that the pol IV-mediated nucleotide incorporation opposite the lesion is error-prone. Similar results were obtained for the 8-oxodG in the 5'-Tg-(8-oxodG)-3' tandem lesion. In this respect, the results from previous steady-state kinetic analysis revealed that human Pol κ, an ortholog of *E. coli* pol IV, is efficient in nucleotide incorporation opposite 8-oxodG (*61*). The nucleotide incorporation, however, is inaccurate; Pol κ incorporated a dAMP opposite 8-oxodG more efficiently than a dCMP by approximately 16-fold (*61*). Therefore, our finding of the error-prone bypass of 8-oxodG by *E. coli* pol IV is consistent with the previous

findings made with human Pol κ. However, no obvious difference in G→T mutation frequency was found for the 5'-(8-oxodG)-Tg-3' tandem lesion in wild-type AB1157 cells and the isogenic cells deficient in pol II, pol IV, pol V, or both pol IV and pol V.

Other than the single-base substitutions, we also detected an approximately 40% TG→GT tandem double mutation for the 5'-Tg-(8-oxodG)-3' in wild-type AB1157 cells and the isogenic cells deficient in SOS-induced DNA polymerases. Here we propose a tentative mechanism to account for this unusual tandem double mutation (Scheme 4-1). We reason that the incorporation of dAMP opposite the 8-oxodG and the resulting presence of the 8-oxoGua:Ade base pair at the primer-template junction may lead to a conformational change of Tg at the polymerase active site, where the *N*-glycosidic bond of the modified nucleoside is altered from the *anti* to *syn* conformation, thereby rendering the Tg to form base pair preferentially with the cytosine base. In this context, it is worth noting that we were not able to detect the T→G single-base substitution from the replication of the 5'-Tg-(8-oxodG)-3'-bearing genome, suggesting that the misincorporation of dAMP across the 8-oxodG might be essential for the mis-insertion of dCMP opposite the downstream 5' Tg.

Together, given the presence of copper ions in normal cells (*3*) and its cellular accumulation under pathophysiological conditions (*62*), we believe that the copper-stimulated formation of the 5'-Tg-(8-oxodG)-3' tandem lesion in DNA exposed with H_2O_2 or γ-rays is very significant. Although the formation of this type of lesion in cells remains to be assessed, the relatively high frequency of its formation *in vitro* suggests that it might also be induced in cells. The lower *in-vivo* bypass efficiencies for tandem

Scheme 4-1. The Tg:Cyt (left) and 8-oxoGua:Ade (right) base pairs formed during the replication of the 5'-Tg-(8-oxodG)-3'-bearing substrate.

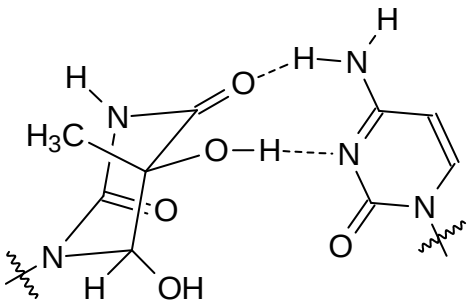

Tg:Cyt Pair

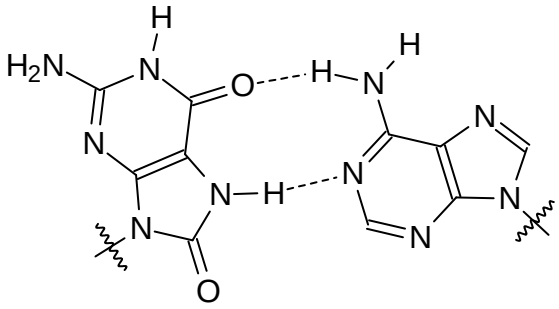

8-oxoGua:Ade Pair

lesions compared to the composing single lesions revealed that, when the two common ROS-induced lesions (i.e., Tg and 8-oxodG) are adjacent to each other, they impose greater cytotoxic effects by blocking more effectively the DNA replication. The tandem lesions also displayed different mutagenic properties than when these lesions are present alone. Moreover, the mutagenic properties of the tandem lesions are also affected by the spatial arrangements of the composing single-nucleobase lesions; the 8-oxodG component in both tandem lesions can lead to G→T transversion, whereas the 5'-Tg-(8-oxodG)-3' tandem lesion could give rise to the unique TG→GT tandem double mutation.

References:

(1) Finkel, T., and Holbrook, N. J. (2000) Oxidants, oxidative stress and the biology of ageing. *Nature 408*, 239-47.

(2) Marnett, L. J. (2000) Oxyradicals and DNA damage. *Carcinogenesis 21*, 361-70.

(3) Agarwal, K., Sharma, A., and Talukder, G. (1989) Effects of copper on mammalian cell components. *Chem. Biol. Interact. 69*, 1-16.

(4) Bach, D., and Miller, I. R. (1967) Polarographic investigation of binding of Cu^{++} and Cd^{++} by DNA. *Biopolymers 5*, 161-72.

(5) Bryan, S. E., and Frieden, E. (1967) Interaction of copper(II) with deoxyribonucleic acid below 30 degrees. *Biochemistry 6*, 2728-34.

(6) Prutz, W. A., Butler, J., and Land, E. J. (1990) Interaction of copper(I) with nucleic acids. *Int J Radiat Biol 58*, 215-34.

(7) Bar-Or, D., and Winkler, J. V. (2002) Copper is involved in hydrogen-peroxide-induced DNA damage. *Free Radic. Biol. Med. 32*, 197-9.

(8) Cao, H., and Wang, Y. (2007) Quantification of oxidative single-base and intrastrand cross-link lesions in unmethylated and CpG-methylated DNA induced by Fenton-type reagents. *Nucleic Acids Res. 35*, 4833-44.

(9) Hong, H., Cao, H., and Wang, Y. (2006) Identification and quantification of a guanine-thymine intrastrand cross-link lesion induced by Cu(II)/H_2O_2/ascorbate. *Chem. Res. Toxicol. 19*, 614-21.

(10) Lee, D. H., O'Connor, T. R., and Pfeifer, G. P. (2002) Oxidative DNA damage induced by copper and hydrogen peroxide promotes CG-->TT tandem mutations

at methylated CpG dinucleotides in nucleotide excision repair-deficient cells. *Nucleic Acids Res. 30*, 3566-73.

(11) Drouin, R., Rodriguez, H., Gao, S. W., Gebreyes, Z., O'Connor, T. R., Holmquist, G. P., and Akman, S. A. (1996) Cupric ion/ascorbate/hydrogen peroxide-induced DNA damage: DNA-bound copper ion primarily induces base modifications. *Free Radic. Biol. Med. 21*, 261-73.

(12) Aruoma, O. I., Halliwell, B., Gajewski, E., and Dizdaroglu, M. (1991) Copper-ion-dependent damage to the bases in DNA in the presence of hydrogen peroxide. *Biochem J. 273*, 601-4.

(13) Sagripant, J. L., and Kraemer, K. H. (1989) Site-specific oxidative DNA damage at polyguanosines produced by copper plus hydrogen peroxide. *J. Biol. Chem. 264*, 1729-34.

(14) Gentil, A., Le Page, F., Cadet, J., and Sarasin, A. (2000) Mutation spectra induced by replication of two vicinal oxidative DNA lesions in mammalian cells. *Mutat. Res. 452*, 51-6.

(15) Kalam, M. A., and Basu, A. K. (2005) Mutagenesis of 8-oxoguanine adjacent to an abasic site in simian kidney cells: tandem mutations and enhancement of G-->T transversions. *Chem. Res. Toxicol. 18*, 1187-92.

(16) Yang, N., Chaudhry, M. A., and Wallace, S. S. (2006) Base excision repair by hNTH1 and hOGG1: A two edged sword in the processing of DNA damage in gamma-irradiated human cells. *DNA Repair 5*, 43-51.

(17) Venkhataraman, R., Donald, C. D., Roy, R., You, H. J., Doetsch, P. W., and Kow, Y. W. (2001) Enzymatic processing of DNA containing tandem dihydrouracil by endonucleases III and VIII. *Nucleic Acids Res. 29*, 407-14.

(18) Budworth, H., and Dianov, G. L. (2003) Mode of inhibition of short-patch base excision repair by thymine glycol within clustered DNA lesions. *Journal of Biological Chemistry 278*, 9378-9381.

(19) Budworth, H., Dianova, II, Podust, V. N., and Dianov, G. L. (2002) Repair of clustered DNA lesions. Sequence-specific inhibition of long-patch base excision repair by 8-oxoguanine. *J. Biol. Chem. 277*, 21300-5.

(20) Lomax, M. E., Cunniffe, S., and O'Neill, P. (2004) 8-oxoG retards the activity of the ligase III/XRCC1 complex during the repair of a single-strand break, when present within a clustered DNA damage site. *DNA Repair 3*, 289-299.

(21) Eot-Houllier, G., Eon-Marchais, S., Gasparutto, D., and Sage, E. (2005) Processing of a complex multiply damaged DNA site by human cell extracts and purified repair proteins. *Nucleic Acids Res. 33*, 260-71.

(22) Wang, Y. (2008) Bulky DNA lesions induced by reactive oxygen species. *Chem. Res. Toxicol. 21*, 276-81.

(23) Box, H. C., Budzinski, E. E., Dawidzik, J. B., Gobey, J. S., and Freund, H. G. (1997) Free radical-induced tandem base damage in DNA oligomers. *Free Radic. Biol. Med. 23*, 1021-30.

(24) Box, H. C., Budzinski, E. E., Dawidzik, J. B., Wallace, J. C., and Iijima, H. (1998) Tandem lesions and other products in X-irradiated DNA oligomers. *Radiat. Res. 149*, 433-9.

(25) Zhang, Q., and Wang, Y. (2005) Generation of 5-(2'-deoxycytidyl)methyl radical and the formation of intrastrand cross-link lesions in oligodeoxyribonucleotides. *Nucleic Acids Res. 33*, 1593-603.

(26) Bellon, S., Ravanat, J. L., Gasparutto, D., and Cadet, J. (2002) Cross-linked thymine-purine base tandem lesions: synthesis, characterization, and measurement in gamma-irradiated isolated DNA. *Chem. Res. Toxicol. 15*, 598-606.

(27) Bourdat, A.-G., Douki, T., Frelon, S., Gasparutto, D., and Cadet, J. (2000) Tandem Base Lesions Are Generated by Hydroxyl Radical within Isolated DNA in Aerated Aqueous Solution. *J. Am. Chem. Soc. 122*, 4549-4556.

(28) Gu, C., and Wang, Y. (2004) LC-MS/MS identification and yeast polymerase η bypass of a novel γ-irradiation-induced intrastrand cross-link lesion G[8-5]C. *Biochemistry 43*, 6745-50.

(29) Hong, H., Cao, H., and Wang, Y. (2007) Formation and genotoxicity of a guanine-cytosine intrastrand cross-link lesion *in vivo*. *Nucleic Acids Res. 35*, 7118-27.

(30) Hong, I. S., Carter, K. N., Sato, K., and Greenberg, M. M. (2007) Characterization and mechanism of formation of tandem lesions in DNA by a nucleobase peroxyl radical. *J. Am. Chem. Soc. 129*, 4089-98.

(31) Jiang, Y., Hong, H., Cao, H., and Wang, Y. (2007) *In vivo* formation and *in vitro* replication of a guanine-thymine intrastrand cross-link lesion. *Biochemistry 46*, 12757-63.

(32) Budzinski, E. E., Dawidzik, J. D., Wallace, J. C., Freund, H. G., and Box, H. C. (1995) The radiation chemistry of d(CpGpTpA) in the presence of oxygen. *Radiat. Res. 142*, 107-9.

(33) Box, H. C., Dawidzik, J. B., and Budzinski, E. E. (2001) Free radical-induced double lesions in DNA. *Free Radic. Biol. Med. 31*, 856-68.

(34) Hayes, R. C., Petrullo, L. A., Huang, H. M., Wallace, S. S., and LeClerc, J. E. (1988) Oxidative damage in DNA. Lack of mutagenicity by thymine glycol lesions. *J. Mol. Biol. 201*, 239-46.

(35) Collins, A. R., Cadet, J., Moller, L., Poulsen, H. E., and Vina, J. (2004) Are we sure we know how to measure 8-oxo-7,8-dihydroguanine in DNA from human cells? *Archives of Biochemistry and Biophysics 423*, 57-65.

(36) McNulty, J. M., Jerkovic, B., Bolton, P. H., and Basu, A. K. (1998) Replication inhibition and miscoding properties of DNA templates containing a site-specific *cis*-thymine glycol or urea residue. *Chem. Res. Toxicol. 11*, 666-73.

(37) Ide, H., Kow, Y. W., and Wallace, S. S. (1985) Thymine glycols and urea residues in M13 DNA constitute replicative blocks *in vitro*. *Nucleic Acids Res. 13*, 8035-52.

(38) Suzuki, N., Ohashi, E., Kolbanovskiy, A., Geacintov, N. E., Grollman, A. P., Ohmori, H., and Shibutani, S. (2002) Translesion synthesis by human DNA

polymerase kappa on a DNA template containing a single stereoisomer of dG-(+)- or dG-(-)-anti-N-2-BPDE (7,8-dihydroxy-anti-9,10-epoxy-7,8,9,10-tetrahydrobenzo[a]pyrene). *Biochemistry 41*, 6100-6106.

(39) Cheng, K. C., Cahill, D. S., Kasai, H., Nishimura, S., and Loeb, L. A. (1992) 8-Hydroxyguanine, an abundant form of oxidative DNA damage, causes G-->T and A-->C substitutions. *J. Biol. Chem. 267*, 166-72.

(40) Bienvenu, C., and Cadet, J. (1996) Synthesis and kinetic study of the deamination of the *cis* diastereomers of 5,6-dihydroxy-5,6-dihydro-5-methyl-2'-deoxycytidine. *J. Org. Chem. 61*, 2632-2637.

(41) Zuo, S., Boorstein, R. J., and Teebor, G. W. (1995) Oxidative damage to 5-methylcytosine in DNA. *Nucleic Acids Res. 23*, 3239-43.

(42) Gibbs, P. E., Kilbey, B. J., Banerjee, S. K., and Lawrence, C. W. (1993) The frequency and accuracy of replication past a thymine-thymine cyclobutane dimer are very different in *Saccharomyces cerevisiae* and *Escherichia coli*. *J. Bacteriol. 175*, 2607-12.

(43) Jarosz, D. F., Beuning, P. J., Cohen, S. E., and Walker, G. C. (2007) Y-family DNA polymerases in *Escherichia coli*. *Trends Microbiol. 15*, 70-7.

(44) Wang, Y., and Wang, Y. (2006) Synthesis and thermodynamic studies of oligodeoxyribonucleotides containing tandem lesions of thymidine glycol and 8-oxo-2'-deoxyguanosine. *Chem. Res. Toxicol. 19*, 837-43.

(45) Delaney, J. C., and Essigmann, J. M. (2006) Assays for determining lesion bypass efficiency and mutagenicity of site-specific DNA lesions *in vivo*. *Methods Enzymol. 408*, 1-15.

(46) Delaney, J. C., and Essigmann, J. M. (2004) Mutagenesis, genotoxicity, and repair of 1-methyladenine, 3-alkylcytosines, 1-methylguanine, and 3-methylthymine in alkB *Escherichia coli*. *Proc. Natl. Acad. Sci. U. S. A. 101*, 14051-6.

(47) Delaney, J. C., and Essigmann, J. M. (1999) Context-dependent mutagenesis by DNA lesions. *Chem. Biol. 6*, 743-753.

(48) Yuan, B., Cao, H., Jiang, Y., Hong, H., and Wang, Y. (2008) Efficient and accurate bypass of N^2-(1-carboxyethyl)-2'-deoxyguanosine by DinB DNA polymerase *in vitro* and *in vivo*. *Proc. Natl. Acad. Sci. U. S. A. 105*, 8679-84.

(49) Rechkoblit, O., Zhang, Y. B., Guo, D. Y., Wang, Z. G., Amin, S., Krzeminsky, J., Louneva, N., and Geacintov, N. E. (2002) trans-lesion synthesis past bulky benzo[a]pyrene diol epoxide N-2-dG and N-6-dA lesions catalyzed by DNA bypass polymerases. *Journal of Biological Chemistry 277*, 30488-30494.

(50) Douki, T., Riviere, J., and Cadet, J. (2002) DNA tandem lesions containing 8-oxo-7,8-dihydroguanine and formamido residues arise from intramolecular addition of thymine peroxyl radical to guanine. *Chem. Res. Toxicol. 15*, 445-54.

(51) Stoewe, R., and Prutz, W. A. (1987) Copper-catalyzed DNA damage by ascorbate and hydrogen peroxide: kinetics and yield. *Free Radic. Biol. Med. 3*, 97-105.

(52) Gao, Y. G., Sriram, M., and Wang, A. H. (1993) Crystallographic studies of metal ion-DNA interactions: different binding modes of cobalt(II), copper(II) and

barium(II) to *N*7 of guanines in Z-DNA and a drug-DNA complex. *Nucleic Acids Res. 21*, 4093-101.

(53) Trumbore, C. N., Ehrlich, R. S., and Myers, Y. N. (2001) Changes in DNA conformation induced by gamma irradiation in the presence of copper. *Radiat. Res. 155*, 453-65.

(54) Savoye, C., Sabattier, R., Charlier, M., and Spotheim-Maurizot, M. (1996) Sequence-modulated radiosensitization of DNA by copper ions. *Int. J. Radiat. Biol. 70*, 189-98.

(55) Jiang, Y., Wang, Y., and Wang, Y. (2009) In vitro replication and repair studies of tandem lesions containing neighboring thymidine glycol and 8-oxo-7,8-dihydro-2'-deoxyguanosine. *Chem. Res. Toxicol. 22*, 574-583.

(56) Basu, A. K., Loechler, E. L., Leadon, S. A., and Essigmann, J. M. (1989) Genetic effects of thymine glycol: site-specific mutagenesis and molecular modeling studies. *Proc. Natl. Acad. Sci. U. S. A. 86*, 7677-81.

(57) Sutton, M. D., and Walker, G. C. (2001) Managing DNA polymerases: coordinating DNA replication, DNA repair, and DNA recombination. *Proc. Natl. Acad. Sci. USA 98*, 8342-9.

(58) Maga, G., Villani, G., Crespan, E., Wimmer, U., Ferrari, E., Bertocci, B., and Hubscher, U. (2007) 8-oxo-guanine bypass by human DNA polymerases in the presence of auxiliary proteins. *Nature 447*, 606-8.

(59) Neeley, W. L., Delaney, S., Alekseyev, Y. O., Jarosz, D. F., Delaney, J. C., Walker, G. C., and Essigmann, J. M. (2007) DNA polymerase V allows bypass of toxic guanine oxidation products *in vivo*. *J. Biol. Chem. 282*, 12741-8.

(60) Kalam, M. A., Haraguchi, K., Chandani, S., Loechler, E. L., Moriya, M., Greenberg, M. M., and Basu, A. K. (2006) Genetic effects of oxidative DNA damages: Comparative mutagenesis of the imidazole ring-opened formamidopyrimidines (Fapy lesions) and 8-oxo-purines in simian kidney cells. *Nucleic Acids Res. 34*, 2305-15.

(61) Johnson, R. E., Washington, M. T., Haracska, L., Prakash, S., and Prakash, L. (2000) Eukaryotic polymerases iota and zeta act sequentially to bypass DNA lesions. *Nature 406*, 1015-9.

(62) Ala, A., Walker, A. P., Ashkan, K., Dooley, J. S., and Schilsky, M. L. (2007) Wilson's disease. *Lancet 369*, 397-408.

CHAPTER 5

Efficient and Accurate Bypass of N^2-(1-carboxyethyl)-2′-deoxyguanosine by DinB DNA Polymerase *In Vitro and In Vivo*

Introduction

Living cells are constantly exposed to environmental and endogenous agents that inflict damage to DNA (*1*). Cells have evolved various strategies to counteract the deleterious effects of DNA lesions by an intricate DNA repair system and certain mechanisms to tolerate unrepaired lesions during DNA replication (*2*). However, the presence of DNA lesions in replicating DNA may lead to replication fork stalling, thereby inducing cell death. It was proposed that, when a high-fidelity replication fork is arrested at the lesion site, translesion synthesis polymerases can take over from replicative polymerases temporarily to bypass synthetically the lesion residing in the template (*3*). Among the Y-family DNA polymerases, DinB (also known as pol IV in *Escherichia coli* and pol κ in eukaryotic cells) is conserved in all domains of life; however, the basis for this marked conservation remains unclear (*4*). In particular, the physiological substrates for the polymerase allowing for the striking conservation have yet been identified.

Similar to pol V (the other Y-family DNA polymerase in *E. coli*) and its eukaryotic homolog pol η, which are specialized in bypassing efficiently and accurately TT cyclobutane pyrimidine dimer (*5, 6*), *E. coli* pol IV and human pol κ can insert

preferentially the correct nucleotide, dCMP, opposite a number of N^2-dG lesions (*7, 8*). It was also found that the DinB polymerase is capable of bypassing N^2-dG adduct induced by benzo[*a*]pyrene-7,8-diol-9,10-epoxide (BPDE) (*9-12*), a cigarette smoke carcinogen.

Aside from the difference in substrate specificity, *E. coli* pol IV and pol V distinguishes from each other in expression levels. In un-induced cells, pol V is not detectable by Western analysis, whereas there are approximately 250 copies of pol IV per cell detected. Upon SOS induction, it is believed that there are only about 15 molecules of pol V per cell; however, the level of pol IV reaches approximately 2,500 molecules per cell (*4*). The high level of expression of pol IV also suggests that there is an important, basic, and yet to-be-discovered function for pol IV in general metabolism (*4*).

Other than ROS, which constitutes a major endogenous source of DNA damage (*13*), genomic DNA in living cells is susceptible to damage from exposure to reactive carbonyl species, and methylglyoxal (MG) is one of them (*14*). In this respect, MG can arise endogenously in all cells and all organisms from the nonenzymatic fragmentation of triose phosphates, which include glyceraldehyde-3-phosphate and dihydroxyacetone phosphate, and are produced as metabolites of the highly conserved glycolysis pathway (*15-20*). In this regard, treatment of human red blood cells with increasing concentrations of glucose *in vitro* can result in increases of intracellular MG concentration (*21*). The accumulation of MG in human cells can also be enhanced by many factors, including aging, hyperglycemia, inflammation, oxidative stress, diabetes, and uremia (*22*). In addition, humans are exposed to exogenous sources of MG including cigarette smoke (*22, 23*), food, and beverages (*24*).

N^2-(1-carboxyethyl)-2'-deoxyguanosine (N^2-CEdG) was the major stable adduct formed in calf thymus DNA upon exposure to MG at physiological concentration and temperature (Figure 1-3) (*25*). N^2-CEdG can also be detected in urine samples from healthy humans, cultured human smooth muscle cells and bovine aorta endothelium cells using immunoaffinity chromatography with a polyclonal antibody raised against N^2-CEdG (*26, 27*).

MG-DNA adducts could induce single-strand breaks and mutations in *E. coli* cells, and G→C and G→T transversions in *supF* gene in mammalian cells (*26, 27*). However, lesion-containing DNA substrates in these previous mutagenesis studies were prepared by direct treatment of undamaged DNA with dihydroxyacetone or MG (*26, 27*); thus, the identity and homogeneity of the DNA adducts were not carefully assessed. In light of the previous findings that DinB is capable of bypassing, in an error-free manner, a number of N^2-dG lesions (*7-12*), we reason that this polymerase may also be involved in the bypass of N^2-CEdG.

In the present study, we prepared single-stranded M13 genomes carrying individual diastereomers of N^2-CEdG and assessed the cytotoxic and mutagenic properties of the lesion in *E. coli* cells. Our results showed that pol IV was the major polymerase responsible for the error-free bypass of N^2-CEdG *in vivo*. Steady-state kinetic measurements revealed that the nucleotide incorporation, catalyzed by *E. coli* pol IV or its human homolog pol κ, is both accurate and efficient. In addition, N^2-CEdG could be detected in untreated human cells, and exposure of cells to glucose or MG enhanced the

formation of N^2-CEdG. These observations support that N^2-CEdG is an important endogenous substrate for DinB DNA polymerase.

Experimental

Materials

Unmodified ODNs used in this study were purchased from Integrated DNA Technologies (Coralville, IA). [γ-^{32}P]ATP was obtained from Amersham Biosciences Co. (Piscataway, NJ). All enzymes unless specified were from New England Biolabs (Ipswich, MA) or Sigma-Aldrich (St. Louis, MO). Shrimp alkaline phosphatase was obtained from Roche Diagnostics (Indianapolis, IN). [3,3,3-D_3]-DL-Alanine (D_3, >98%) was obtained from Cambridge Isotope Laboratories (Andover, MA). 1,1,1,3,3,3-hexafluoro-2-propanol (HFIP) was purchased from TCI America (Portland, OR).

M13mp7(L2) and wild-type *E. coli* strains were provided by Prof. John M. Essigmann, and polymerase-deficient AB1157 strains [*Δ*pol B1::spec (pol II-deficient), *Δ*dinB (pol IV-deficient) and *Δ*umuC::kan (pol V-deficient)] were generous gifts from Prof. Graham Walker (*28*). *E. coli* DNA polymerase IV was provided by Prof. Myron F. Goodman (*29*). Human polymerase κ was purchased from Enzymax (Lexington, KY).

Synthesis of [2, 2, 2-D_3]-N^2-(1-Carboxyethyl)-2'-deoxyguanosine (D_3-N^2-CEdG)

This compound was synthesized from 2-fluoro-2'-deoxyinosine and D_3-DL-alanine employing previously reported procedures (*30*). The resulting two diastereomers of D_3-N^2-CEdG were separated by HPLC and used as internal standards for the quantification of N^2-CEdG formed in cells, and the concentrations of the stock solutions

of D_3-N^2-CEdG were determined by UV absorbance measurements using molar extinction coefficients of 13600 L/mol/cm at 260 nm (*30*).

Cell Culture and Methylglyoxal/D-Glucose Treatment

WM-266-4 human melanoma skin cancer cells (ATCC, Manassas, VA) were cultured at 37°C in 5% CO_2 atmosphere and in Eagle's minimum essential medium supplemented with 10% fetal bovine serum (Invitrogen, Carlsbad, CA), 100 unit/mL penicillin, and 100 μg/mL streptomycin (ATCC). After growing to 80% confluence, cells were detached by trypsin-EDTA treatment and harvested by centrifugation to remove the medium. The cell pellets were subsequently washed twice with phosphate-buffered saline (PBS) and resuspended in 20 mL PBS (10^6 cells/mL) containing desired concentration of methylglyoxal (MG). The cells were incubated with MG at room temperature for 3.0 hours with occasional shaking.

For D-glucose treatment, the cells were cultured in the same media containing certain concentrations of D-glucose. The media was discarded and the cells were resuspended in fresh media containing the same concentration of glucose on day 3. The cells were harvested at the end of day 5. The nuclear DNA was isolated from cell lysates with phenol extraction and desalted by ethanol precipitation.

Enzymatic Digestion

Eight units of nuclease P1, 0.02 unit of calf spleen phosphodiesterase, and a 10-μL solution carrying 300 mM sodium acetate (pH 5.0) and 10 mM zinc acetate were added to 90 μl aqueous solution with 200 μg genomic DNA, and the digestion was

carried out at 37°C for 4 h. To the digestion mixture were then added 50 units of alkaline phosphatase, 0.2 unit of snake venom phosphodiesterase, and 10 μL of 0.5 M Tris-HCl buffer (pH 8.9). The digestion was continued at 37°C for 4 h and the enzymes were removed by passing through a 10-kDa cut-off Centricon membrane (Millipore, Billerica, MA). The amount of nucleosides in the mixture was quantified by UV absorbance measurements, and to the mixture were then added 300 fmol of D_3-S-N^2-CEdG and D_3-R-N^2-CEdG. The resulting aliquots were subsequently subjected to HPLC enrichment and LC-MS/MS analysis.

HPLC Enrichment

The enrichment of DNA lesions from the digestion mixture of genomic DNA was performed on a Beckman Gold HPLC system (pump module 125, 32 Karat software version 3.0, Fullerton, CA) with a UV detector (module 126) monitoring at 260 nm. A 4.6 × 250 mm Grace Apollo reverse phase C18 column (5 μm in particle size, Deerfield, IL) was used, and 10 mM ammonium formate buffer (pH 6.4, solvent A) and a mixture of 10 mM ammonium formate and acetonitrile (70/30, v/v, solvent B) were employed as mobile phases. A gradient of 5 min 0-10% B followed by 40 min 10-35% was used, and the flow rate was 0.60 mL/min. We collected fractions in a wide retention time range (3-4 min) to ensure that the lesions were completely collected while the unmodified nucleosides were excluded as much as possible. The collected fractions were dried in a Speed-vac, reconstituted in 6 μL of H_2O, and 3 μL was injected for LC-MS/MS analysis.

LC-MS/MS Quantification of N^2-CEdG

Quantitative analysis of N^2-CEdG in the above DNA hydrolysates was performed by online capillary HPLC-ESI-MS/MS using an Agilent 1100 capillary HPLC pump (Agilent Technologies) interfaced with an LTQ linear ion-trap mass spectrometer (Thermo Fisher Scientific, San Jose, CA), which was set up for monitoring the fragmentation of N^2-CEdG and isotope-labeled internal standard D_3-N^2-CEdG. A 0.5×150 mm Zorbax SB-C18 column (5 μm in particle size, Agilent Technologies) was used for the separation of the DNA hydrolysis mixture, and the flow rate was 6.0 μL/min. A 5-min gradient of 2–20% methanol in 0.1% formic acid, followed by a 35-min gradient of 20–45% methanol in 0.1% formic acid, was employed for the separation. To eliminate the isobaric impurities present in MS/MS, we quantified N^2-CEdG using MS^3, which monitored the further fragmentation of the protonated ions of nucleobase portions of N^2-CEdG and D_3-N^2-CEdG (i.e., the ions of *m/z* 224 and 227), respectively.

Preparation of ODN Substrates Containing an S-N^2-CEdG or R-N^2-CEdG

The 16mer and 20mer N^2-CEdG-containing ODNs (16mer, 5'-GAAGACCAXCGACGCC-3'; 20mer, 5'-ATGGCXCACTATGATCCTAG-3', X =S/R-N^2-CEdG) were prepared as described previously (*30*).

In Vitro Replication Studies with Human Polymerase κ

Primer extension assays were performed under standing-start conditions. The 20mer lesion-containing template or non-damaged template (20 nM) with dG in place of the N^2-CEdG was annealed with a 5'-[^{32}P]-labeled 15mer primer

d(GCTAGGATCATAGTG) (10 nM), to which mixture were then added a mixture of all four dNTPs (200 μM) as well as the human polymerase κ. The reaction was carried out at 37°C in a 20-μL solution containing 10 mM Tris-HCl (pH 7.5), 5 mM $MgCl_2$, and 7.5 mM dithiothreitol (DTT) for 60 min. The concentrations of the polymerase are indicated in the figures. The reaction was terminated by adding 8 μL of gel-loading buffer containing 80% formamide, 10 mM EDTA (pH 8.0), 1 mg/mL xylene cyanol, and 1 mg/mL bromophenol blue. The products were resolved on 20% (29:1) cross-linked polyacrylamide gels containing 8 M urea. Gel band intensities for the substrates and products were quantified by using a Typhoon 9410 Variable Mode Imager (Amersham Biosciences Co.) and ImageQuant version 5.2 (Amersham Biosciences Co.).

The steady-state kinetic analyses were performed as described previously (*31*). The primer-template duplex (10 nM) was incubated with human polymerase κ (5 ng) in the presence of an individual dNTP at various concentrations as indicated in the figures. The reaction was carried out at room temperature with the same reaction buffer as described above. The dNTP concentration was optimized for different insertion reactions to allow for less than 20% primer extension (*32, 33*). The products were resolved again by denaturing PAGE analysis. The observed rate of dNTP incorporation (V_{obs}) was plotted as a function of dNTP concentration, and the apparent K_m and V_{max} steady-state kinetic parameters for the incorporation of both the correct and incorrect nucleotides were determined by fitting the rate data with the Michaelis-Menten equation.

The efficiency for nucleotide incorporation was determined by the ratio of V_{max}/K_m. The fidelity of nucleotide incorporation was then calculated by the frequency of misincorporation (f_{inc}) with the following equation:

$$f_{inc} = \frac{(V_{max} / K_m)_{incorrect}}{(V_{max} / K_m)_{correct}}$$

In Vitro Replication Studies with E.coli DNA Polymerase IV

Primer extension assays and steady-state kinetic measurements with *E. coli* pol IV were performed under similar conditions as described above for human pol κ. For primer extension assays, a mixture of all four dNTPs (200 μM) as well as the *E. coli* Pol IV were added to the same primer-template complex as described above. The reaction was carried out at 37°C in a 20-μL solution containing 20 mM Tris-HCl (pH = 7.5), 8 mM $MgCl_2$, 5 mM dithiothreitol (DTT), 0.1 mM EDTA, 50mM NaCl, 40 ug/mL BSA and 4% glycerol for 60 min. The concentrations of the polymerase are indicated in the figures. The reaction was terminated by adding 8 μL of gel-loading buffer containing 80% formamide, 10 mM EDTA (pH 8.0), 1 mg/mL xylene cyanol, and 1 mg/mL bromophenol blue. The products were again resolved on 20% (acrylamie:bis-acrylamide, 29:1, wt/wt) cross-linked polyacrylamide gels containing 8 M urea.

For steady-state kinetic measurements, the primer-template duplex (10 nM) was incubated with *E. coli* Pol IV (20 ng) in the presence of an individual dNTP at various concentrations as indicated in the figures. The reaction was carried out at 37°C for 10 min with the same reaction buffer as described above. The dNTP concentration was optimized for different insertion reactions to allow for less than 20% primer extension.

Construction of ss-M13 Genomes Harboring a Site-specifically Inserted S-N^2-CEdG, R-N^2-CEdG or dG

The M13mp7 (L2) viral genomes, either lesion-free or carrying a site-specifically inserted S- or R-N^2-CEdG, were prepared following the procedures described by Delaney and Essigmann (*33*). Briefly, 20 pmol of ss-M13mp7 (L2) was digested with 40 U EcoRI at 23°C for 8 h to linearize the vector. Two scaffolds, 5'-GGTCTTCCACTGAATCATGGTCATAGC-3' and 5'-AAAACGACGGCCAGTGAATTGGCGTC-3' (25 pmol), each spanning one end of the cleaved vector and the modified ODN insert, were annealed with the linearized vector. The 16mer insert [d(GAAGACCAXCGACGCC), where "X" is dG, S-N^2-CEdG, or R-N^2-CEdG, 30 pmol] was 5'-phosphorylated in a 30-μl solution containing 1×T4 polynucleotide kinase buffer, 1 mM ATP, 5 mM dithiothreitol (DTT), and 15 U polynucleotide kinase at 37°C for 1 h. The 5'-phosphorylated 16mer inserts were ligated, by using T4 DNA ligase, to the above vector in the presence of the two scaffolds at 16°C for 8 h. T4 DNA polymerase (22.5 U) was subsequently added and incubated at 37°C for 4 h to remove the scaffolds. The solution was extracted once with phenol/chloroform/isoamyl alcohol (25:24:1, v/v), and the aqueous phase was passed through a Sephadex-G50 column (Amersham) to remove traces of phenol and salt. The constructed genomes were normalized against a lesion-free competitor genome, which was constructed by inserting a 19-mer unmodified ODN to the EcoRI-linearized genome, following the method described by Delanely et al. (*33*)

Transfection of E. coli Cells with ss-M13 Vectors Containing S-N^2-CEdG, R-N^2-CEdG or dG

Desalted genomes containing a lesion or unmodified dG (150 fmol) were mixed with the competitor genome at a ratio of 6:1 and transfected into the electrocompetent AB1157 *E. coli* cells. The M13 genome-carrying *E. coli* cells were grown in 3 mL LB culture at 37°C for 6 h, after which the phage was recovered from the supernatant by centrifugation at 13,000 rpm for 5 min. The resulting phage was further amplified in SCS110 *E. coli* cells to increase the progeny/lesion-genome ratio (*33*). The phage recovered from the supernatant (700 μl) was passed through a QIAprep Spin M13 kit (Qiagen, Valencia, CA) to isolate the ss-M13 DNA.

Determination of the Bypass Efficiency Using Competitive Replication and Adduct Bypass (CRAB) assay

PCR amplification of the region of interest in the resulting progeny genome was performed in a 100-μl solution containing 1 μM of each primer, 0.3 mM of each dNTP, 15 μl ss-M13 DNA, 1 U Phusion high-fidelity DNA polymerase, and 1× polymerase reaction buffer. The primers were 5'-YCAG GGT TTT CCC AGT CAC GAC GTT GTA A-3' and 5'-YCAG CTA TGA CCA TGA TTC AGT GGA AGA C-3' (Y is an amino group), and the amplification cycle was 30, each consisting of 10 s at 98 °C, 30 s at 62 °C, 15 s at 72 °C, with a final extension at 72 °C for 5 min. The PCR products were purified by using QIAquick nucleotide removal kit (Qiagen, Valencia, CA).

For the bypass efficiency assay, a portion of the above PCR fragments was treated in a 10-μl reaction volume with 5 U BbsI and 1 U shrimp alkaline phosphatase (Roche) in 1× NEB buffer 2 at 37 °C for 4 h, followed by heating at 65 °C for 20 min to deactivate the phosphatase. The above mixture was then treated in a 15-μl solution containing 1× NEB buffer 2, 5 mM DTT and ATP (50 pmol cold, premixed with 1.66 pmol [γ-^{32}P] ATP) and 10 U polynucleotide kinase at 37 °C for 1 h, followed by heating at 65 °C for 20 min to deactivate the polynucleotide kinase. After supplementation with 10 U Tsp509I, the reaction mixture was incubated at 65 °C for 1 h, followed by quenching with 15 μl formamide gel loading buffer containing xylene cyanol FF and bromophenol blue dyes. The mixture was loaded onto a 20% denaturing gel and products were quantified by phosphorimager analysis. After the restriction cleavages, the DNA fragment of interest from the full-length replication product was liberated as an 8mer ODN, d(p*XCGACGCC), where 'X' designates the nucleobase present at the original lesion site after *in vivo* DNA replication and "p*" represents the 5'-radiolabeled phosphate. On the other hand, the corresponding DNA fragment released from the competitor genome was an 11mer ODN, d(p*GCTAGCTGCGG). The bypass efficiency was calculated using the following formula, %bypass= (lesion signal/competitor signal)/(non-lesion control signal/its competitor signal) (*34*).

Determination of Bypass Efficiency and Mutation Frequency Using LC-MS

To examine the bypass efficiency using LC-MS, PCR products were treated in a 250-μl reaction volume with 45 U BbsI and 20 U shrimp alkaline phosphatase in 1× NEB

buffer 2 at 37°C for 4 h, followed by heating at 65°C for 20 min. After supplementation with 50 U of Tsp509I, the reaction mixture was incubated at 65°C for 1 h followed by extraction once with phenol/chloroform/isoamyl alcohol (25:24:1, v/v), and the aqueous portion was dried with Speed-vac and desalted with HPLC.

The resulting ODN fragments were separated using a 0.5×150 mm Zorbax SB-C18 column (5 μm in particle size, Agilent Technologies) and the flow rate was 8.0 μl/min, which was delivered by using the Agilent 1100 capillary HPLC pump. A 5-min gradient of 0-20% methanol followed by a 35 min of 20-50% methanol in 400 mM HFIP buffer (pH was adjusted to 7.0 by the addition of triethylamine) was used for the separation (*34*). The effluent from the LC column was coupled directly to the LTQ linear ion trap mass spectrometer, which was set up for monitoring the fragmentation of the $[M-2H]^{2-}$ ions of the 8mer and 11mer ODNs.

Results

To explore the possibility that N^2-CEdG might constitute an endogenous substrate for DinB polymerase, we first assessed the formation of N^2-CEdG in WM-266-4 human melanoma cells that are either untreated or treated with glucose or MG. LC-MS/MS analysis using the accurate isotope-dilution method revealed that both diastereomers of N^2-CEdG could be detected in untreated cells at a level of one lesion per 10^7 nucleotides (Figure 5-1, LC-MS/MS data and calibration curves are shown in Figures 5-2 and 5-3, respectively). In addition, incubation of melanoma cells with MG led to a dose-dependent increase in the level of N^2-CEdG (Figure 5-1). Moreover, culturing of these cells in media

containing 5 and 25 mM glucose for 5 days resulted in the increase of the levels of the lesions to approximately 2.5 and 4 lesions in 10^7 nucleosides (Figure 5-1). In this context, it is worth noting that, in response to change in blood glucose level, glucose transporters are regulated in some types of cells (*35*). Therefore, the intracellular glucose concentration in WM-266-4 human cells may not increase proportionally with the glucose concentration in the culture media, which may explain why the levels of N^2-CEdG lesions induced in glucose-treated cells are not proportional to the applied glucose dose. Taken together, both diastereomers of N^2-CEdG can be induced endogenously in WM-266-4 human melanoma cells, and the exposure of cells to MG or glucose further enhances the formation of N^2-CEdG. In this context, it is worth noting that the two diastereomers of N^2-CEdG can also be detected readily in HeLa-S3 cells (data not shown).

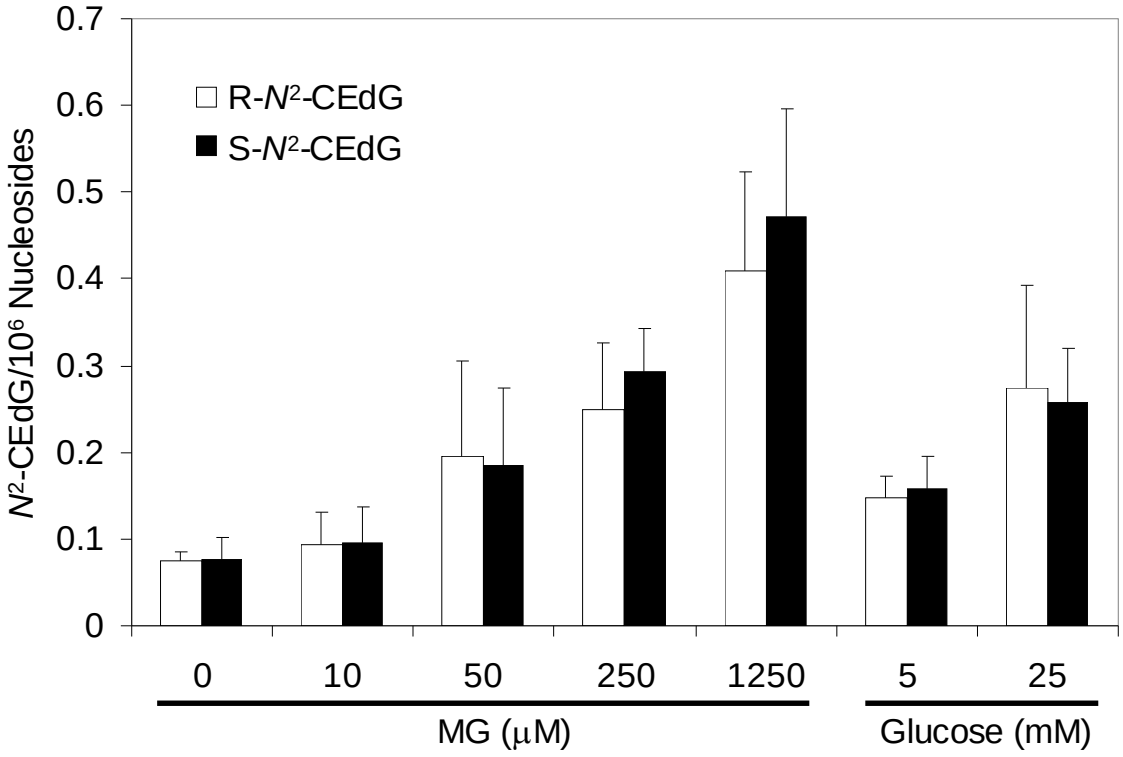

Figure 5-1. The dose-dependant formation of N^2-CEdG in WM266-4 cells, either untreated or treated with methylglyoxal for 3 hrs or D-glucose for 5 days. The concentrations of methylglyoxal and D-glucose are indicated. The data represent the means and standard deviations of results from three independent cell culture and treatments.

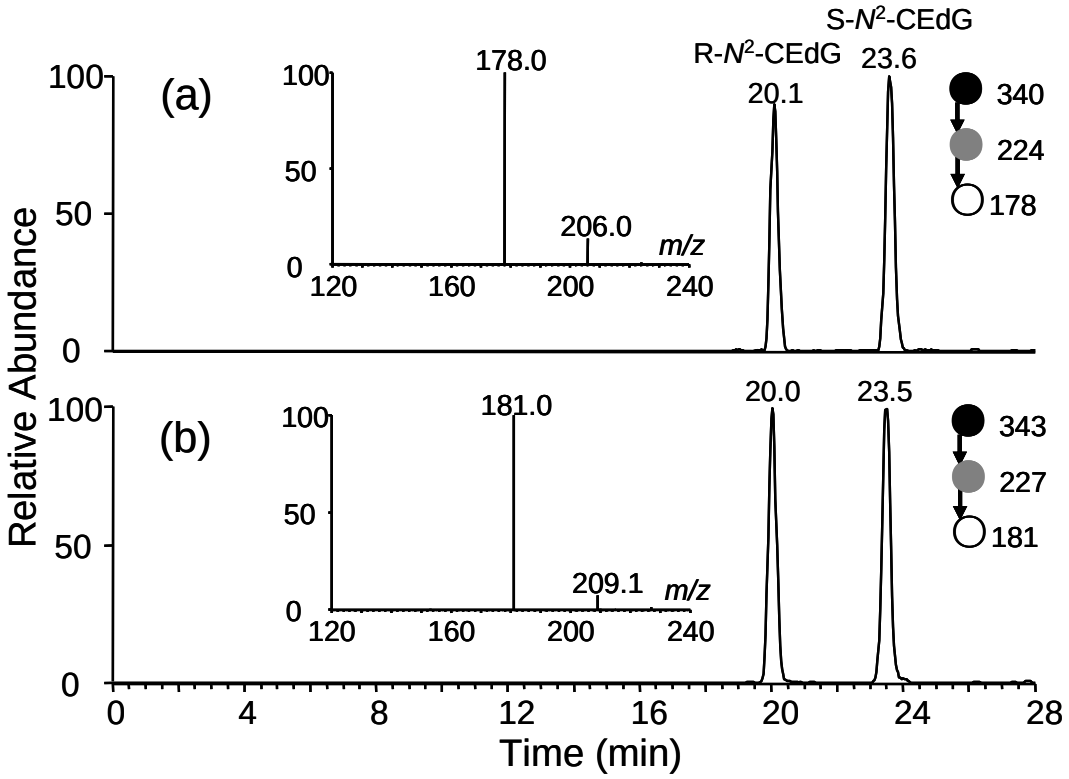

Figure 5-2. SICs for the monitoring of the *m/z* 340.1→224.1→178.1 (a, for N^2-CEdG) and *m/z* 343.1→ 227.1→181.1 (b, for D_3-N^2-CEdG) transitions of the digestion mixtures of genomic DNA extracted from cells treated with 25 μM methylglyoxal. 300 fmol of D_3-N^2-CEdG internal standard was added before HPLC enrichment.

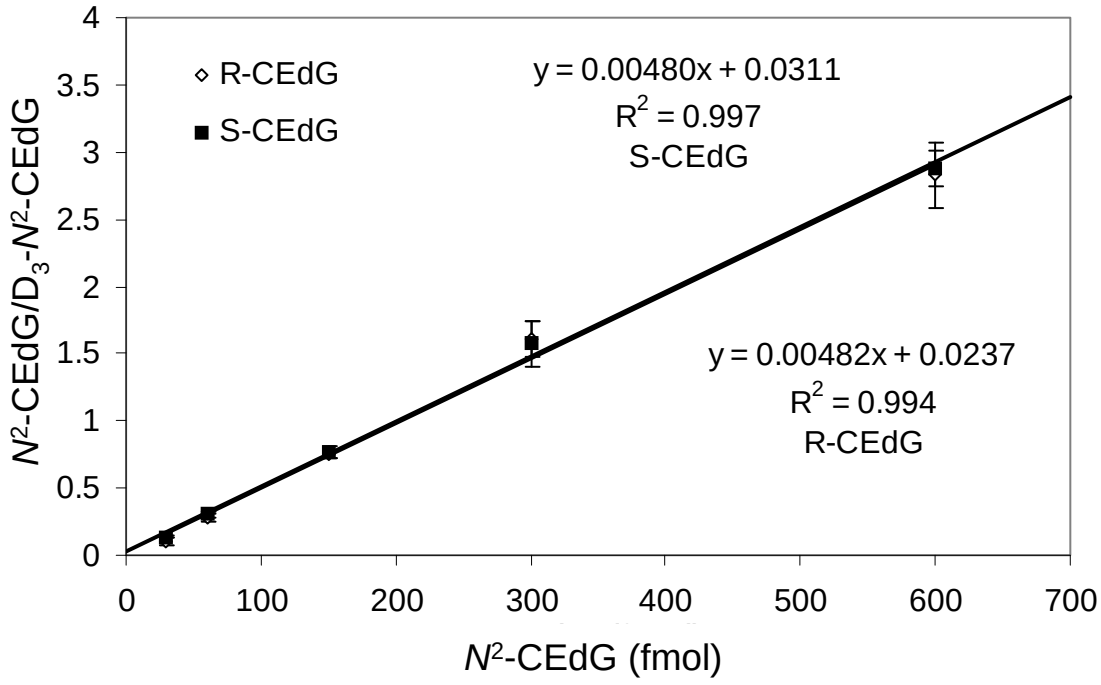

Figure 5-3. Calibration curve for quantification of S-N^2-CEdG and R-N^2-CEdG

We next examined how the presence of N^2-CEdG compromises DNA replication and which SOS-induced DNA polymerase is involved in bypassing the lesion in *E. coli* cells. To this end, we synthesized ODNs harboring a site-specifically incorporated S- or R-N^2-CEdG, following our procedures (*30*). We then ligated the ODNs into single-stranded M13 genome and assessed the bypass efficiencies and mutation frequencies of the two diastereomers by using the CRAB (competitive replication and adduct bypass) and REAP (restriction endonuclease and post-labeling) assays introduced by Essigmann and coworkers (Figure 5-4) (*32, 33*).

If there is no deletion mutation, restriction digestion of the PCR products of progeny M13 genome arising from the replication of the lesion-carrying vector affords a 8mer fragment harboring the site where the N^2-CEdG was initially incorporated. The corresponding digestion of PCR products of the progeny of the competitor genome gives an 11mer fragment (Figure 5-4). The failure to detect any radiolabeled fragments with lengths shorter than 8 mer supports that neither diastereomer gives rise to deletion muations (Figure 5-5). The bypass efficiency canbe calculated from the ratio of the 8mer product over the 11mer product with the consideration of the genome ratio used in the initial transfection experiment. The bypass efficiency for the lesion-carrying genome is then normalized against that for the control lesion-free genome (Figure 5-6A).

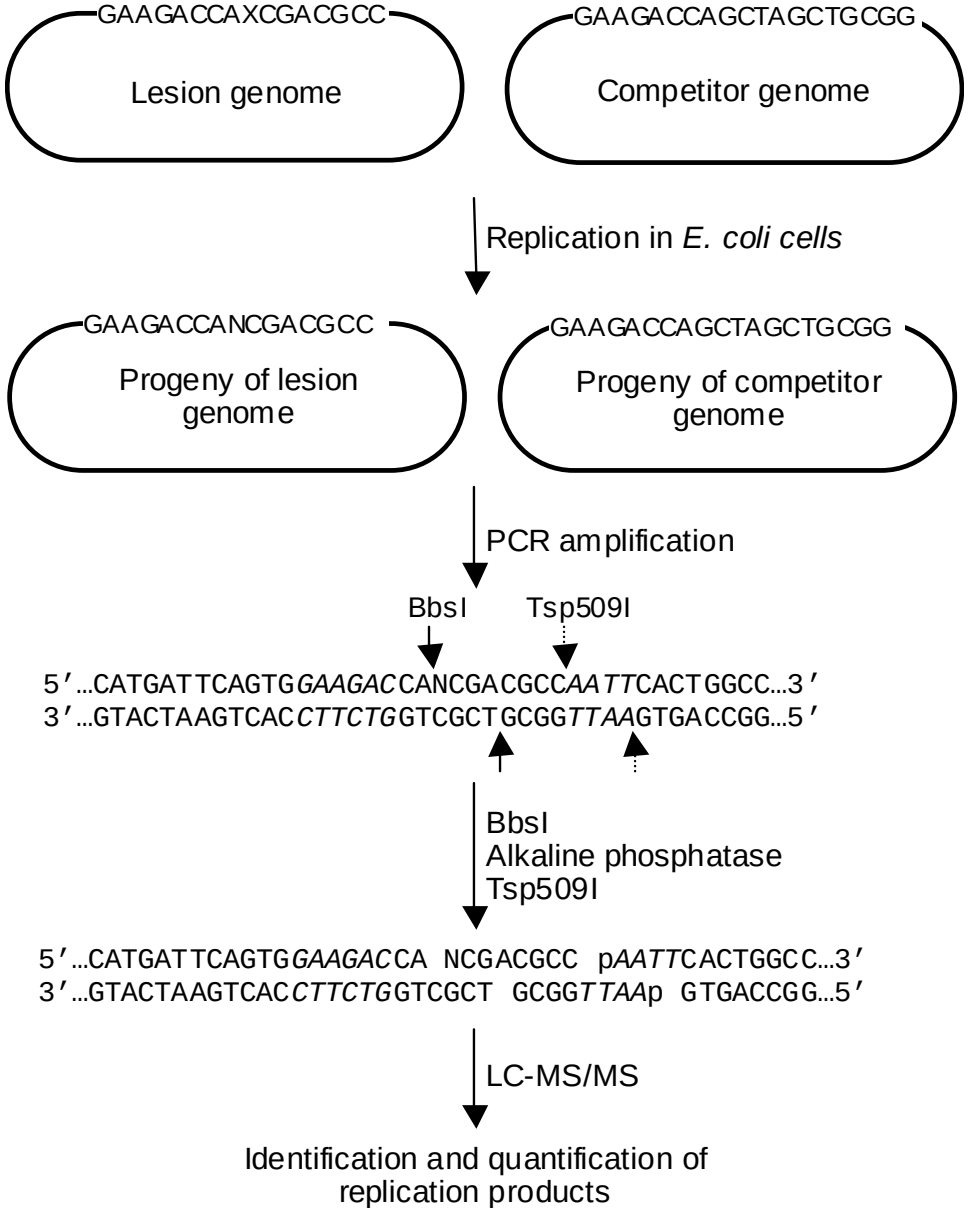

Figure 5-4. Determination of cytotoxicity and mutagenicity of the N^2-CEdG lesion in *E. coli* cells. "X" in the 16mer ODN represents S-N^2-CEdG, R-N^2-CEdG or unmodified dG. "N" in the progeny of lesion genome represents the nucleoside inserted at the original lesion site. BbsI and Tsp509I restriction endonuclease recognition sites are indicated in italic and the cleavage sites induced by the two enzymes are designated by broken and solid arrows. Only partial sequence of PCR products for the lesion genome is shown, and the PCR products of competitor genome are not shown.

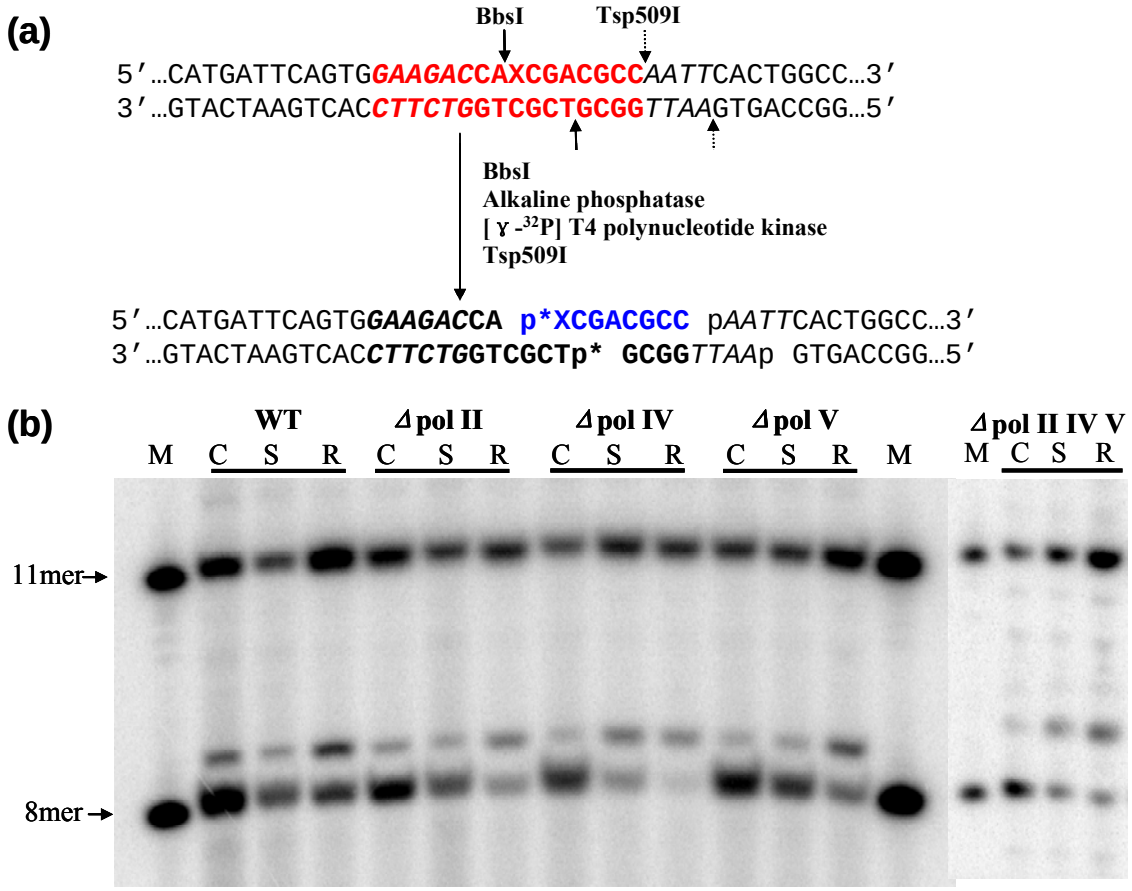

Figure 5-5. Measurement of the bypass efficiencies of the two diastereomers of N^2-CEdG *in vivo by* CRAB assay. (a) Sample processing ("p*" represents ^{32}P-labeled phosphate group); (b) Gel image showing the 11mer and 8mer released from the PCR products of the progeny resulting from the replication of competitor genome and the control or lesion-carrying genome. "M" represents markers which include the un-mutated 8mer sequence from the control genome and authentic 11mer sequence from the competitor genome. "C", "S", and "R" represent control as well as S- N^2-CEdG - and R- N^2-CEdG -bearing genomes, respectively. The band above the 8mer is most likely a non-specific digestion product from the competitor genome because, in each lane, the intensity for this band is proportional to the band intensity of the 11mer.

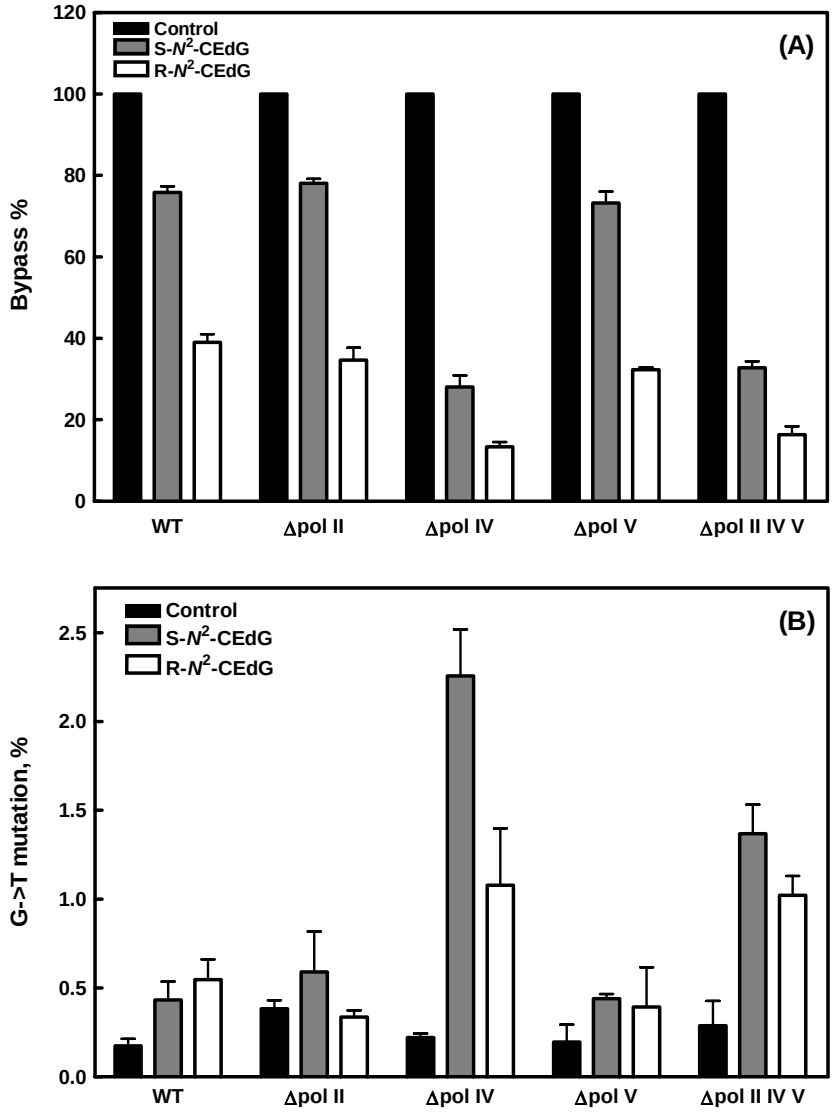

Figure 5-6. Bypass efficiencies (A) and mutation frequencies (B) of dG, S-N^2-CEdG and R-N^2-CEdG lesions in wild-type, pol II-, pol IV- and pol V-deficient AB1157 *E. coli* cells determined by CRAB and REAP assays, respectively. Black, gray and white column represent the results for substrates carrying dG, S-N^2-CEdG and R-N^2-CEdG, respectively. The data represent the means and standard deviations of results from three independent experiments.

It turned out that the bypass efficiencies for S- and R-N^2-CEdG in wild-type AB1157 cells are approximately 75% and 35%, respectively; deficiency in pol II or pol V in the isogenic AB1157 background does not appreciably affect the bypass efficiencies for the two diastereomers (Figure 5-6A). However, the bypass efficiency dropped to approximately 28% and 13%, respectively, in the corresponding pol IV-deficient cells (Figure 5-6A). Therefore, pol IV is the major polymerase involved in the bypass of N^2-CEdG in *E. coli* cells. In addition, regardless of the *E. coli* strains used, the bypass efficiency for R-N^2-CEdG is approximately one half of that for S-N^2-CEdG (Figure 5-6A), demonstrating that R-N^2-CEdG is a stronger block to DNA replication than S-N^2-CEdG. Moreover, the bypass efficiencies for N^2-CEdG were similar in pol IV-deficient and triple-knockout AB1157 cells, underscoring the lack of involvement of pol II and pol V in bypassing the lesion *in vivo*. We also measured the bypass efficiencies by using the recently introduced LC-MS/MS method (*33, 36*), and the results are consistent with those measured by using the conventional CRAB assay (Figure 5-7).

We then assessed the mutation frequencies of N^2-CEdG in wild-type and bypass polymerase-deficient *E. coli* strains with the REAP assay (*32, 33*), and we used LC-MS/MS for interrogating the replication fragments (Figure 5-4) (*37*). In this respect, the restriction digestion mixture was analyzed by LC-MS/MS, and we monitored the fragmentation of the $[M - 2H]^{2-}$ ions of d(NCGACGCC), where "N" is an A, T, C or G. It turned out that only d(GCGACGCC) and d(TCGACGCC) could be found in the digestion mixture. We then quantified the relative amounts of different replication

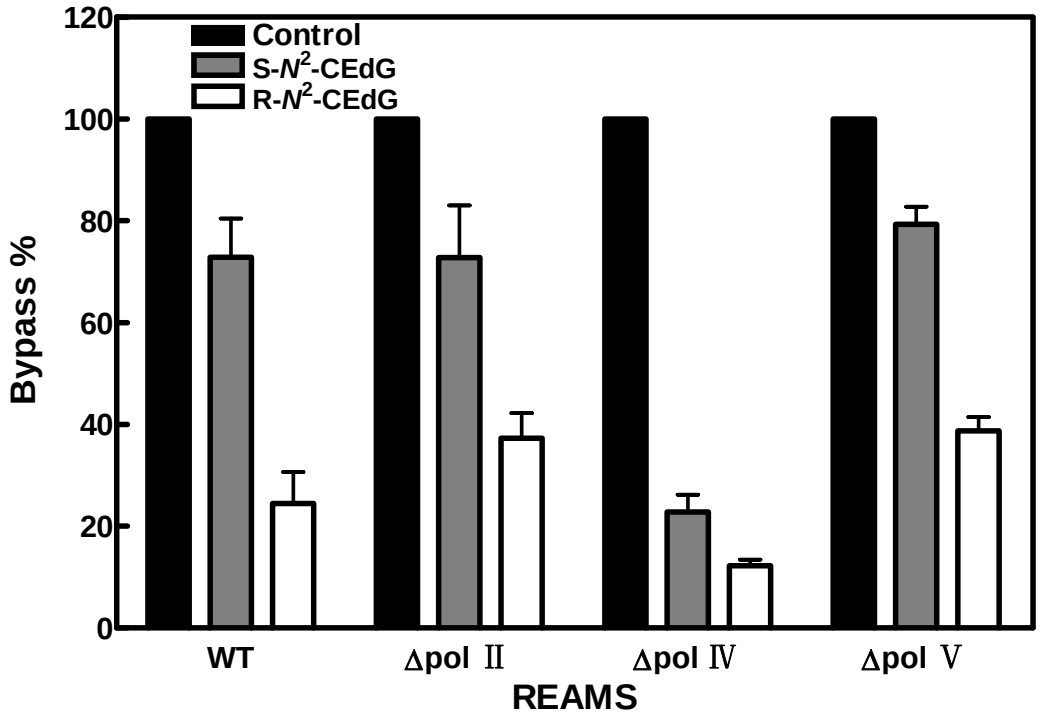

Figure 5-7. *In vivo* bypass efficiency of S-N^2-CEdG, R-N^2-CEdG lesions in wild-type, pol II-, pol IV- and pol V-deficient AB1157 *E. coli* determined by LC-MS/MS assay. Black, gray and white column represent control DNA, S- N^2-CEdG and R- N^2-CEdG, respectively. The data represent the means and standard deviations of results from three independent transformation and LC-MS/MS experiments.

products with the consideration of difference in ionization efficiencies for different ODNs [LC-MS/MS for monitoring the formation of d(GCGACGCC) and d(TCGACGCC) are shown in Figure 5-8, and calibration curves are depicted in Figure 5-9]. Our results revealed that both S-N^2-CEdG and R-N^2-CEdG are weakly mutagenic in wild-type AB1157 cells and the deficiency in pol II or pol V does not confer apparent increase in mutation frequency (Figure 5-6B). However, deficiency in pol IV causes considerable increase in G→T mutation. Moreover, the mutation frequency induced by R-N^2-CEdG is approximately one half of that by S-N^2-CEdG in pol IV-deficient background (1.1% and 2.3%, respectively, Figure 5-6B). Along this line, triple-knockout cells again exhibited significant increase in G→T mutation relative to the wild-type strain (Figure 5-6B). On the grounds that low mutation frequencies were found for N^2-CEdG, we may conclude that DinB plays an important role in avoiding the cytotoxic, rather than the mutagenic, effects of N^2-CEdG and its structurally related derivatives.

The above results unveiled that approximately two thirds of the bypass of N^2-CEdG in AB1157 *E. coli* cells requires pol IV, and the deficiency in pol IV leads to a marked increase in mutation frequency. Therefore, the pol IV-mediated bypass of N^2-CEdG in *E. coli* cells is error-free. To further substantiate this conclusion, we accessed quantitatively the efficiency and fidelity of pol IV-mediated nucleotide insertion opposite both S- and R- N^2-CEdG by using the steady-state kinetic measurements (Figure 5-10 and 5-11, and Table 5-1) (*29, 31*). It turned out that the nucleotide insertion opposite both diastereomers of N^2-CEdG is remarkably accurate, with mis-insertion frequencies similar to those found for nucleotide incorporation opposite an unmodified dG. Furthermore, the

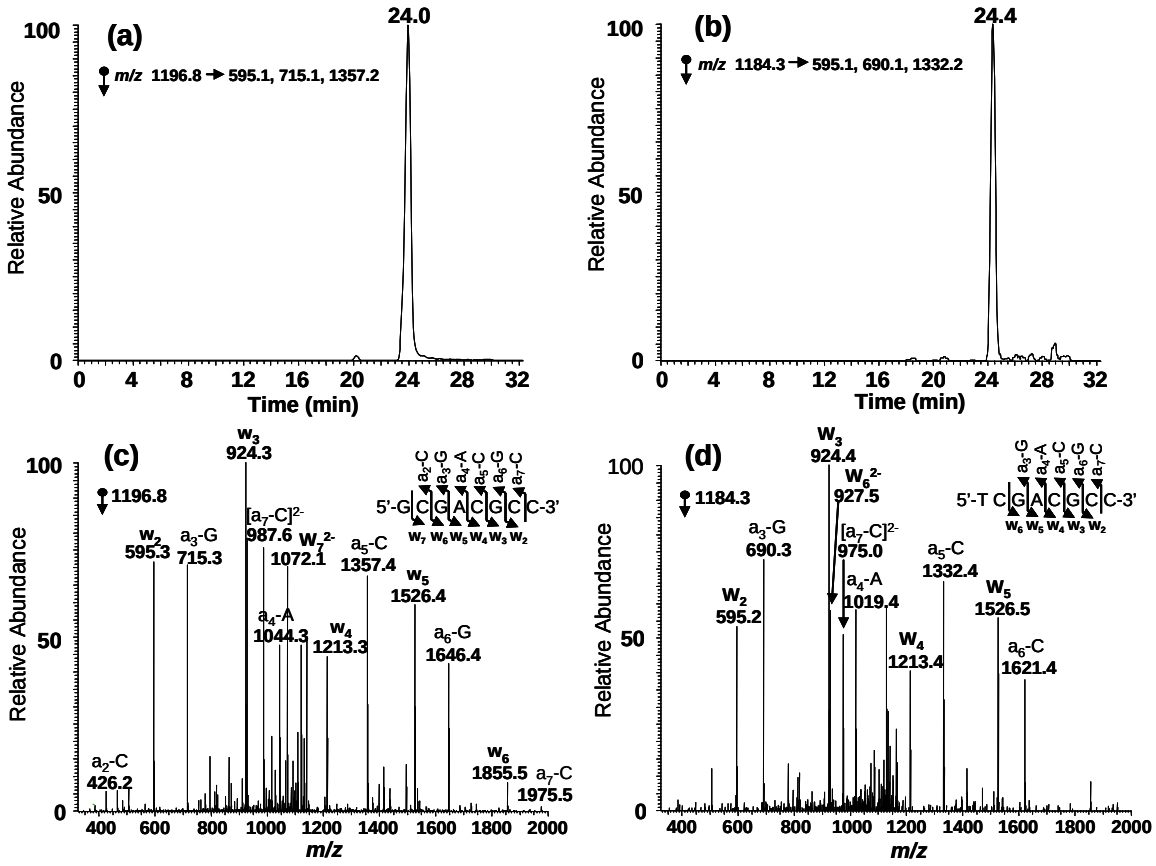

Figure 5-8. LC-MS/MS for monitoring the restriction fragments of interest without mutation or with a G◊T mutation at the original N^2-CEdG site [i.e., d(GCGACGCC) (8mer-G) and d(TCGACGCC) (8-mer T)]. Shown in (a) and (b) are the SICs for the formation of indicated fragment ions of these two ODNs, and illustrated in (c) and (d) are the MS/MS of the $[M–2H]^{2-}$ ions (*m/z* 1196.9 and 1184.3)of these two ODNs.

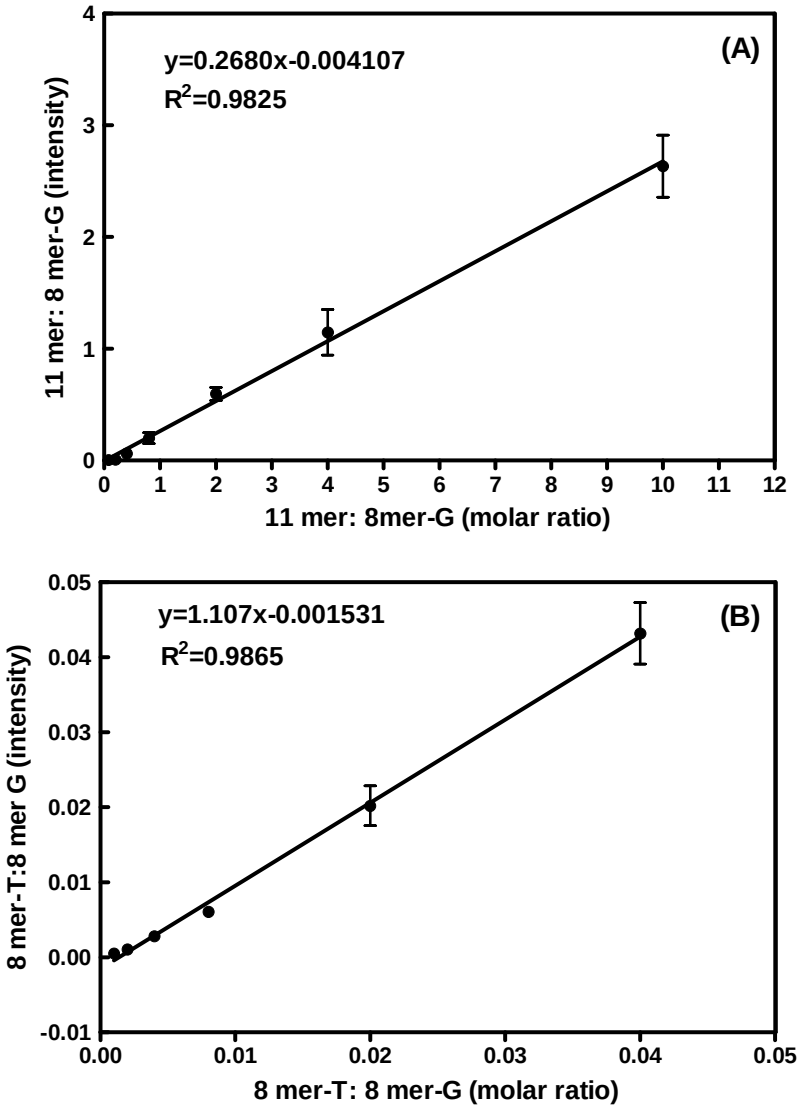

Figure 5-9. Calibration curves for the quantification of 11mer [i.e., d(GCTAGCTGCGG)] (a) and 8mer-T [i.e., d(TCGACGCC)] (b). 2.5 pmol of 8mer-G [i.e., d(GCGACGCC)] was mixed with 11mer and 8mer-T at different ratios. The normalized peak area ratios of 11mer and 8mer-T over 8mer-G in the selected-ion chromatograph (SIC) were plotted against the molar ratio for these ODNs to give the calibration curves. The fragment ions, w_2, [a_3-Base] and [a_5-Base] ions were selected for the SIC monitoring of 8mer ODN while the fragment ions, w_3, [a_4-base], and [a_5-Base] ions were selected for SIC monitoring of 11mer ODN. The conditions for analysis are identical for the replication mixture and the calibration curves. The data represent three independent measurements.

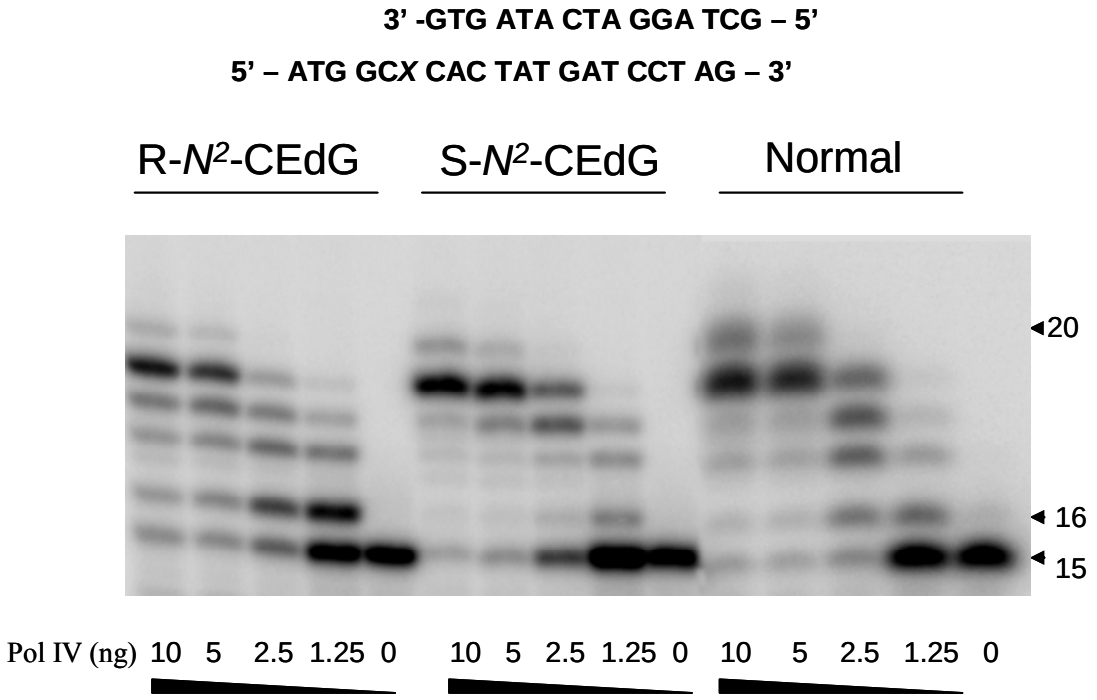

Figure 5-10. *In vitro* replication studies of N^2-CEdG-bearing and control undamaged substrates with *E. coli* polymerase IV (*X* represents S-N^2-CEdG, R-N^2-CEdG or unmodified dG). The primer extension was carried out at 37 °C in the presence of all four dNTPs at a concentration of 200 μM each for 60 min, and the amounts of pol IV were indicated. A 5'-[^{32}P]-labeled d(GCT AGG ATC ATA GTG) was used as the primer.

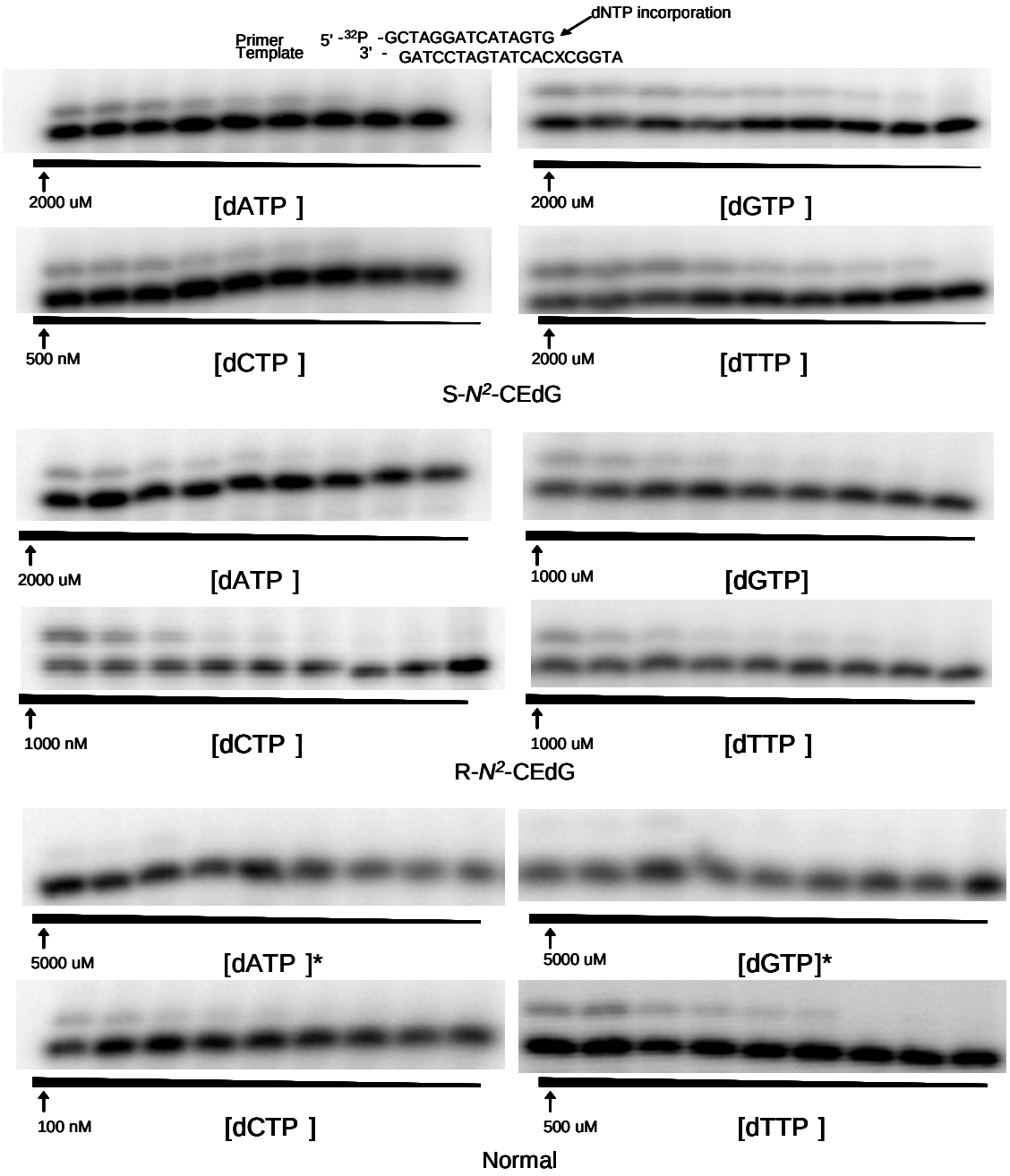

Figure 5-11. Steady-state kinetic measurements for incorporation of dAMP, dGMP, dCMP and dTMP opposite the S-N^2-CEdG, R-N^2-CEdG or undamaged dG on the 20 mer ODNs. *E.coli* DNA Pol IV (20 ng) was incubated with 10 nM primer-template duplex substrate at 37 °C for 10 minutes for each reaction. The highest dNTP concentration is shown in the figure, and the concentration ratio of dNTP between adjacent lanes was 0.5 - 0.6.
* The incorporation of dATP and dGTP opposite undamaged dG is barely detectable even at extraordinarily high concentration.

Table 5-1: Fidelity of nucleotide incorporation by *E.coli* DNA polymerae IV on N^2-CEdG-containing substrates and the undamaged substrate as determined by steady-state kinetic measurements (K_m and V_{max} are average values based on three independent measurements)

dNTP	V_{max} *(nM/min)*	K_m*(nM)*	V_{max} / K_m	f_{inc}
		S-N^2-CEdG crosslink containing substrates		
dATP	0.62 ± 0.07	(8.41 ± 0.74) x	7.37 x 10^{-7}	2.91 x 10^{-4}
dGTP	0.23 ± 0.02	(6.83 ± 0.63) x	3.36 x 10^{-7}	1.33 x 10^{-4}
dCTP	0.19 ± 0.02	75 ± 8.4	2.53 x 10^{-3}	1.00
dTTP	0.46 ± 0.06	(5.83 ± 0.68) x	7.89 x 10^{-7}	3.12 x 10^{-4}
		R-N^2-CEdG crosslink containing substrates		
dATP	0.16 ± 0.01	(7.90 ± 0.89) x	2.02 x 10^{-7}	1.44 x 10^{-4}
dGTP	0.49 ± 0.08	(1.49 ± 0.26) x	3.28 x 10^{-7}	2.34 x 10^{-4}
dCTP	0.16 ± 0.03	(1.14± 0.28) x 10	1.40 x 10^{-3}	1.00
dTTP	0.48 ± 0.05	(1.23± 0.05) x 10	3.89 x 10^{-7}	2.78 x 10^{-4}
		Control normal substrates		
dATP	n/a	n/a	n/a	n/a
dGTP	n/a	n/a	n/a	n/a
dCTP	0.34 ± 0.07	53 ± 8.2	6.42 x 10^{-3}	1.00
dTTP	0.073 ± 0.001	(4.61 ± 0.56) x	1.58 x 10^{-6}	2.46x 10^{-4}

replacements of dG with an S- or R-N^2-CEdG caused decreases in the efficiency (V_{max}/K_m, Table 5-1) for nucleotide insertion by 2.5- and 4.6-fold, respectively, which is consistent with the observation that R-N^2-CEdG is a stronger block to DNA replication than S-N^2-CEdG in *E. coli* cells (see above).

We also measured the steady-state kinetic parameters for nucleotide incorporation opposite the N^2-CEdG lesion by human pol κ (Figure 5-12 and 5-13). The nucleotide insertion by human pol κ is again highly accurate, and the polymerase inserts preferentially dCMP opposite the lesion (Table 5-2). More strikingly, the efficiencies for human pol κ to incorporate the correct nucleotide, dCMP, opposite S- and R-N^2-CEdG, were increased by 6- and 3.5-fold, respectively, relative to the unmodified substrate. Thus, N^2-CEdG is a better substrate for human pol κ than an unmodified dG.

Discussion

MG is induced endogenously as a byproduct of glycolysis, a metabolic process conserved in all organisms (*22, 23, 38*). The concentration of MG human cells can be elevated under various pathological conditions (e.g., diabetes) (*24*). It was found recently that MG induces modifications in calf thymus DNA mainly on dG to give N^2-CEdG (*39*). N^2-CEdG can also be detected in urine samples of healthy human subjects (*40*), and in kidney and aorta cells of diabetic and uremic patients (*41*). LC-MS/MS with the isotope dilution method revealed that N^2-CEdG can be formed in untreated WM-266-4 cells at a level of approximately one lesion per 10^7 nucleosides; treatment of cells with MG or glucose can further stimulate the formation of the lesion, supporting that N^2-CEdG is an

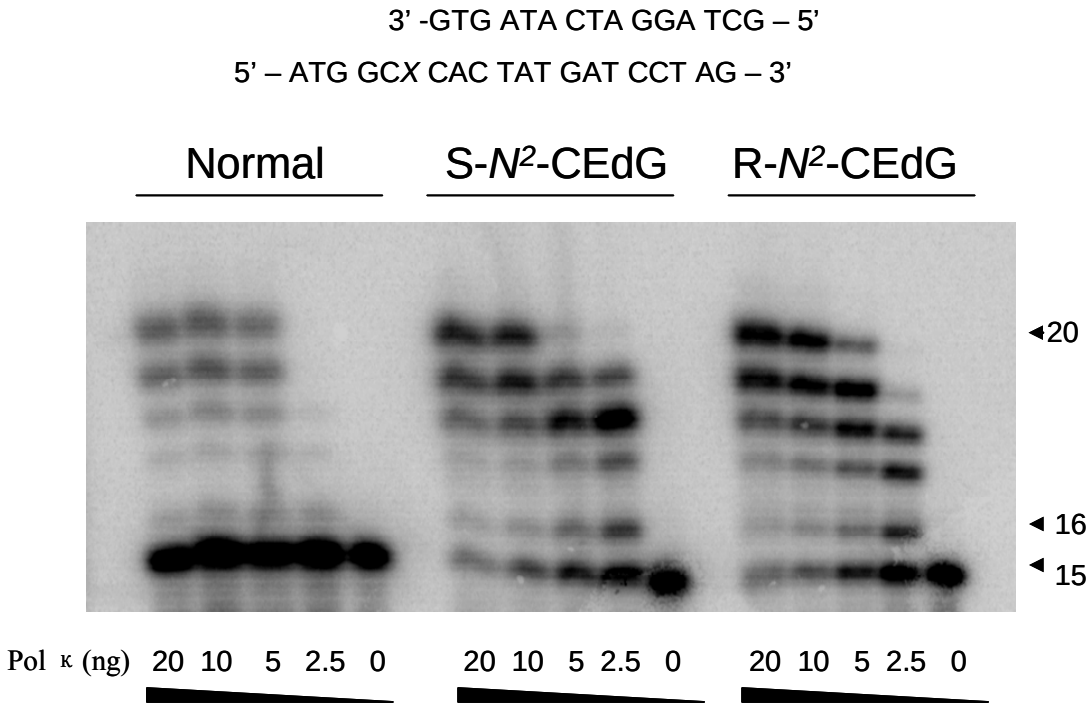

Figure 5-12. In vitro replication studies of N^2-CEdG-bearing and control undamaged substrates with human polymerase κ (*X* represents S-N^2-CEdG, R-N^2-CEdG or unmodified dG). The primer extension was carried out at 37 °C in the presence of all four dNTPs at a concentration of 200 μM each for 60 min, and the amounts of human pol κ were indicated. A 5'-[^{32}P]-labeled d(GCTAGGATCATAGC) was used as the primer.

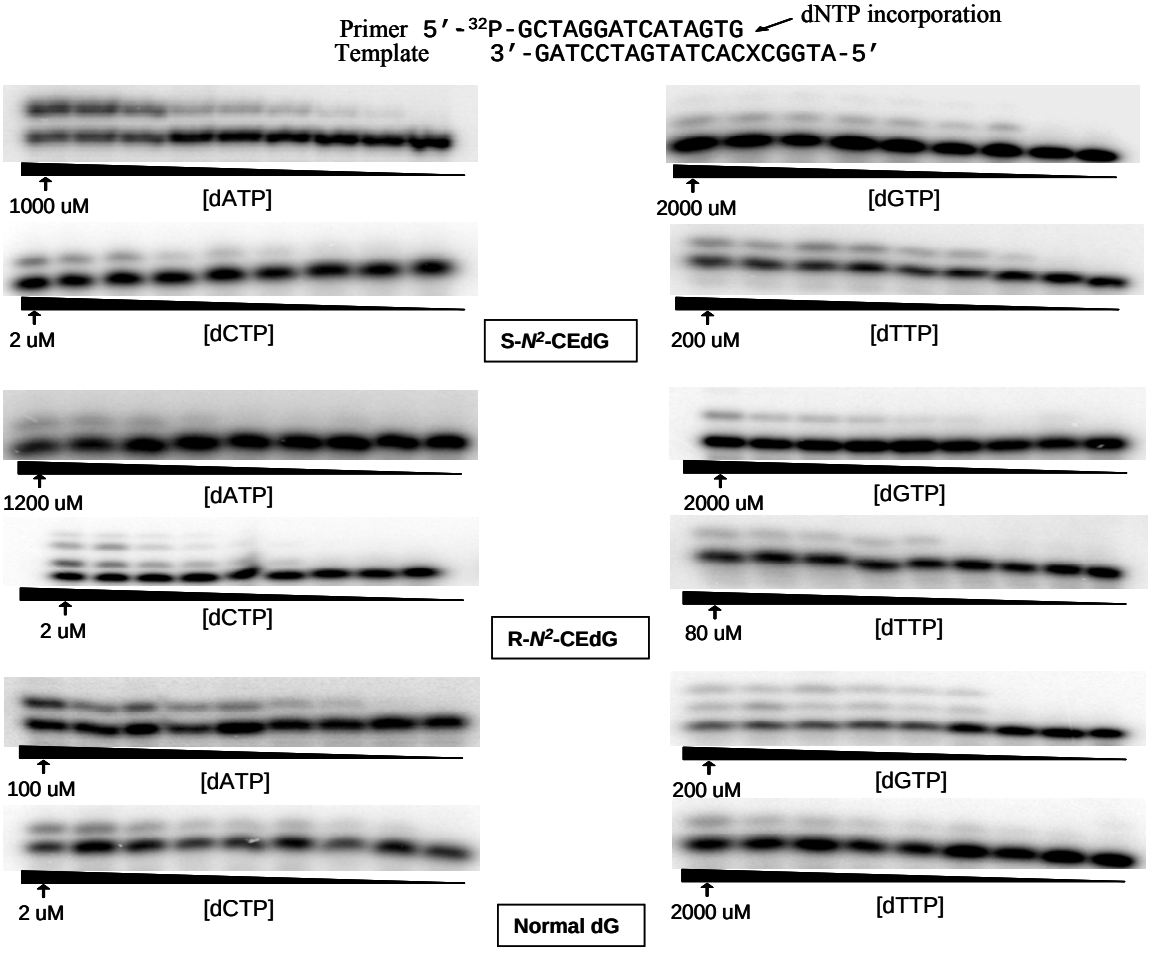

Figure 5-13. Steady-state kinetic measurements for incorporation of dAMP, dGMP, dCMP and dTMP opposite the S- N^2-CEdG, R- N^2-CEdG or undamaged dG on the 20 mer ODNs. Human pol κ (5 ng) was incubated with 10 nM primer-template duplex substrate at room temperature for 10 minutes for each reaction. The highest dNTP concentration is shown in the figure, and the concentration ratio of dNTP between adjacent lanes was 0.5-0.6.

Table 5-2. Fidelity of nucleotide incorporation by human polymerase κ on N^2-CEdG-containing substrates and the undamaged substrate as determined by steady-state kinetic measurements (K_m and V_{max} are average values based on three independent measurements).

dNTP	V_{max} (nM min^{-1})	K_m (nM)	V_{max} / K_m (min^{-1})	f_{inc}
S-N^2-CEdG-containing substrate				
dATP	0.24 ± 0.004	(1.21 ± 0.10) × 10^5	1.98 × 10^{-6}	6.39 × 10^{-3}
dGTP	0.08 ± 0.01	(3.31 ± 0.32) × 10^5	2.41 × 10^{-7}	7.77 × 10^{-4}
dCTP	0.25 ± 0.03	(8.06 ± 0.95) × 10^2	3.10 × 10^{-4}	1.00
dTTP	0.30 ± 0.02	(3.46 ± 0.55) × 10^4	8.67 × 10^{-6}	2.80 × 10^{-2}
R-N^2-CEdG-containing substrate				
dATP	0.28 ± 0.02	(9.83 ± 0.20) × 10^5	2.84 × 10^{-7}	1.49 × 10^{-3}
dGTP	0.10 ± 0.01	(5.28 ± 1.05) × 10^5	1.89 × 10^{-7}	9.90 × 10^{-4}
dCTP	0.91 ± 0.09	(4.77 ± 0.39) × 10^3	1.91 × 10^{-4}	1.00
dTTP	0.14 ± 0.02	(2.53 ± 0.43) × 10^4	5.53 × 10^{-6}	2.90 × 10^{-2}
dG-containing substrate				
dATP	0.26 ± 0.002	(7.48 ± 1.17) × 10^4	3.48 × 10^{-6}	6.4 × 10^{-2}
dGTP	0.30 ± 0.01	(1.84 ± 0.26) × 10^5	1.63 × 10^{-6}	3.0 × 10^{-2}
dCTP	0.27 ± 0.01	(5.00 ± 0.54) × 10^3	5.40 × 10^{-5}	1.00
dTTP	0.16 ± 0.06	(7.75 ± 0.02) × 10^5	2.06 × 10^{-7}	3.81 × 10^{-3}

endogenous DNA lesion and the amount of the lesion can be enhanced by byproducts of glycolysis.

Replication studies using single-stranded M13 shuttle vectors harboring a site-specifically incorporated N^2-CEdG revealed that the two diastereomers of the lesion exhibited significantly different bypass efficiencies in *E. coli* cells. The R-N^2-CEdG is twice as effective as S-N^2-CEdG in blocking DNA replication in all strains of *E. coli* cells that we examined. Although the absence of pol II or V does not give rise to apparent alteration in bypass efficiency, deficiency in pol IV results in a significant drop in bypass efficiency by 63% and 66% for the S and R diastereomers, respectively (Figure 5-6A).

Both diastereomers are weakly mutagenic in wild-type AB1157 cells and the isogenic *E. coli* cells that are deficient in pol II or pol V. However, the frequency of G→T mutation in pol IV-deficient background was increased significantly for both diastereomers, supporting that the pol IV-mediated lesion bypass is largely error-free. Along this line, it was found that G→T transversion accounts for 70% of benzo[*a*]pyrene-induced mutations in pol κ-defective cells, whereas G→T and G→A mutations occur at an equal frequency of approximately 30% of total mutations in parental cells (*7*).

These results are also in accordance with *in vitro* replication data showing that nucleotide insertion opposite N^2-CEdG is both accurate and efficient. In this respect, the efficiencies (V_{max}/K_m) for *E. coli* pol IV to incorporate the correct nucleotide, dCMP, opposite dG, S-, and R-N^2-CEdG were 6.42×10^{-3}, 2.53×10^{-3}, and 1.40×10^{-3} min^{-1}, respectively (Table 5-1). In addition, the corresponding efficiencies for human pol κ to

insert dCMP were 5.40×10^{-5}, 3.10×10^{-4}, and 1.91×10^{-4} min^{-1}, respectively (Table 5-2). In keeping with our observations, *E. coli* pol IV and human pol κ insert dCMP opposite N^2-furfuryl-dG with 10- to 15-fold greater catalytic efficiency than opposite an undamaged dG (*7*). It is of note that N^2-furfuryl-dG is a structure analog of the principal N^2-dG adduct induced by nitrofurazone (*7*), and there is no evidence showing that N^2-furfuryl-dG is an endogenously induced DNA adduct. Furthermore, *E. coli* pol IV and human pol κ can bypass accurately the bulky N^2-dG-BPDE adduct (*10*-*12*), and the M13 genome bearing an N^2-dG-BPDE gave 4-fold fewer plaques when transfected into SOS-induced pol IV-deficient *E. coli* cells relative to the isogenic wild-type cells (*11*). Different from what we found for the bypass of N^2-CEdG, the efficiency for human pol κ to insert dCMP across N^2-dG-BPDE was at least 70 times less than opposite an undamaged dG (*10*).

Recently, the x-ray crystal structure for the catalytic core of human pol κ in ternary complex with DNA and an incoming nucleotide has been solved (*42*). The structure reveals the absence of steric hindrance in the minor groove at the primer-template junction (*42*), which may explain the tolerance of the polymerase toward the minor-groove adduct, N^2-CEdG.

Taken together, the results from the present study offer solid evidence supporting that N^2-CEdG, a DNA adduct arising from MG, is an endogenous substrate for DinB DNA polymerase.

References:

(1) Lindahl, T. (1993) Instability and decay of the primary structure of DNA. *Nature 362*, 709-15.

(2) Friedberg, E. C., Walker, G. C., Siede, W., Wood, R. D., Schultz, R. A., and Ellenberger, T. (2006) *DNA Repair and Mutagenesis*, ASM Press, Washington, D.C.

(3) Goodman, M. F. (2002) Error-prone repair DNA polymerases in prokaryotes and eukaryotes. *Annu. Rev. Biochem. 71*, 17-50.

(4) Fuchs, R. P., Fujii, S., and Wagner, J. (2004) Properties and functions of *Escherichia coli*: Pol IV and Pol V. *Adv. Protein Chem. 69*, 229-64.

(5) Tang, M., Pham, P., Shen, X., Taylor, J. S., O'Donnell, M., Woodgate, R., and Goodman, M. F. (2000) Roles of E. coli DNA polymerases IV and V in lesion-targeted and untargeted SOS mutagenesis. *Nature 404*, 1014-8.

(6) Johnson, R. E., Washington, M. T., Haracska, L., Prakash, S., and Prakash, L. (2000) Eukaryotic polymerases iota and zeta act sequentially to bypass DNA lesions. *Nature 406*, 1015-9.

(7) Jarosz, D. F., Godoy, V. G., Delaney, J. C., Essigmann, J. M., and Walker, G. C. (2006) A single amino acid governs enhanced activity of DinB DNA polymerases on damaged templates. *Nature 439*, 225-8.

(8) Choi, J. Y., Zang, H., Angel, K. C., Kozekov, I. D., Goodenough, A. K., Rizzo, C. J., and Guengerich, F. P. (2006) Translesion synthesis across 1,N^2-ethenoguanine by human DNA polymerases. *Chem. Res. Toxicol. 19*, 879-86.

(9) Zhang, Y., Yuan, F., Wu, X., Wang, M., Rechkoblit, O., Taylor, J. S., Geacintov, N. E., and Wang, Z. (2000) Error-free and error-prone lesion bypass by human DNA polymerase k *in vitro*. *Nucleic Acids Res. 28*, 4138-46.

(10) Rechkoblit, O., Zhang, Y. B., Guo, D. Y., Wang, Z. G., Amin, S., Krzeminsky, J., Louneva, N., and Geacintov, N. E. (2002) trans-lesion synthesis past bulky benzo[a]pyrene diol epoxide N-2-dG and N-6-dA lesions catalyzed by DNA bypass polymerases. *Journal of Biological Chemistry 277*, 30488-30494.

(11) Shen, X., Sayer, J. M., Kroth, H., Ponten, I., O'Donnell, M., Woodgate, R., Jerina, D. M., and Goodman, M. F. (2002) Efficiency and accuracy of SOS-induced DNA polymerases replicating benzo[*a*]pyrene-7,8-diol 9,10-epoxide A and G adducts. *J. Biol. Chem. 277*, 5265-74.

(12) Suzuki, N., Ohashi, E., Kolbanovskiy, A., Geacintov, N. E., Grollman, A. P., Ohmori, H., and Shibutani, S. (2002) Translesion synthesis by human DNA polymerase kappa on a DNA template containing a single stereoisomer of dG-(+)- or dG-(-)-anti-N-2-BPDE (7,8-dihydroxy-anti-9,10-epoxy-7,8,9,10-tetrahydrobenzo[a]pyrene). *Biochemistry 41*, 6100-6106.

(13) Finkel, T., and Holbrook, N. J. (2000) Oxidants, oxidative stress and the biology of ageing. *Nature 408*, 239-47.

(14) De Bont, R., and van Larebeke, N. (2004) Endogenous DNA damage in humans: a review of quantitative data. *Mutagenesis 19*, 169-85.

(15) Fothergill-Gilmore, L. A., and Michels, P. A. (1993) Evolution of glycolysis. *Prog. Biophys. Mol. Biol. 59*, 105-235.

(16) Kalapos, M. P. (1999) Methylglyoxal in living organisms: chemistry, biochemistry, toxicology and biological implications. *Toxicol. Lett. 110*, 145-75.

(17) Phillips, S. A., Mirrlees, D., and Thornalley, P. J. (1993) Modification of the Glyoxalase System in Streptozotocin-Induced Diabetic Rats - Effect of the Aldose Reductase Inhibitor Statil. *Biochemical Pharmacology 46*, 805-811.

(18) Ramasamy, R., Yan, S. F., and Schmidt, A. M. (2006) Methylglyoxal comes of AGE. *Cell 124*, 258-60.

(19) Chaplen, F. W., Fahl, W. E., and Cameron, D. C. (1998) Evidence of high levels of methylglyoxal in cultured Chinese hamster ovary cells. *Proc. Natl. Acad. Sci. U S A 95*, 5533-8.

(20) Mclellan, A. C., Thornalley, P. J., Benn, J., and Sonksen, P. H. (1994) Glyoxalase System in Clinical Diabetes-Mellitus and Correlation with Diabetic Complications. *Clinical Science 87*, 21-29.

(21) Thornalley, P. J. (1988) Modification of the Glyoxalase System in Human Red Blood-Cells by Glucose Invitro. *Biochemical Journal 254*, 751-755.

(22) Saint-Jalm, Y., and Moree-Testa, P. (1980) Study of nitrogen-containing compounds in cigarette smoke by gas chromatography-mass spectrometry. *J. Chromatogr 198*, 188-92.

(23) do Rosario, P. M., Cordeiro, C. A., Freire, A. P., and Nogueira, J. M. (2005) Analysis of methylglyoxal in water and biological matrices by capillary zone electrophoresis with diode array detection. *Electrophoresis 26*, 1760-7.

(24) Frischmann, M., Bidmon, C., Angerer, J., and Pischetsrieder, M. (2005) Identification of DNA adducts of methylglyoxal. *Chem. Res. Toxicol. 18*, 1586-92.

(25) Schneider, M., Georgescu, A., Bidmon, C., Tutsch, M., Fleischmann, E. H., Popov, D., and Pischetsrieder, M. (2006) Detection of DNA-bound advanced glycation end-products by immunoaffinity chromatography coupled to HPLC-diode array detection. *Mol. Nutr. Food Res. 50*, 424-9.

(26) Murata-Kamiya, N., Kamiya, H., Kaji, H., and Kasai, H. (2000) Methylglyoxal induces G:C to C:G and G:C to T:A transversions in the supF gene on a shuttle vector plasmid replicated in mammalian cells. *Mutat. Res. 468*, 173-82.

(27) Pischetsrieder, M., Seidel, W., Munch, G., and Schinzel, R. (1999) N-2-(1-carboxyethyl)deoxyguanosine, a nonenzymatic glycation adduct of DNA, induces single-strand breaks and increases mutation frequencies. *Biochemical and Biophysical Research Communications 264*, 544-549.

(28) Jarosz, D. F., Beuning, P. J., Cohen, S. E., and Walker, G. C. (2007) Y-family DNA polymerases in Escherichia coli. *Trends Microbiol. 15*, 70-77.

(29) Kobayashi, S., Valentine, M. R., Pham, P., O'Donnell, M., and Goodman, M. F. (2002) Fidelity of Escherichia coli DNA polymerase IV - Preferential generation of small deletion mutations by dNTP-stabilized misalignment. *Journal of Biological Chemistry 277*, 34198-34207.

(30) Cao, H., Jiang, Y., and Wang, Y. (2007) Stereospecific synthesis and characterization of oligodeoxyribonucleotides containing an N^2-(1-carboxyethyl)-2'-deoxyguanosine. *J. Am. Chem. Soc. 129*, 12123-12130.

(31) Creighton, S., Bloom, L. B., and Goodman, M. F. (1995) Gel fidelity assay measuring nucleotide misinsertion, exonucleolytic proofreading, and lesion bypass efficiencies. *Methods Enzymol. 262*, 232-56.

(32) Delaney, J. C., and Essigmann, J. M. (1999) Context-dependent mutagenesis by DNA lesions. *Chem. Biol. 6*, 743-53.

(33) Delaney, J. C., and Essigmann, J. M. (2006) Assays for determining lesion bypass efficiency and mutagenicity of site-specific DNA lesions in vivo. *Methods Enzymol. 408*, 1-15.

(34) Gu, C. N., and Wang, Y. S. (2007) In vitro replication and thermodynamic studies of methylation and oxidation modifications of 6-thioguanine. *Nucleic Acids Research 35*, 3693-3704.

(35) Kaiser, N., Sasson, S., Feener, E. P., Boukobzavardi, N., Higashi, S., Moller, D. E., Davidheiser, S., Przybylski, R. J., and King, G. L. (1993) Differential Regulation of Glucose-Transport and Transporters by Glucose in Vascular Endothelial and Smooth-Muscle Cells. *Diabetes 42*, 80-89.

(36) Delaney, J. C., and Essigmann, J. M. (1999) Context-dependent mutagenesis by DNA lesions. *Chem. Biol. 6*, 743-753.

(37) Hong, H., Cao, H., and Wang, Y. (2007) Formation and genotoxicity of a guanine-cytosine intrastrand cross-link lesion in vivo. *Nucleic Acids Res 35*, 7118-27.

(38) Nagao, M., Fujita, Y., Wakabayashi, K., Nukaya, H., Kosuge, T., and Sugimura, T. (1986) Mutagens in coffee and other beverages. *Environ. Health Perspect. 67*, 89-91.

(39) Schneider, M., Thoss, G., Hubner-Parajsz, C., Kientsch-Engel, R., Stahl, P., and Pischetsrieder, M. (2004) Determination of glycated nucleobases in human urine by a new monoclonal antibody specific for N2-carboxyethyl-2'-deoxyguanosine. *Chem. Res. Toxicol. 17*, 1385-90.

(40) Li, H., Nakamura, S., Miyazaki, S., Morita, T., Suzuki, M., Pischetsrieder, M., and Niwa, T. (2006) N-2-carboxyethyl-2 '-deoxyguanosine, a DNA glycation marker, in kidneys and aortas of diabetic and uremic patients. *Kidney International 69*, 388-392.

(41) Masutani, C., Araki, M., Yamada, A., Kusumoto, R., Nogimori, T., Maekawa, T., Iwai, S., and Hanaoka, F. (1999) Xeroderma pigmentosum variant (XP-V) correcting protein from HeLa cells has a thymine dimer bypass DNA polymerase activity. *Embo J. 18*, 3491-501.

(42) Lone, S., Townson, S. A., Uljon, S. N., Johnson, R. E., Brahma, A., Nair, D. T., Prakash, S., Prakash, L., and Aggarwal, A. K. (2007) Human DNA polymerase k encircles DNA: implications for mismatch extension and lesion bypass. *Mol. Cell 25*, 601-14.

CHAPTER 6

Concluding Remarks and Future Directions

In this dissertation, three types of DNA lesions, namely, an oxidatively induced intrastrand cross-link lesion (G[8-5m]T), two tandem ROS-induced nucleobase lesions [5'-Tg-(8-oxodG)-3' and 5'-(8-oxodG)-Tg-3'] and a N^2-dG DNA adduct (N^2-CEdG), were identified and quantified by LC-MS/MS methods; their cytotoxicity and mutagenicity were further characterized by traditional steady-state kinetics techniques and LC-MS/MS-based strategies.

In Chapter 2, a cross-link lesion, G[8-5m]T, in which the C8 carbon atom of guanine and the 5-methyl carbon atom of its 3' neighboring thymide are covalently bonded, was identified by LC-MS/MS from the γ ray-treated Hela-S3 cells for the first time, and its yield of formation is proportional to the dose of the γ-rays applied. Our *in-vitro* replication studies showed that the DNA synthesis mediated by Klenow fragment, a representative replicative DNA polymerase, was stopped mostly after incorporating the correct nucleotide dAMP opposite the 3′-thymine moiety of the lesion, suggesting strong blocking effect of this lesion toward replicative polymerases. By contrast, translesion synthesis polymerase, i.e. yeast pol η, could replicate past the lesion with a markedly reduced efficiency as well as with considerable frequencies of nucleotide misincorporation (i.e., dAMP and dGMP were inserted opposite the 5′-guanine moiety of the G[8-5m]T). Taken together, our data suggested that this ionizing radiation-inducible

intrastrand cross-link lesion may render certain difficulty for DNA replication and lead to mutations.

In Chapters 3 and 4, we discussed our study on tandem nucleobase lesions. An efficient dose-dependent formation of the 5'-Tg-(8-oxodG)-3' tandem lesion in isolated DNA upon treatment with Fenton type reagents or γ-rays in the presence of Cu(II) /ascorbate was revealed for the first time. It is worth highlighting our strategy for the quantification of this lesion, where we took advantage of the fact that nuclease P1 can not cleave the phosphodiester bond between Tg and its 3' adjacent nucleotide. This results the release of the tandem lesion as a unique chemical entity, i.e. 5'-p-Tg-p-(8-oxodG)-3', which could be easily detected and quantified by LC-MS/MS. The high yield of this lesion may indicate novel mechanisms of its formation as well as potentially high biological significance of this lesion. In light of this finding, we further assessed the cytotoxic and mutagenic properties of this tandem lesion together with 5'-(8-oxodG)-Tg-3' both *in vitro* and *in vivo*. Chapter 3 focused on examining how they are replicated with purified DNA polymerases and how they are interpreted by purified BER enzymes. We found that both tandem lesions blocked primer extension mediated by the Klenow fragment and yeast pol η more readily than when the Tg or 8-oxodG was present alone and the mutagenic properties of Tg or 8-oxodG differed while they were present alone or in tandem; in addition, the activities of purified BER enzymes were also altered when they encountered substrates bearing the tandem lesions. In Chapter 4, we extended our replication studies on these tandem lesions from *in vitro* to *in vivo* by assessing their bypass efficiencies and mutation frequencies in *E. coli* cells. In consistency with our *in-*

vitro results, the bypass efficiencies for the tandem lesions were considerably reduced comparing to those for the two isolated single-nucleobase lesions. Surprisedly, the 5′-Tg-(8-oxodG)-3′ could also give rise to a significant frequency of TG→GT tandem double mutation, which has never been reported before. Taken together, both *in-vitro* and *in-vivo* results indicated that tandem lesions could exert a greater cytotoxic effect than when the composing lesions are present alone and the mutagenic properties of the tandem lesions could be markedly altered.

In Chapter 5, we assessed the formation, cytotoxic and mutagenic properties of the N^2-CEdG, a major stable DNA adduct formed from methylglyoxal. We found that N^2-CEdG could be detected at a frequency of one lesion per 10^7 nucleosides in WM-266-4 human melanoma cells, and treatment of these cells with MG or glucose led to a dose-responsive increase in its formation. Furthermore, our *in-vitro* replication results showed that *E. coli* pol IV and its human counterpart polymerase κ were able to bypass N^2-CEdG accurately and efficiently. Our *in-vivo* replication study on this lesion in wild-type and bypass polymerase-deficient *E. coli* cells also confirmed that pol IV is the major DNA polymerase responsible for bypassing N^2-CEdG in *E. coli* cells. Taken together, our data support that N^2-CEdG, a minor-groove DNA adduct arising from MG, is an important endogenous substrate for DinB DNA polymerase.

Future studies can be conducted focusing on the identification and quantification of these lesions in other biological samples, i.e. tissues. For example, the accumulation of intrastrand cross-link lesions may be associated with neurodegeneration in NER-deficient

patients, thus it is helpful to assess the lesion formation in NER-deficient animals or human tissues. In this dissertation we showed the efficient formation of the 5′-Tg-(8-oxodG)-3′ tandem lesion in isolated DNA upon exposure to Fenton-type reagents. It is necessary to analyze its formation *in vivo*. In this regard, Cu ions are accumulated abnormally in liver, brain, kidney and other tissues of Wilson's disease patients. Therefore, reagent-treated cultured cells, Wilson's disease model animal or patient tissues could be assessed. This may help to illustrate the significance of Cu ions and DNA damage involved in the pathogenesis. In addition, it is important to further extend *in-vivo* replication study from *E. coli* to mammalian cells, viewing that, both replication and repair systems in the mammalian cells are much more complicated than those in prokaryotes. The strategies discussed in Chapters 4 and 5 should be readily adaptable for such studies. In addition, we assessed how tandem lesions are recognized by purified BER enzymes in Chapter 3, it is of interest to investigate whether intrastrand cross-link lesions and tandem nucleobase lesions are substrates for eukaryotic NER repair system.